



**Politecnico
di Torino**

Politecnico di Torino

Corso di Laurea Magistrale
A.a. 2023/2024
Sessione di Laurea Marzo 2024

**Determination of global resistance
safety factors for RC beams failing in
bending according to strain-based
method using NLNAs**

Relatori:

Prof. GINO Diego
Ing. MICELI Elena

Candidato:

BARGETTO Stefano

Abstract

The purpose of this thesis is to define a methodology for the design and verification of reinforced concrete structural elements subject to flexural collapse using non-linear numerical analysis (NLTAs). This methodology is based on the global resistance method (GRM) based on the strain-based method, establishing a correlation between the structural response of reinforced concrete beams and structural and geometric response characteristics of the system. These characteristics include the maximum strain of the primary reinforcement obtained through non-linear numerical analysis using mean values of material properties and nominal values for geometric properties, as well as the amount of reinforcement characterizing the resistant section (identified through the geometric reinforcement ratio). To achieve this goal, firstly, 16 beams tested to collapse, found in the scientific literature and subjected to flexural collapse, were selected. Using their geometry and material properties, it was possible to develop a non-linear numerical model for each beam, aiming to minimize the discrepancy between numerical prediction and experimental result. Subsequently, these numerical models were used to conduct an extensive series of probabilistic simulations, assuming appropriate hypotheses regarding the modelling of random variables related to material properties. The results of the probabilistic simulations allow correlating the estimation of statistical parameters with the response of the structures and their geometric characteristics, in order to propose a useful methodology for design or verification, aimed at defining the values of the global resistance safety factor within the GRM.

Ringraziamenti

La conclusione di un percorso di studi come la Laurea Magistrale è un importante traguardo frutto dell'impegno dello studente, ma non solo.

Io infatti mi sento di voler ringraziare la mia famiglia, soprattutto i miei genitori: Margherita e Luigi. Genitori che non hanno avuto l'opportunità di specializzarsi a livello universitario, perché non era economicamente possibile, ma che hanno fatto molti sacrifici affinché tutti e tre i loro figli potessero farlo, ognuno nel proprio campo.

Vorrei ricordare il supporto di mia sorella Elena, una seconda mamma per me, e di mio fratello Lorenzo. In questi anni mi hanno visto nei momenti gioiosi e in quelli più di sconforto. In questi ultimi casi, il tempo per una pausa pranzo rigenerativa si trovava sempre.

Voglio ringraziare Erri, che con il suo amore mi sprona in tutte le cose che faccio e crede sempre in me, anche nei momenti in cui faccio fatica a farlo da solo.

Voglio ringraziare il mio relatore, Diego Gino. Lo ringrazio per la disponibilità che mi ha sempre concesso in questi mesi.

Fiducioso nel futuro, ringrazio di essere al Politecnico, oggi, 15 Marzo 2024. Una data importante che segna l'inizio di una nuova avventura e di nuovi orizzonti ai quali ambire.

*Ai miei genitori,
che mi hanno supportato
lasciandomi libero di fare la mie scelte*

Contents

1	Introduction	1
2	Global Resistance Format (GRF).....	4
2.1	Safety formats.....	6
2.2	Strain-based methodology	7
3	Experimental benchmark	11
3.1	Typology of tests.....	11
3.2	Database	12
3.2.1	Giuseppe Campione [1].....	13
3.2.2	Qian Chunxiang [2].....	15
3.2.3	Hussein M. Elsanadedy [3].....	18
3.2.4	Alberto Meda [4]	20
3.2.5	Evangelista L. [5].....	22
3.2.6	M. A. Rashid and M. A. Mansur [6]	24
4	FEM modelling.....	28
4.1	ATENA 2D: FEM software.....	28
4.1.1	Pre processing.....	29
4.1.2	Post processing	45
4.1.3	CCT and CCO files.....	47
4.2	Finite Elements Models: hypothesis and NLNAs results.....	49
5	Probabilistic modelling	55
5.1	Relevant random variables	55
5.1.1	Latin Hypercube Sampling (LHS)	56
5.2	Probabilistic analysis of the global structural resistance	57
6	Results and comments	62
6.1	Strain-based method for RC structures failing in bending.....	64

6.1.1	Expressions for practical applications	67
6.2	Comparison with the other safety formats within the GRF	69
7	Conclusions.....	70
	References.....	72
	List of figures.....	74
	List of tables	77

1 Introduction

Non-linear numerical analysis (NLNAs) for reinforced concrete structural elements is a quite novel method used for the design and the assessment of new and existing structures. Particularly, NLNAs permits to predict a more real mechanical behaviour of a reinforced concrete element considering both the aleatory uncertainties, due to the inherent physical properties of the system, and epistemic ones, which can be reduced by increasing the level of knowledge. As well as considering the geometrical and mechanical non-linearities, NLNAs allows to also treat the deterioration phenomena. Even if these advantages require a more refinement model phase, the next generation of Eurocodes will permit to use NLNAs to perform the safety verifications of reinforced concrete structures.

A safety verification may be conducted by means of a local or a global approach. The cross-sectional analysis is considered the best example of local approach. In this case the verification is carried out comparing the design value of the internal action E_d with the related design value of the local resistance R_d . In this case E_d is evaluated by means of linear elastic analysis and the capability of the reinforced concrete structure to redistribute the internal forces is not considered.

On the contrary, looking at the global approach the comparison is made between the design value of the external actions F_d and the design global resistance R_d . In the figure below (Figure 1.1) the differences between the two approaches can be appreciated. This is base of the Global Resistance Format (GRF). The global structural resistance R_{NLNAs} can be evaluated using the NLNAs according to the selected safety format and then the design value R_d is estimated applying two specific factors which consider the aleatory and the epistemic uncertainties respectively γ_R and γ_{Rd} according to the following formula:

$$R_d = \frac{R_{NLNA}(f_{rep}; a_{rep})}{\gamma_R \cdot \gamma_{Rd}} \quad (1)$$

In this work of thesis only the evaluation of the coefficient γ_R is performed as a function of the target reliability imposed. As a mention, according to [7] the evaluation of the coefficient γ_{R_d} can be carried out by means of the comparison between the structural resistance estimated with NLNAs, R_{NLNAs} , and the experimental one, R_{exp} . However, in this work of thesis it will be considered a fixed reasonable value of γ_{R_d} .

One of the disadvantages of the adoption of NLNAs for safety evaluations is related to the significant computational demand, in terms both of time and economical costs. In particular, the entire process is characterized by three main steps:

- i. *Characterization of input variables and model definition:* in this case, it is the first step which includes the phase of research of the scientific articles and the definition of the mechanical and geometrical characteristics of the reinforced concrete beams in order to perform the structural analysis.
- ii. *Structural analysis:* Using the fem software ATENA 2D, presented in the following, it is possible to evaluate the structural response of the structural element through a structural analysis.
- iii. *Post-processing phase and results:* In this case, the analyst has to be able to discern the real failure mode from the numerical one. In general, the achieved material strain in concomitance of the global failure mode is representative of the structural resistance. It is necessary to consider that NLNAs results can be significantly sensitive by the values set for materials properties. For this aim, if it is necessary, the value of R_d should be reduced applying an additional factor of 1.15.

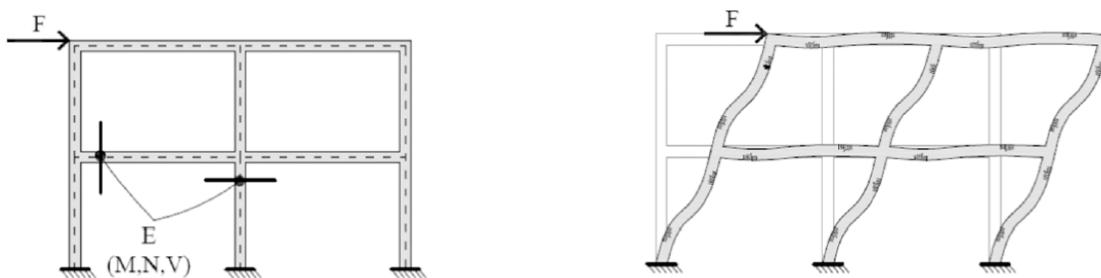


Figure 1.1: Comparison between local structural analysis and global structural analysis [8]

Considering these precautions and the time demand previously discussed, the NLNAs use for the design and assessment of reinforced concrete structures requires a lot of skills for the analyst. In this context, it is important to define a simplified procedure in order to incentivize the utilization of this method.

With this idea, the aim of this work of thesis is to define a simplified methodology within the Global Resistance Method (GRM) following a strain-based approach for assessing the value of the global structural resistance R_d .

The same approach has been studied by [7] focusing on the non-slender structures. This thesis expands the strain-based method from the non-slender structures to the structures characterized by a beam behaviour.

As first thing, an experimental benchmark consisting of 16 reinforced concrete beams has been compiled. The experimental values and the material properties have been used to establish NLN models used to perform probabilistic analysis of the global structural resistance to characterize the statistics of the corresponding probabilistic distribution. Then, it has been associated these statistical parameters with the peak strain occurred in the primary reinforcement. As also introduced previously, this latter value represents an indicator of the ultimate limit state condition to assess the global resistance of the structure. The value of the structural resistance takes into account the mean properties of the structures. This correlation permits to evaluate the structural resistance as a function of the peak strain observed in the primary reinforcement. In this way, the statistical parameters can be directly considered to determine the design value of the structural resistance. It is important to specify that the predictive equations are useful to evaluate the factor γ_R as a function of the CoV (Coefficient of Variation) $V_{R,m}$, which can be used to calculate the global structural resistance R_d .

In the following chapters, the different types of safety formats will be explained focusing on the Global Resistance Method (GRM). It will also present a proper explanation of the strain-based methodology, which is the purpose of this thesis, correlated to the main steps of the probabilistic analysis.

2 Global Resistance Format (GRF)

As it has been presented previously, to design or verify a structure considering the entire structural system it is necessary to use a global approach according to the GRF proposed by [11]. The global structural resistance R_d represents the ultimate global response to compare with the design value of the actions F_d applied on the structure. According to the GRF, the limit state condition can be formulated with the following equation:

$$F_d \leq R_d$$

As it has been affirmed, the term R_d represents the global structural resistance and it can be evaluated using the following formula:

$$R_d = \frac{R_{NLNA}(f_{rep}; a_{rep})}{\gamma_R \cdot \gamma_{Rd}} \quad (1)$$

In the Eq.(1), R_{NLNA} represents the global resistance estimated using NLNAs through the fem software. R_{NLNA} is a function of two terms: f_{rep} and a_{rep} , useful to consider the material and geometric properties of the structural system. The structural resistance R_d is reduced applying two factors: γ_R and γ_{Rd} . The first one, the global resistance safety factor, is related to the aleatory uncertainties (i.e. material and geometric properties), the second one denotes the model uncertainty safety factor and it take into account the epistemic uncertainties in NLNAs. As it has been mentioned before, this latter value is not evaluated in this work of thesis.

Regarding the evaluation of the global resistance safety factor γ_R , it can be determined using the Eq.(2) considering a lognormal probabilistic distribution for the global structural resistance, as explained in the chapter of probabilistic modelling.

$$\gamma_R = \frac{\exp(\alpha_R \cdot \beta_t \cdot V_R)}{\delta_R} \quad (2)$$

In the Eq.(2), the terms β_t and α_R are known quantity because the former represents the target reliability index and the latter is the first order reliability method sensitivity factor, set equal to 0.8 considering as dominant the aleatory uncertainties. Regarding the term δ_R , it is obtained considering two factors according to the Eq.(3):

$$\delta_R = \delta_{R,m} \cdot \delta_{R,g} \quad (3)$$

In particular, $\delta_{R,m}$ is the so-called mean-to-mean deviation as it is useful to quantify the discrepancy between the mean value of the global structural resistance given by a probabilistic analysis $\mu_{R,m}$ and the value of the global resistance obtained performing a NLN analysis considering the mean values of material properties and nominal values for geometric characteristics $R_{NLNA}(f_{rep}; a_{rep})$, according to the Eq.(4). The second factor $\delta_{R,g}$ it can be set equal to 1 because it has not been considered a slender system.

$$\delta_{R,m} = \frac{\mu_{R,m}}{R_{NLNA}(f_{rep}; a_{rep})} \quad (4)$$

Coming back to the Eq.(2), the term V_R represents the Coefficient of Variation (CoV) of the global structural resistance. Assumed as a lognormal distributed function, it takes into account the aleatory uncertainties due to material and geometric properties and it can be evaluated according to the Eq.(5).

$$V_R = \sqrt{V_{R,m}^2 + V_{R,g}^2} \quad (5)$$

In the Eq.(5) $V_{R,m}$ represents the CoV of the global structural resistance due to the aleatory uncertainty of material properties while, $V_{R,g}$ is collected with the aleatory uncertainty of the geometric properties of the system. Now it is necessary to follow two distinct procedures to evaluate these parameters. The value of $V_{R,g}$ can reasonably be set equal to 0.05 for non-slender systems, according to [...]. The value of $V_{R,m}$ has to define according to a specific safety format within the Global Resistance Format (GRF) or explicitly derived through a probabilistic analysis of the global structural resistance. In the next paragraph the different types of safety formats are listed.

2.1 Safety formats

As mentioned above regarding the value of $V_{R,m}$, it has to be evaluated in accordance with a specific safety format within the Global Resistance Format (GRF) or derived from a probabilistic analysis of the global structural resistance, as better described in the following:

1. *Partial Factor Method (PFM)*: using this safety format, the verification is carried out performing 1 NLNA considering the design values as representative one of material and geometrical properties, f_d and a_d . These design values has to be evaluated according to the structural codes and the uncertainties due to the model have to be deleted. In conclusion, for this safety format f_d and a_d are the representative values applied to the Eq.(1), γ_R is set as unit and it has to considerate an appropriate value of γ_{Rd} .
2. *Global Resistance Method (GRM)*: using this safety format, the mean values of material properties f_m and the nominal values of geometrical ones a_n are considered as representative. The value of the global resistance safety factor γ_R it has to be evaluated according to the Eq.s(2)-(5). Regarding the value of γ_{Rd} has to be determined if it is necessary. Finally, the value of the CoV $V_{R,m}$ can be evaluated according to two procedures:
 - *standard Estimation of Coefficient of Variation Method (ECoV)* considering a lognormal distribution for the global structural resistance and performing two NLNAs having as representative values of material and geometrical properties mean/nominal (i.e. f_m and a_n) in the first analysis and characteristics/nominal (i.e. f_k and a_n) in the second one.
 - *Probabilistic evaluation of Coefficient of Variation* with the probabilistic analysis of the global structural resistance evaluating $V_{R,m}$ considering the aleatory uncertainties relating to material properties. This is the procedure which has been used in this work of thesis to estimate the CoV useful to evaluate the global resistance safety factor γ_R .

3. *Probabilistic method (PM)*: using this safety format, they have to be considered both the aleatory and epistemic uncertainties as random variables and the design value of global resistance R_d is directly derived as a function of the target reliability level.

2.2 Strain-based methodology

The aim of this subsection is to explain the strain-based methodology from two different point of view: from the point of view of the analyst and from the point of view of the designer, who needs to design or verify a reinforced concrete structure.

The function of the analyst is to define a proper equation which correlates the structural response of the reinforced concrete structure, in terms maximum strain corresponding to the failure condition $\varepsilon_{s,max}$, with the global resistance safety factor γ_R . Defined the $\varepsilon_{s,max} - \gamma_R$ law which assign a specific value of γ_R as a function of $\varepsilon_{s,max}$, the designer can utilize it for the evaluation of the global structural resistance using the Eq.(1).

The procedure which has to be followed by the analyst is presented in the Figure 2.1. For a better comprehension the entire procedure has been divided into the main steps. As first step, an experimental benchmark of 16 reinforced concrete beams, subjected to flexural collapse, is organised considering a various range of different material properties and reinforcement steel arrangement. This precaution permit to consider a comprehensive methodology to assess the global structural resistance. After that, it has been necessary to idealize the 16 reinforced concrete beams creating a NLN model for each structure with the aim to minimize the related model uncertainties. These models have been used to conduct a set of probabilistic analysis of the global structural resistance. The probabilistic analyses have been carried out by means of the Latin Hypercube Sampling (LHS) method. The latter uses 30 samples to approximate the random response of each one of the 16 reinforced concrete beams. In this case it has been considered one value for the Coefficient of Variation of the concrete V_c equal to 0.15. To conduct all the probabilistic analyses, a total of 480 NLNAs have been performed. This procedure permit to estimate the probability distribution of the global structural resistance, considering

for each structure the mean value $\mu_{R,m}$ and the CoV $V_{R,m}$. Finally, it is possible to correlate statistical parameters obtained by the probabilistic analyses with the peak strain $\epsilon_{s,max}$ occurred in the primary reinforcement in concomitance of the failure step. This latter value is carried out by performing a single NLNA considering the mean values f_m of the material properties and the nominal values a_n for the geometrical ones. In this way, the analyst defines an equation which correlate the structural response of the reinforced concrete structure with the global resistance safety factor.

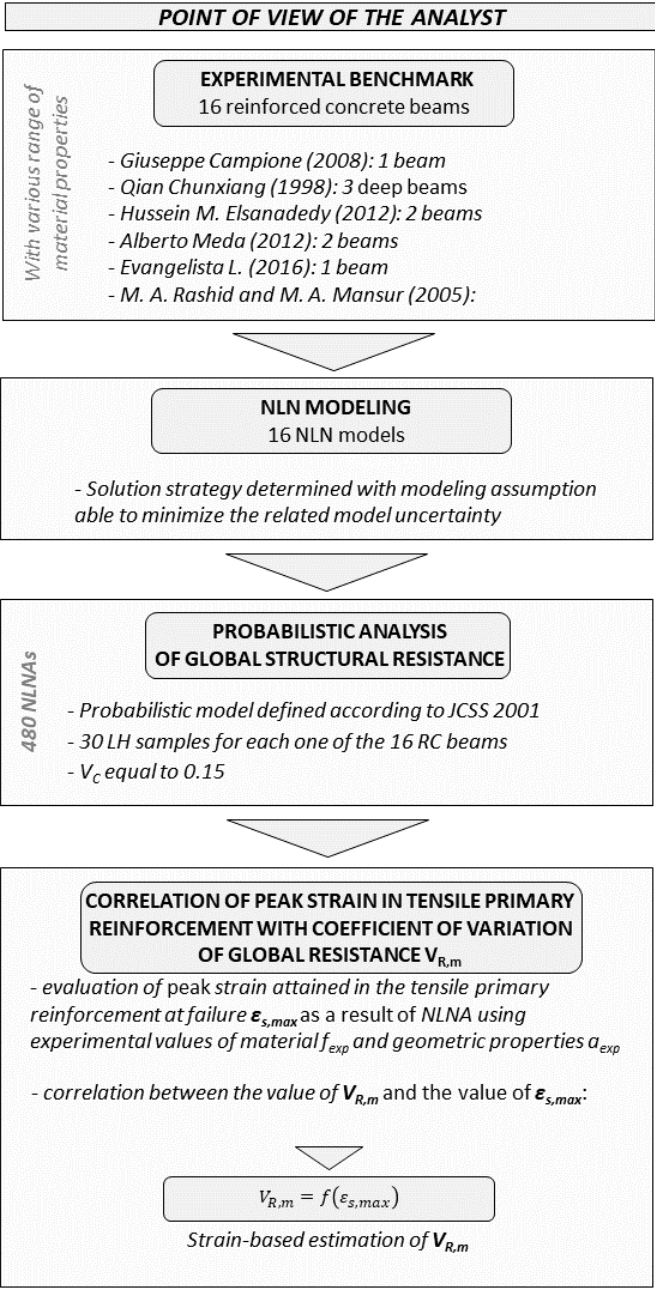


Figure 2.1: Strain-based methodology from the point of view of the analyst

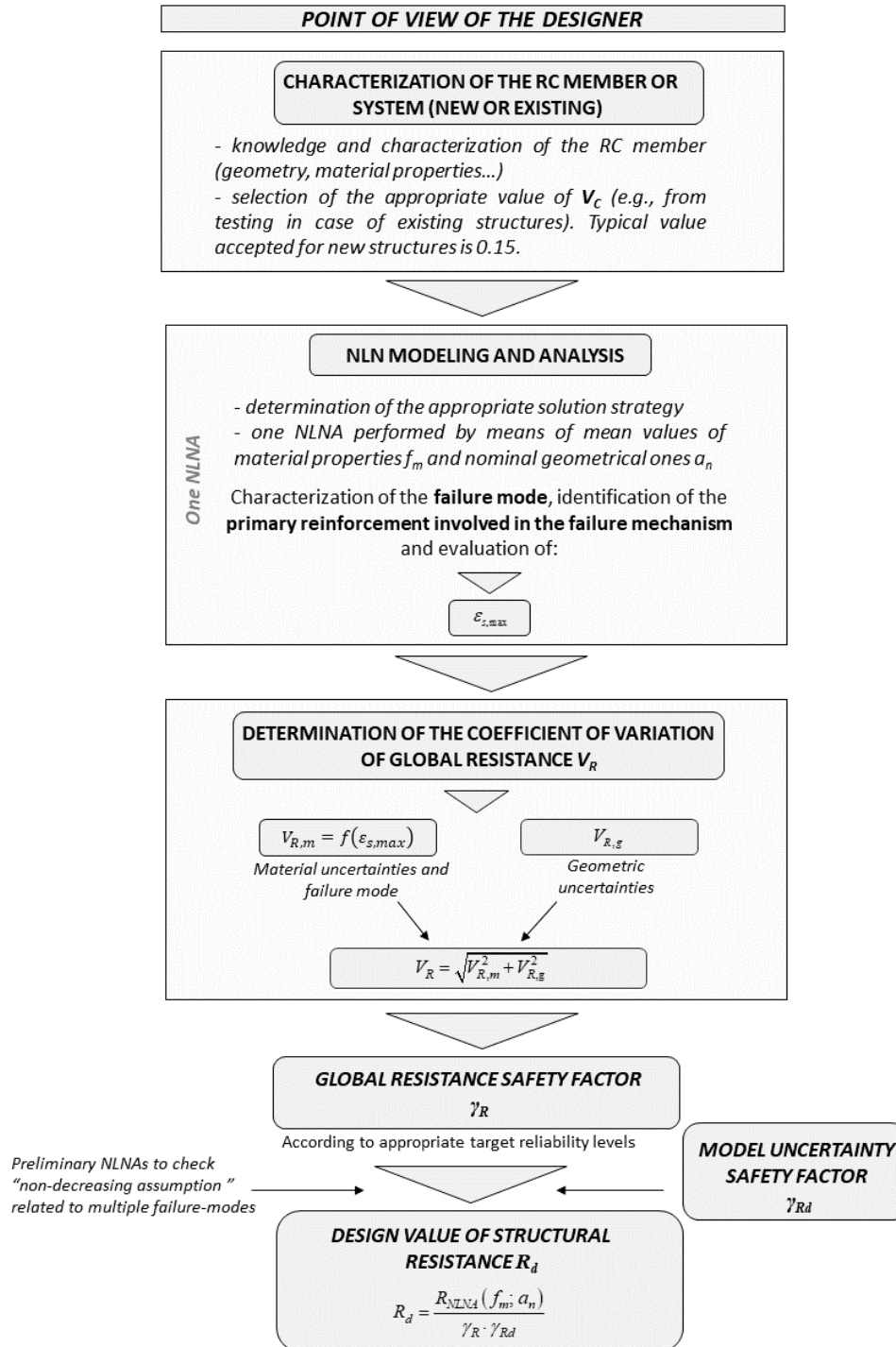


Figure 2.2: Strain-based methodology from the point of view of the designer

The strain-based methodology analysed from the point of view of the designer clarifies the utility of this simplified procedure to design and assess a reinforced concrete structure. Looking at the Figure 2.2, the first step for the designer is to characterize the reinforced concrete member or system in terms of geometry and material properties. Using these parameters, it has to perform only one NLNA and it has to save the value of $\varepsilon_{s,max}$, associated with the failure step

of the primary reinforcement. Knowing this latter parameter and using the proper equation given by the analyst, it is possible to evaluate the CoV $V_{R,m}$ and then the value of the V_R considering a set $V_{R,g}$. After that it is possible to calculate the global resistance safety factor γ_R , according to the target reliability levels. Finally, setting a proper value of γ_{Rd} , it is possible to evaluate the global structural resistance R_d for the structural verifications.

3 Experimental benchmark

First, it has been necessary to choose 16 reinforced concrete beams as case studies characterized by a certain distribution of geometrical and mechanical properties in terms of concrete and reinforcement. This operation permits to consider a various ranging of possible structures.

These experimental values reported into the articles for each specimen will be compared with the analytic ones in the following paragraphs.

3.1 Typology of tests

In this Thesis they have been considered two types of tests:

1. Three-point bending test.
2. Four-point bending test.

In the three-point bending test the beam is considered simply supported and it is loaded with a concentrated force in the middle of the top surface of the specimen (Figure 2.1). It can also be considered a distributed force when there is a steel plate between the concrete face and the loading pin. The same considerations are available for the supporting pins.

The only difference between the two types of tests consists of the number the loading pins. In the case of four-point bending test there are two loading pins placed at a certain distance from each other.

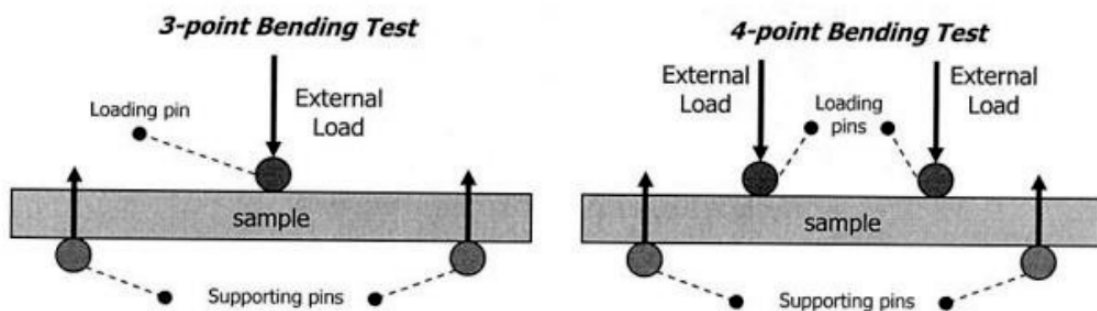


Figure 3.1: Three-point bending test and four-point bending test

The aim of the test is to determine the yielding and the ultimate characteristic of the beam in terms of displacement and load.

3.2 Database

In this paragraph, the experimental values regarding the flexural behaviour of a certain number of reinforced concrete beams are explained. In the following table the bibliography is grouped.

N°	Specimen	Authors
1	5.0.1	Giuseppe Campione
2	CF	
3	CS	Qian Chunxiang
4	CT	
5	BF-1 (1)	Hussein M. Elsanadedy
6	BF-1 (2)	
7	2 ϕ 16-B-PC	Alberto Meda
8	4 ϕ 16-B-PC	
9	RC-1	Evangelista L.
10	A211	
11	B312	
12	B313	M. A. Rashid and M. A. Mansur
13	B321	
14	C211	
15	C311	
16	C411	

Table 3.1: Experimental tests

In the following paragraphs it has been considered each case study and the relative selected specimens. According to the Table 3.1, six papers from the scientific literature are presented.

The main information searched for each beam regard material properties of concrete and reinforcement (i.e. f_c for the first and f_y and f_u for the latter), the geometrical characteristics (i.e. dimensions of the sample and amount of reinforcement), the yielding and ultimate characteristics in terms of load and displacement.

3.2.1 Giuseppe Campione [1]

Consulting this article, a first beam has been selected. In this study a certain number of reinforced concrete beams characterized by different values of concrete cover are presented. It has been chosen the first sample with 5 mm of concrete cover, without steel fibres named for this work of thesis as 5.0.1.

In the following the geometry and the steel reinforcement of the 5.0.1 are presented (Figure 3.2).

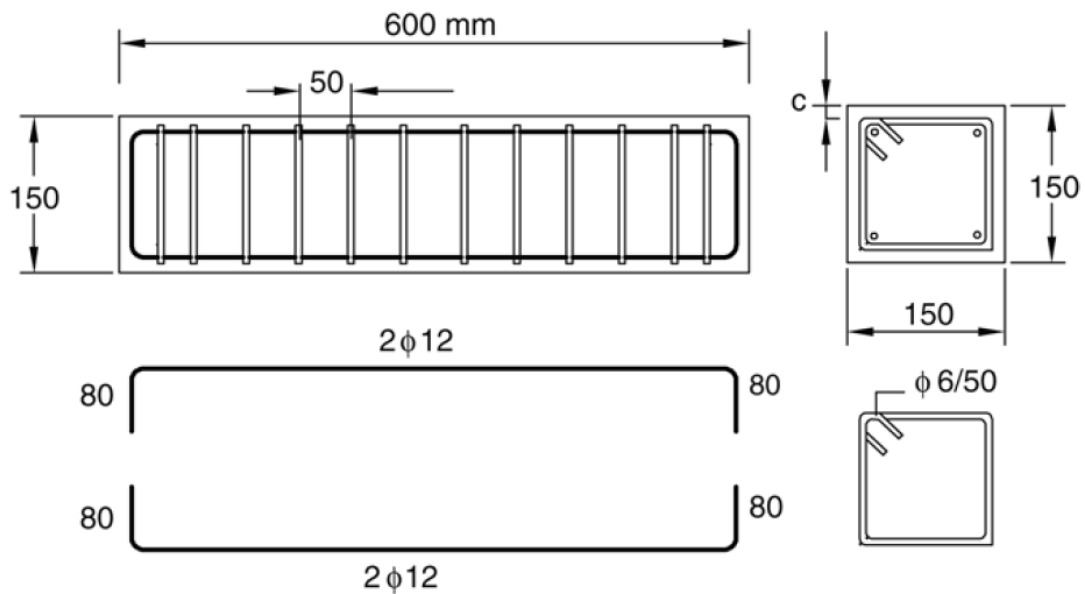


Figure 3.2: Geometry and steel arrangement of 5.0.1

The main information in terms of material properties for the concrete and the steel reinforcement are reported in the table below.

Material properties			
Specimen	Compressive strength	Yielding strength	Ultimate strength
	f_c	f_y	f_u
	[N/mm ²]	[N/mm ²]	[N/mm ²]
5.0.1	32.50	467	546

Table 3.2: Material properties of 5.0.1

In the next tables the geometrical reinforcement arrangement is presented with the values of the amount embedded into the cross section.

Longitudinal steel reinforcement

Specimen	A'_s [mm ²]	A_s [mm ²]	d [mm]	ρ [%]
5.0.1	2Φ12	2Φ12	133	1.13

Table 3.3: Longitudinal steel reinforcement of 5.0.1

Shear steel reinforcement

Specimen	A_{sw} [mm ²]	s [mm]	ρ_{sw} [%]
5.0.1	Φ6	50	0.76

Table 3.4: Shear steel reinforcement

Finally, it has been important to consider the yielding and the ultimate characteristics in terms of load and displacement. For this aim the stress-strain curve of the flexural test is useful to estimate these characteristics.

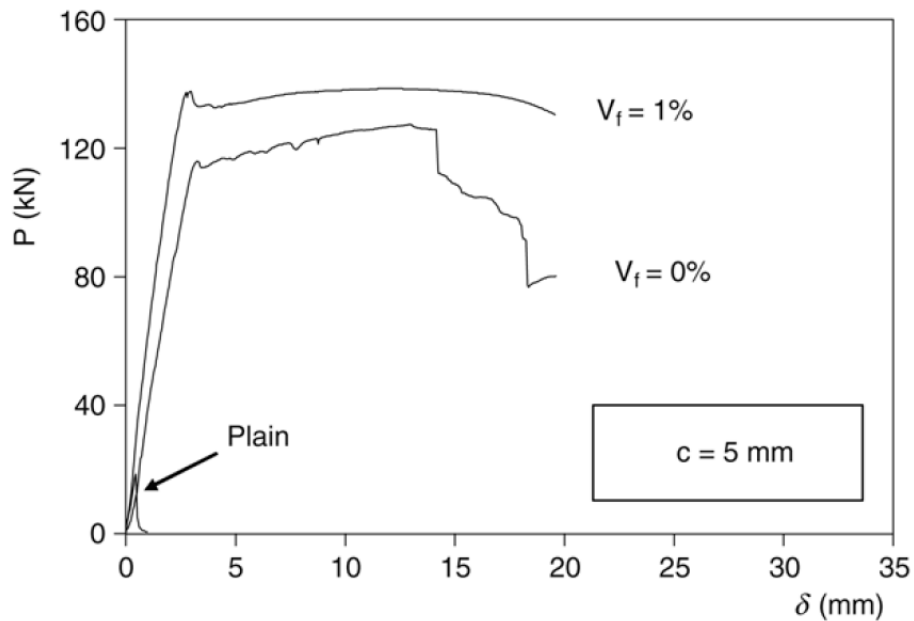


Figure 3.3: Stress-strain curve of 5.0.1

Yielding and ultimate characteristics

Specimen	P_y [kN]	δ_y [mm]	P_u [kN]	δ_u [mm]
5.0.1	118.20	2.94	133	1.13

Table 3.5: Yielding and ultimate characteristics of 5.0.1

3.2.2 Qian Chunxiang [2]

From this study three reinforced concrete beams have been selected and put into the database of the thesis. These beams have been considered as control specimens during the test because they didn't have steel fibres embedded into the concrete matrix. Their names are CF, CS, CT.

In the following the geometry and the steel reinforcement of the CF, CS and CT are presented (Figure 3.4).

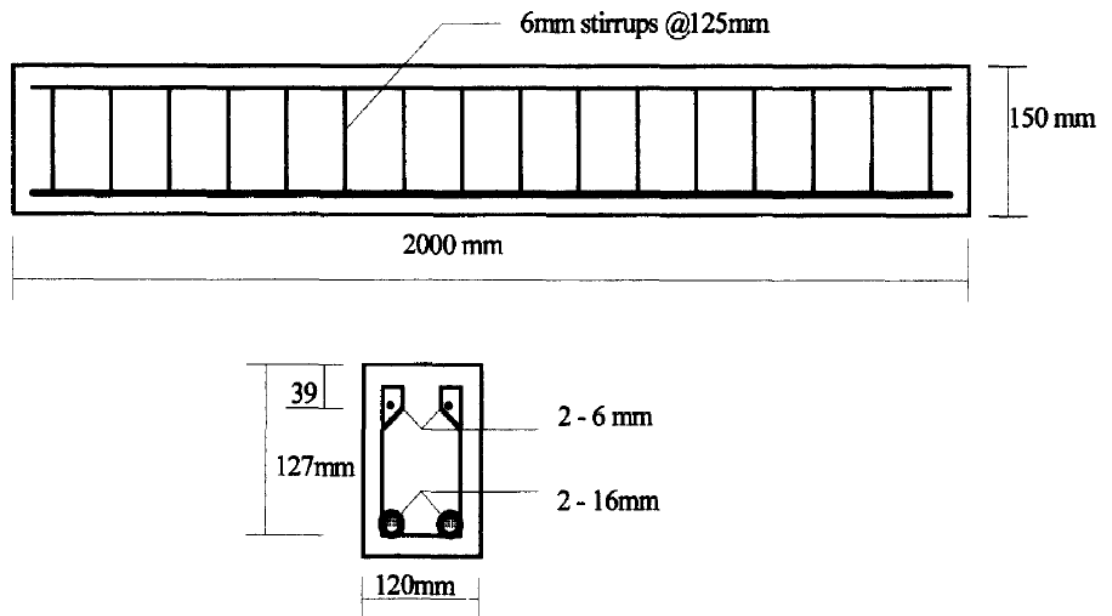


Figure 3.4: Geometry and steel arrangement of CF, CS and CT

The main information in terms of material properties for the concrete and the steel reinforcement are reported in the table below. In this case the f_u of the of steel reinforcement is evaluated applying a coefficient of 1.15 to f_y .

Specimen	Material properties		
	Compressive strength	Yielding strength	Ultimate strength
	f_c	f_y	f_u
	[N/mm ²]	[N/mm ²]	[N/mm ²]
CF	64.80	400	460
CS	68.10	400	460
CT	64.60	400	460

Table 3.6: Material properties of CF, CS and CT

In the next tables the geometrical reinforcement arrangement is presented with the values of the amount embedded into the cross section.

Longitudinal steel reinforcement

Specimen	A'_s [mm ²]	A_s [mm ²]	d [mm]	ρ [%]
CF/CS/CT	2Φ6	2Φ16	127	2.64

Table 3.7: Longitudinal steel reinforcement of CF, CS and CT

Shear steel reinforcement

Specimen	A_{sw} [mm ²]	s [mm]	ρ_{sw} [%]
CF/CS/CT	Φ6	125	0.38

Table 3.8: Shear steel reinforcement of CF, CS and CT

Finally, it has been important to consider the yielding and the ultimate characteristics in terms of load and displacement. For this aim the stress-strain curve of the flexural tests is useful to estimate these characteristics. In particular, it has been considered the B curve in order to evaluate the displacement at the midspan of the beam.

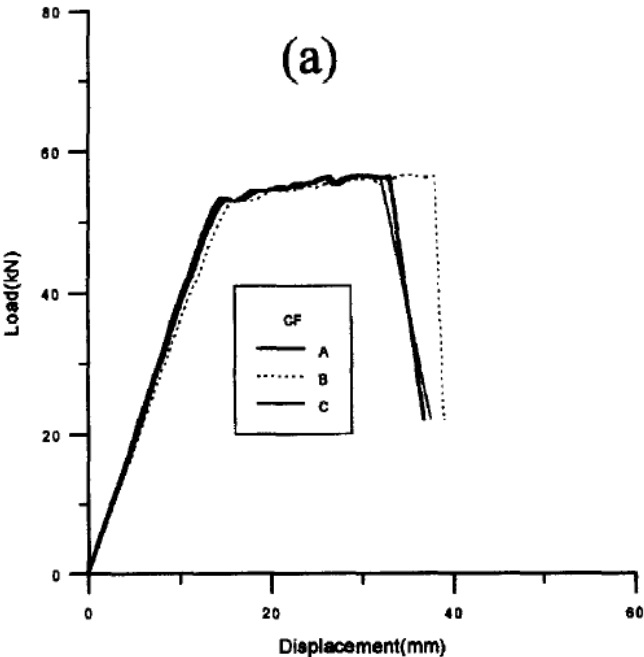


Figure 3.5: Stress-strain curve of CF

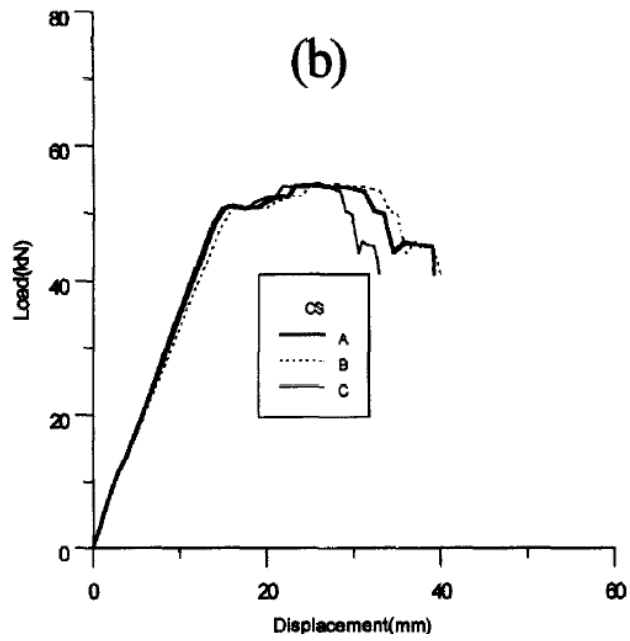


Figure 3.6: Stress-strain curve of CS

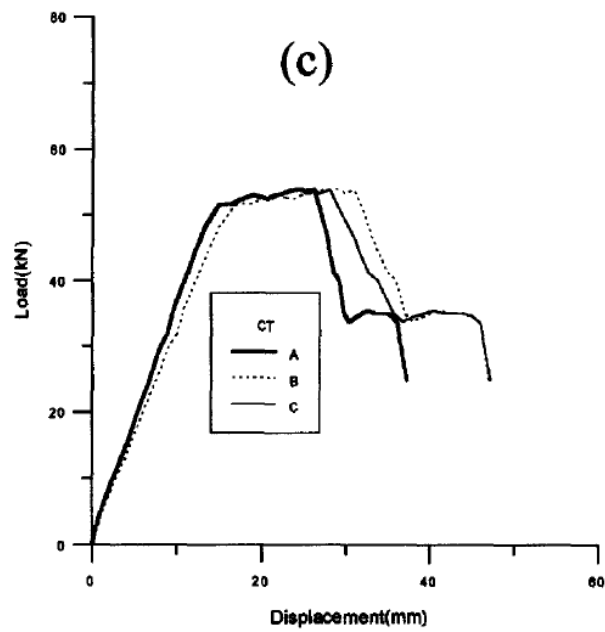


Figure 3.7: Stress-strain curve of CT

Yielding and ultimate characteristics

Specimen	P_y [kN]	δ_y [mm]	P_u [kN]	δ_u [mm]
CF	53	16	56.40	31
CS	50.60	16	54.20	28
CT	51.60	18	53.80	28

Table 3.9: Yielding and ultimate characteristics of CF, CS and CT

3.2.3 Hussein M. Elsanadedy [3]

In this article it has been studied the structural resistance of the reinforced concrete beam strengthened with such a type of steel plates. For this work of thesis two beams without strengthening have been selected and put into the database. Their names are BF-1 (1) and BF-1 (2).

In the following the geometry and the steel reinforcement of the BF-1 (1) and BF-1 (2) are presented (Figure 3.8).

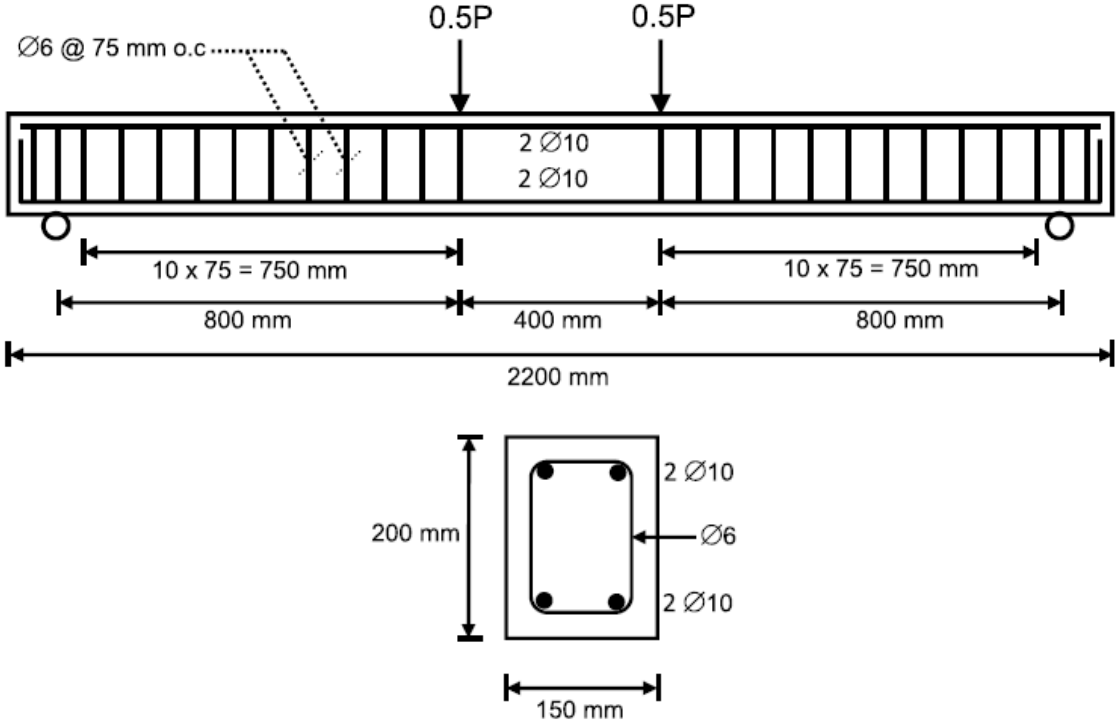


Figure 3.8: Geometry and steel arrangement of BF-1 (1) and BF-1 (2)

The main information in terms of material properties for the concrete and the steel reinforcement are reported in the table below.

Material properties			
Specimen	Compressive strength f_c [N/mm ²]	Yielding strength f_y [N/mm ²]	Ultimate strength f_u [N/mm ²]
BF-1 (1)/BF-1 (2)	20	578	684

Table 3.10: Material properties of BF-1 (1) and BF-1 (2)

In the next tables the geometrical reinforcement arrangement is presented with the values of the amount embedded into the cross section.

Longitudinal steel reinforcement

Specimen	A'_s [mm ²]	A_s [mm ²]	d [mm]	ρ [%]
BF-1 (1)/BF-1 (2)	2 Φ 10	2 Φ 10	175	0.60

Table 3.11: Longitudinal steel reinforcement of BF-1 (1) and BF-1 (2)

Shear steel reinforcement

Specimen	A_{sw} [mm ²]	s [mm]	ρ_{sw} [%]
BF-1 (1)/BF-1 (2)	Φ 6	75	0.51

Table 3.12: Shear steel reinforcement of BF-1 (1) and BF-1 (2)

Finally, it has been considered the stress-strain curve.

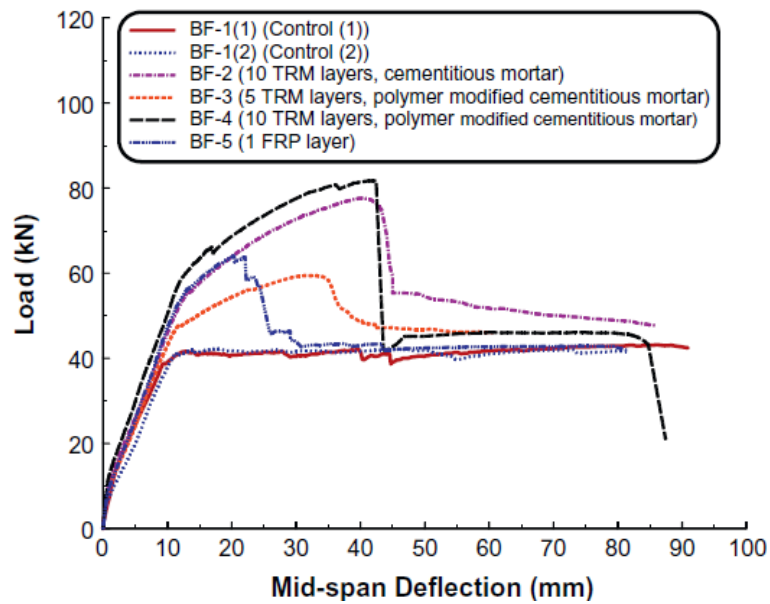


Figure 3.9: Stress-strain curve of BF-1 (1) and BF-1 (2)

Yielding and ultimate characteristics

Specimen	P_y [kN]	δ_y [mm]	P_u [kN]	δ_u [mm]
BF-1 (1)	37.18	8.87	43.22	86.19
BF-1 (2)	34.39	8.85	42.28	81.74

Table 3.13: Yielding and ultimate characteristics of BF-1 (1) and BF-1 (2)

3.2.4 Alberto Meda [4]

In this article it has been studied the structural resistance of the reinforced concrete beam with steel fibres embedded into the concrete matrix. In this case, two beams without steel fibres and characterized by a different ratio of steel reinforcement have been selected and put into the database. Their names are 2φ16-B-PC and 4φ16-B-PC.

In the following the geometry and the steel reinforcement of the 2φ16-B-PC and 4φ16-B-PC are presented (Figure 3.10).

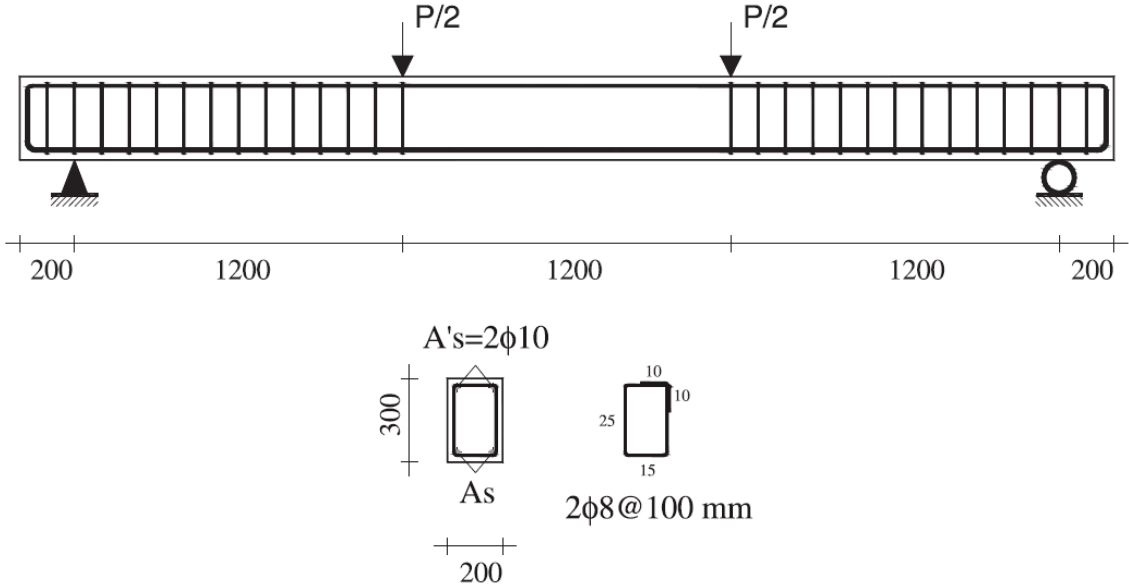


Figure 3.10: Geometry and steel arrangement of 2φ16-B-PC and 4φ16-B-PC

The main information in terms of material properties for the concrete and the steel reinforcement are reported in the table below.

Material properties			
Specimen	Compressive strength	Yielding strength	Ultimate strength
	f_c	f_y	f_u
	[N/mm ²]	[N/mm ²]	[N/mm ²]
2φ16-B-PC/ 4φ16-B-PC	49.70	534	630

Table 3.14: Material properties of 2φ16-B-PC and 4φ16-B-PC

In the next tables the geometrical reinforcement arrangement is presented with the values of the amount embedded into the cross section.

Longitudinal steel reinforcement

Specimen	A'_s [mm ²]	A_s [mm ²]	d [mm]	ρ [%]
2 ϕ 16-B-PC	2 Φ 10	2 Φ 16	260	0.77
4 ϕ 16-B-PC	2 Φ 10	4 Φ 16	260	1.55

Table 3.15: Longitudinal steel reinforcement of 2 ϕ 16-B-PC and 4 ϕ 16-B-PC

Shear steel reinforcement

Specimen	A_{sw} [mm ²]	s [mm]	ρ_{sw} [%]
2 ϕ 16-B-PC	Φ 8	100	0.50
4 ϕ 16-B-PC	Φ 8	100	0.50

Table 3.16: Shear steel reinforcement of 2 ϕ 16-B-PC and 4 ϕ 16-B-PC

Finally, it has been important to consider the yielding and the ultimate characteristics in terms of load and displacement. For this aim the stress-strain curve of the flexural tests is useful to estimate these characteristics.

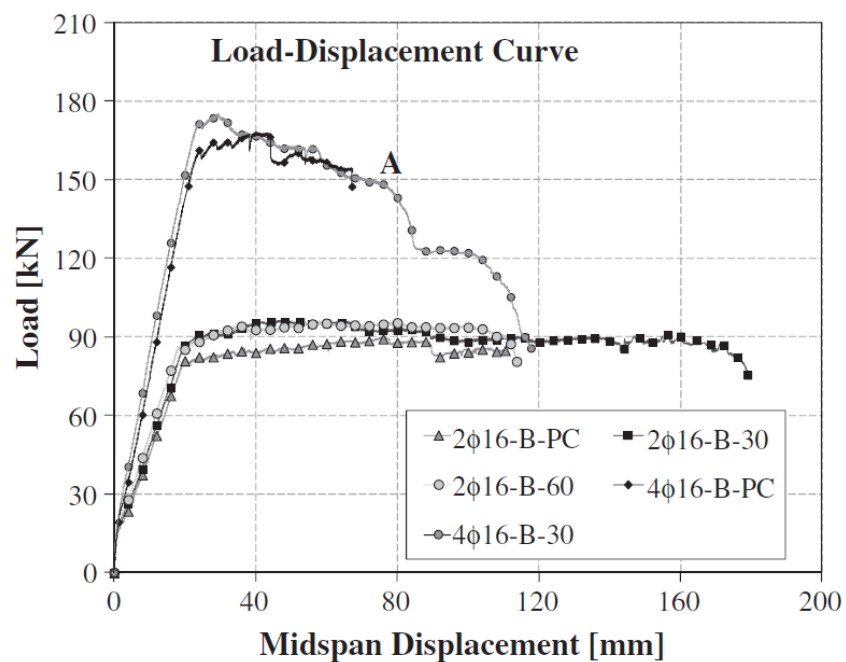


Figure 3.11: Stress-strain curve of 2 ϕ 16-B-PC and 4 ϕ 16-B-PC

Yielding and ultimate characteristics

Specimen	P_y [kN]	δ_y [mm]	P_u [kN]	δ_u [mm]
2 ϕ 16-B-PC	81	21	90	110
4 ϕ 16-B-PC	161	24	168	67

Table 3.17: Yielding and ultimate characteristics of 2 ϕ 16-B-PC and 4 ϕ 16-B-PC

3.2.5 Evangelista L. [5]

In this article it has been studied the structural resistance of the reinforced concrete beam with recycled aggregates embedded into the concrete matrix. In this context, it has been selected one control beam and it has been put into the database. Its name is RC-1.

In the following the geometry and the steel reinforcement of the RC-1 are presented (Figure 3.12).

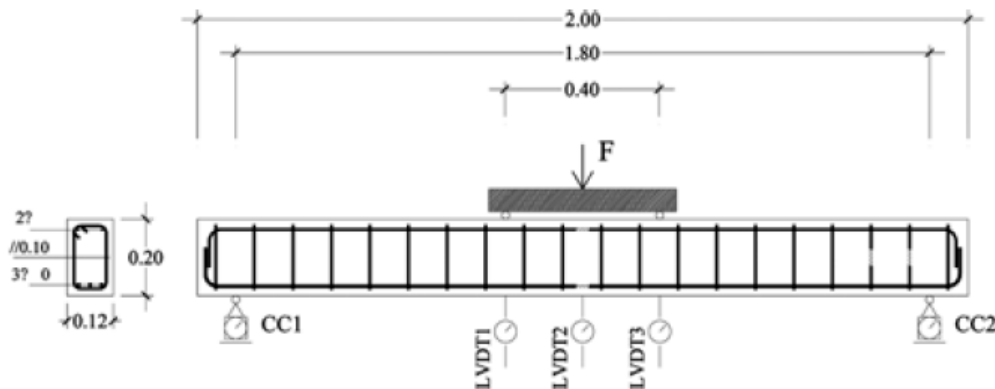


Figure 3.12: Geometry and reinforcement arrangement of RC-1

The main information in terms of material properties for the concrete and the steel reinforcement are reported in the table below.

Material properties			
Specimen	Compressive strength f_c [N/mm ²]	Yielding strength f_y [N/mm ²]	Ultimate strength f_u [N/mm ²]
RC-1	33.56	525	670

Table 3.18: Material properties of RC-1

In the next tables the geometrical reinforcement arrangement is presented with the values of the amount embedded into the cross section.

Longitudinal steel reinforcement

Specimen	A'_s [mm ²]	A_s [mm ²]	d [mm]	ρ [%]
RC-1	2Φ6	3Φ10	185	1.06

Table 3.19: Longitudinal steel reinforcement of RC-1

Shear steel reinforcement

Specimen	A_{sw} [mm ²]	s [mm]	ρ_{sw} [%]
RC-1	Φ6	100	0.48

Table 3.20: Shear reinforcement of RC-1

Finally, it has been important to consider the yielding and the ultimate characteristics in terms of load and displacement. For this aim the stress-strain curve of the flexural tests is useful to estimate these characteristics.

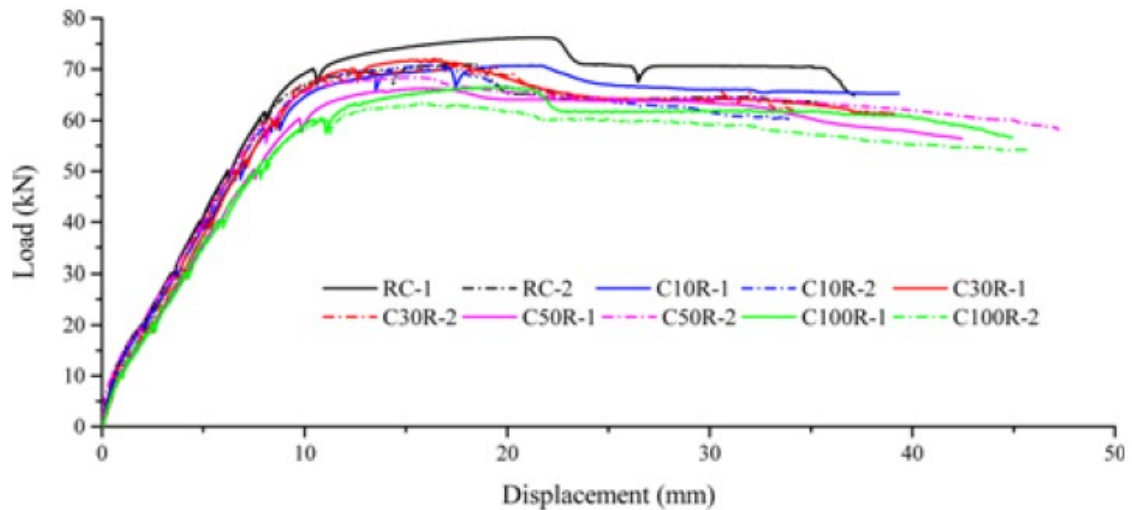


Figure 3.13: Stress-strain curve of RC-1

Yielding and ultimate characteristics

Specimen	P_y [kN]	δ_y [mm]	P_u [kN]	δ_u [mm]
RC-1	69.83	9.72	65.61	37.12

Table 3.21: Yielding and ultimate characteristics of RC-1

3.2.6 M. A. Rashid and M. A. Mansur [6]

In this article a group of reinforced concrete beams is tested in flexure in order to determine the structural resistance of the elements. The benchmark is quite various both in terms of f_c and amount of steel reinforcement embedded into the concrete matrix. From this study seven reinforced concrete beams are selected and used in this work of thesis.

In the following the geometry and the steel reinforcement of the RC-1 are presented (Figure 3.14).

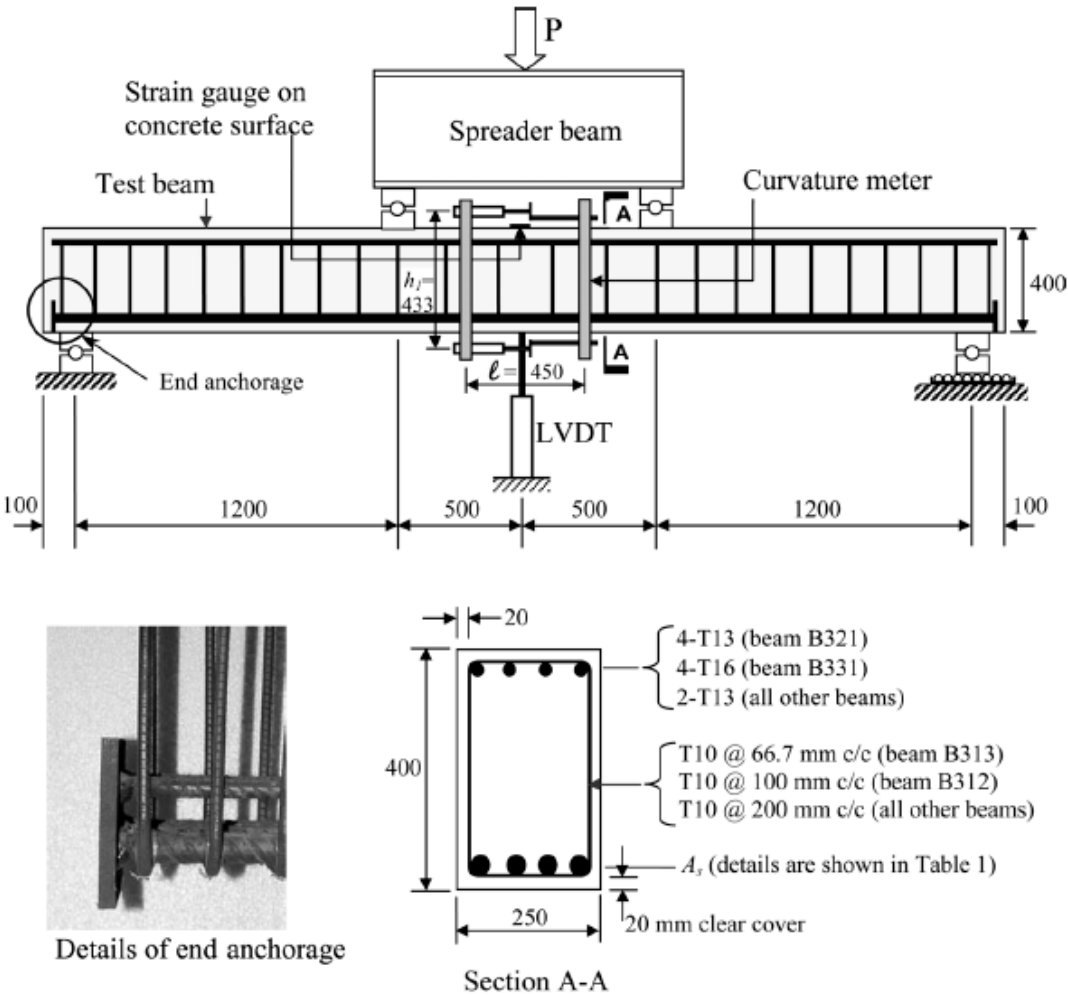


Figure 3.14: Geometry and reinforcement arrangement of A211, B312, B313, B321, C211, C311, C411

The main information in terms of material properties for the concrete and the steel reinforcement are reported in the table below. In this case the f_u of the of steel reinforcement is evaluated applying a coefficient of 1.15 to f_y .

Material properties

Specimen	Compressive	Yielding	Ultimate
	strength	strength	strength
	f_c	f_y	f_u
	[N/mm ²]	[N/mm ²]	[N/mm ²]
A211	42.80	460	529
B312	72.80	460	529
B313	72.80	460	529
B321	77	460	529
C211	85.60	460	529
C311	88.10	460	529
C411	85.60	460	529

Table 3.22: Material properties of A211, B312, B313, B321, C211, C311, C411

In the next tables the geometrical reinforcement arrangement is presented with the values of the amount embedded into the cross section.

Longitudinal steel reinforcement

Specimen	A'_s	A_s	d	ρ
	[mm ²]	[mm ²]	[mm]	[%]
A211	2 ϕ 13	4 ϕ 25	380	2.07
B312	2 ϕ 13	6 ϕ 25	380	3.10
B313	2 ϕ 13	6 ϕ 25	380	3.10
B321	4 ϕ 13	6 ϕ 25	380	3.10
C211	2 ϕ 13	4 ϕ 25 + 2 ϕ 16	380	2.49
C311	2 ϕ 13	4 ϕ 25 + 4 ϕ 16	380	2.91
C411	2 ϕ 13	6 ϕ 25 + 2 ϕ 20	380	3.76

Table 3.23: Longitudinal steel reinforcement of A211, B312, B313, B321, C211, C311, C411

Shear steel reinforcement

Specimen	A_{sw} [mm ²]	s [mm]	ρ_{sw} [%]
A211	$\phi 10$	200	0.31
B312	$\phi 10$	100	0.63
B313	$\phi 10$	66.7	0.94
B321	$\phi 10$	200	0.31
C211	$\phi 10$	200	0.31
C311	$\phi 10$	200	0.31
C411	$\phi 10$	200	0.31

Table 3.24: Shear steel reinforcement of A211, B312, B313, B321, C211, C311, C411

Finally, it has been important to consider the yielding and the ultimate characteristics in terms of load and displacement. For this aim the stress-strain curve of the flexural tests is useful to estimate these characteristics.

Yielding and ultimate characteristics

Specimen	P_y [kN]	δ_y [mm]	P_u [kN]	δ_u [mm]
A211	440.48	15.5	461.3	37
B312	560.36	16.9	730.22	24.4
B313	580.26	16.1	742.94	27
B321	551.16	15.5	765.06	34.4
C211	560.94	18.2	650.42	44.1
C311	605.46	18	730.12	28.3
C411	722.56	19.3	901.4	29

Table 3.25: Yielding and ultimate characteristics of A211, B312, B313, B321, C211, C311, C411

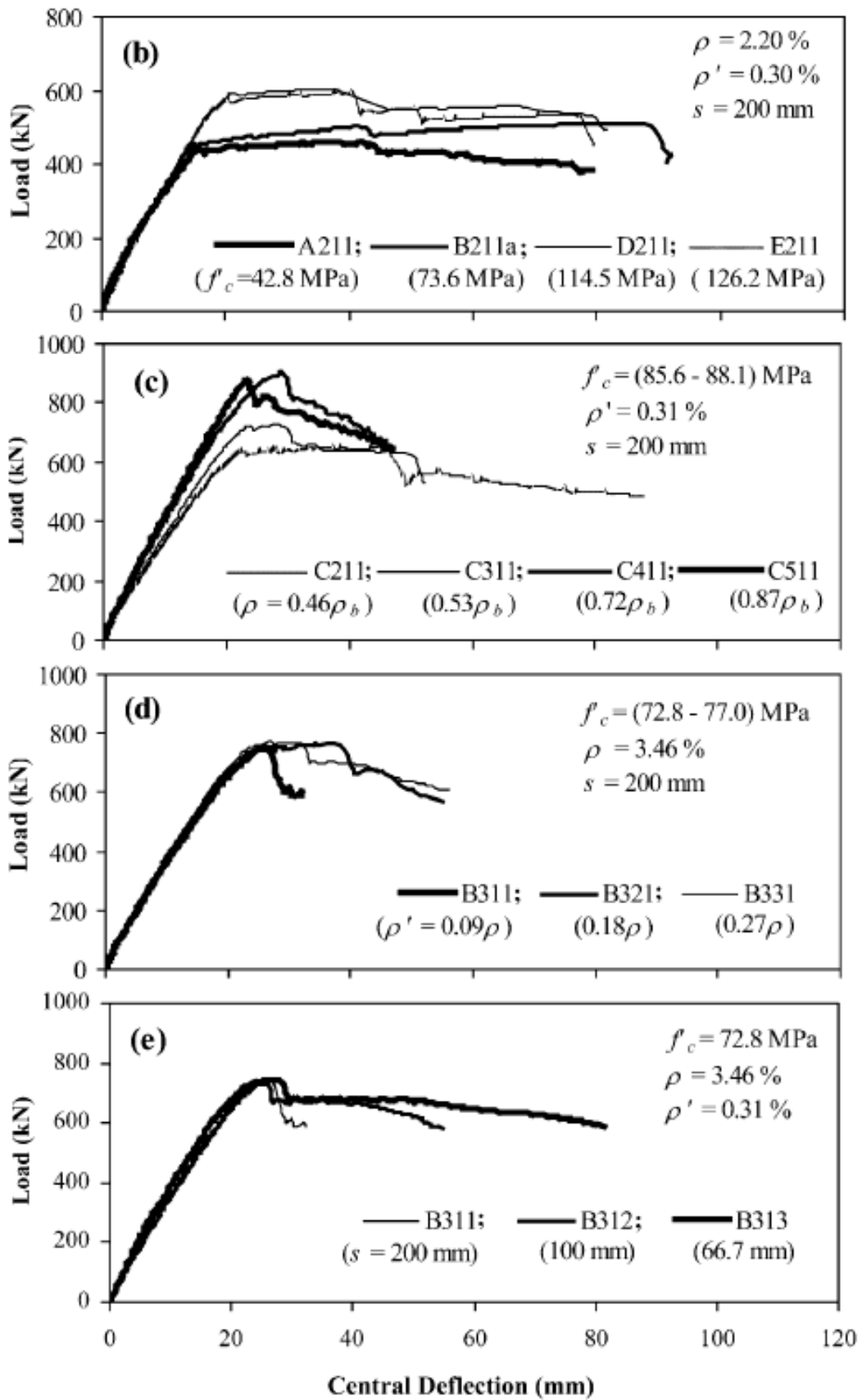


Figure 3.15: Stress-strain curve of A211, B312, B313, B321, C211, C311, C411

4 FEM modelling

This chapter is composed by two main paragraphs. In the first one, it has been presented the FEM software used to the set the 16 NLN models, one for each structure. In the second one the modelling assumptions and the comparison between experimental and FEM values is presented.

4.1 ATENA 2D: FEM software

According to the official site (www.cervenka.cz), ATENA is a user-friendly non-linear analysis, and it is specially designed for concrete. The name stands for Advanced Tool for Engineering Nonlinear Analysis. The software is characterized by a certain number of key features:

- Simulate the real behaviour of reinforced concrete structures modelling discrete bars or smeared reinforcement (Figure 4.1).
- Real-time display of results even during the non-linear analysis and visualization of crack propagation (Figure 4.1).
- It is possible to consider the moisture and thermal load.
- It is possible to model high temperature due to the presence of fire.
- A 3D environmental is available to model a structure.

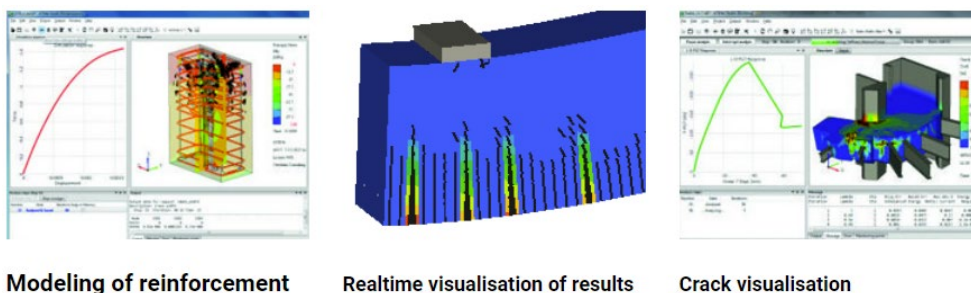


Figure 4.1: Key features of ATENA 2D (www.cervenka.cz)

Another software's strength is the possibility to create new models from the reading of CCT files. These files can be read written by text creator software, and it can be imported into ATENA 2D. A CCT file contains all the necessary information to run an analysis. This option will be used during the probabilistic modelling when it will be necessary to create 30 models for each beam.

4.1.1 Pre processing

The pre-processing phase is useful to define all the initial parameters of the model. It is structured as follows:

1. General data
2. Materials
3. Topology
4. Load and supports
5. Run

4.1.1.1 General data

As it can be shown from the figure below, ATENA 2D is characterized by a user-friendly graphical interface (Figure 4.2). Focusing on the higher part of the interface there are some icons placed horizontally with different functions. Beginning at the first icon they permit to save a model, create a mesh, perform the analysis, zoom in or out and commands useful to select nodes or lines.

Finally, selecting the general data command from the tree menu situated on the left side of the interface, it is possible to insert a description or a note. It is also important to mention that the general data groups all the numbering information (i.e. number of nodes, lines, macro-elements and so on).

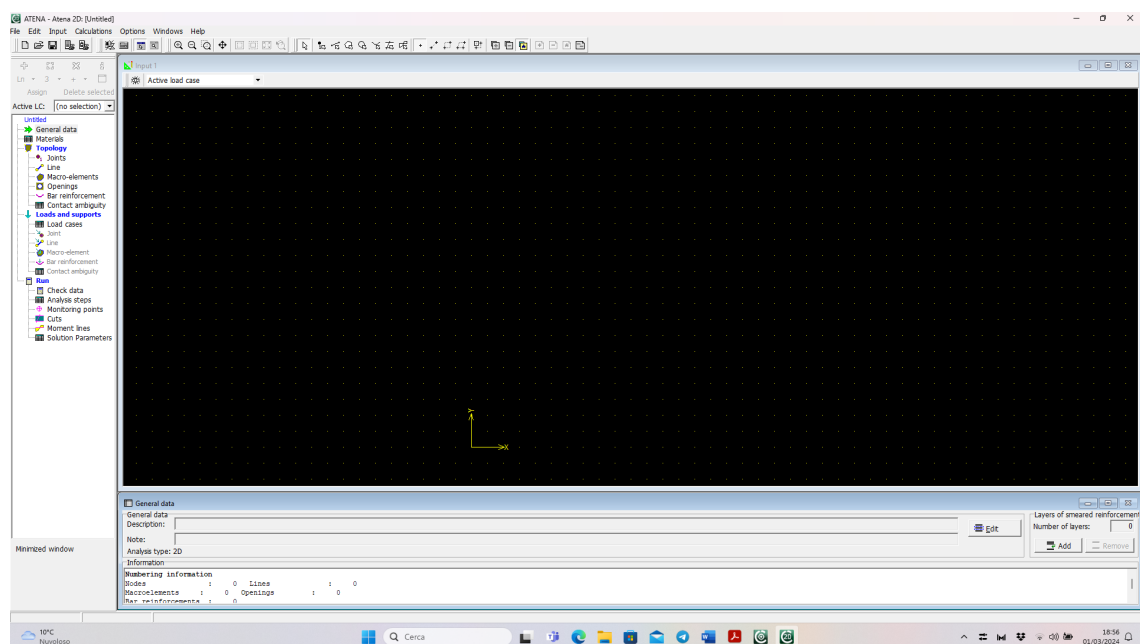


Figure 4.2: Pre processing graphical interface

4.1.1.2 Materials

ATENA 2D proposes several possible models to define the behaviour of a material. For this work of thesis, they have been used three types of materials: *SBeta Material* for the concrete, *Reinforcement* for the rebars and *Plane stress elastic isotropic* for the infinitely rigid steel plates.

4.1.1.2.1 SBeta Material

SBeta is the acronym for StahlBETonAnalyse which stands for “analysis of reinforced concrete”. To define properly the concrete behaviour, it is necessary to compile five tabs presented in the following. In general, in addition to the possibility of considering the non-linear behaviour of the concrete there are also some considerations regarding the cracking mode.

Basic

In the Basic tab the main information required regarded the Elastic modulus, the Poisson’s ratio, the Tensile strength and the Compressive strength. As it can be show in the figure below, these information permit to define the Stress-strain Law and the Biaxial failure law.

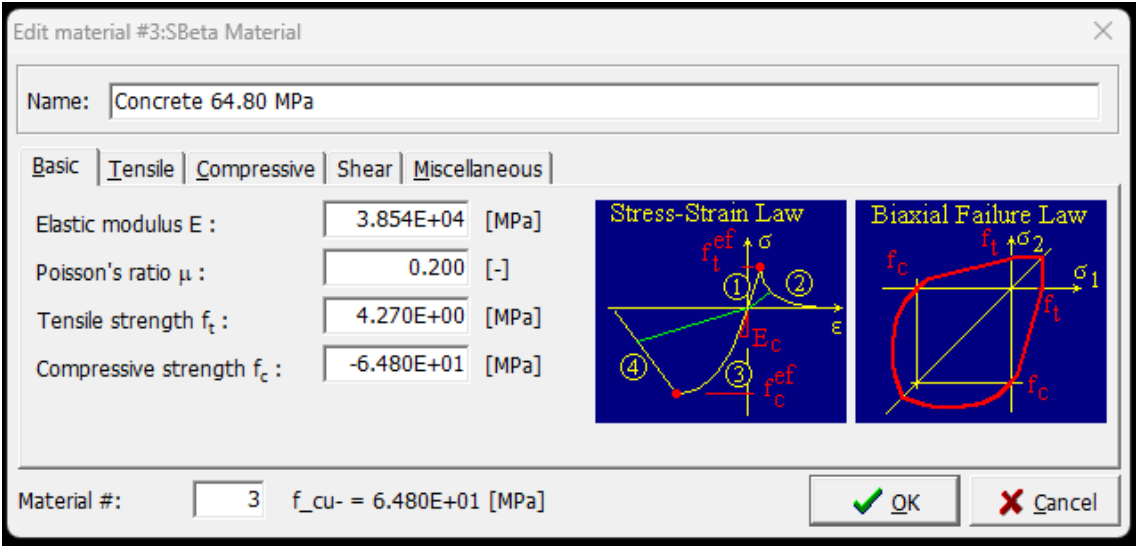


Figure 4.3: Basic tab for SBeta Material

Tensile

In the Tensile tab it is possible to choose the type of tension softening and the Crack model, as it can be appreciated looking the following figure.

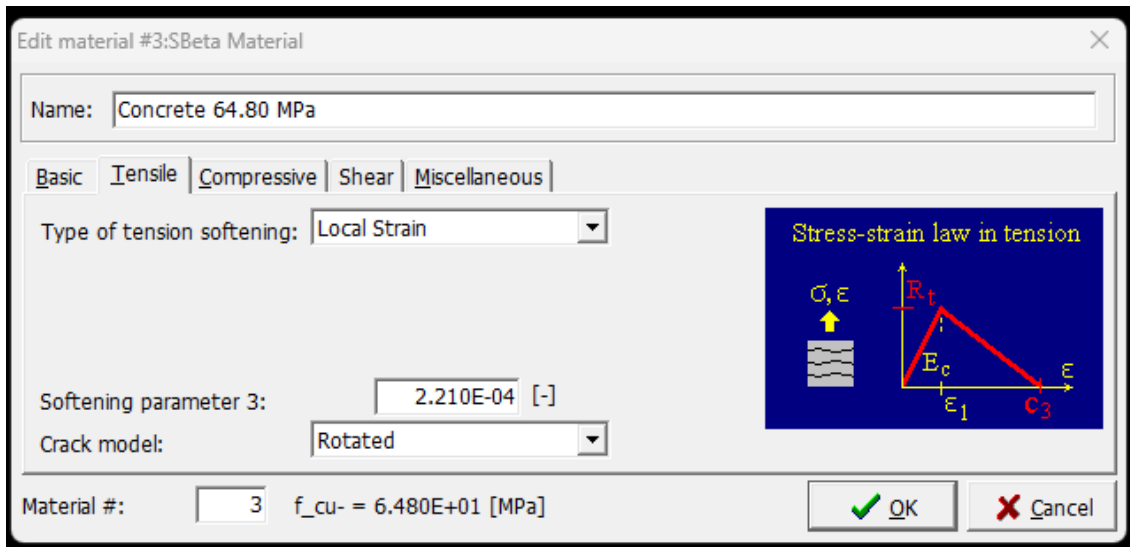


Figure 4.4: Tensile tab - Type of tension softening for SBeta Material

Choosing the *Local Strain* model, the second branch of the stress-strain law is governed by the value C_3 , which represent the end strain at the complete release of stress. This ultimate value can vary between 2 and 15 times of the strain corresponding to the axial tensile strength of concrete.

Regarding the crack model, there are two types: *fixed* crack model or *rotated* crack model. In the first case, the crack direction remains aligned by the principal stress direction during further loading. In the second case, the direction of the crack can rotate if the direction of the principal strain axes changes as it can be show below (Figure 4.5).

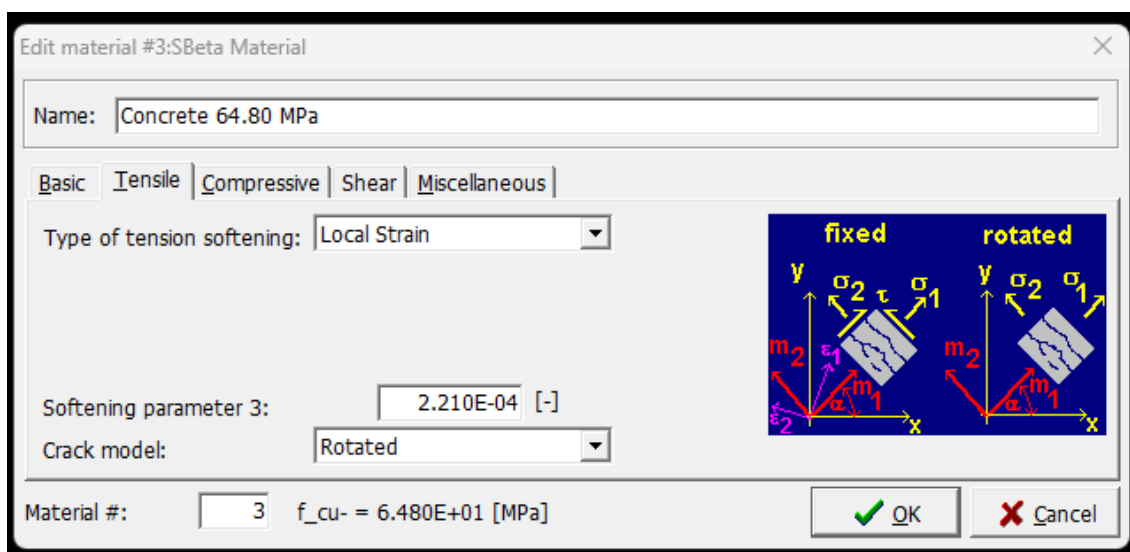


Figure 4.5: Tensile tab - Crack model for SBeta Material

Compressive

In this tab it is necessary to insert the value of strain at compressive strength in the uniaxial compressive test and the RCS parameter set to 0.8. It is also necessary to define the type of compression softening. There are two different types of compression softening: *Softening modulus* and the *Crush band*.

Choosing the Softening modulus, it has been defined a slope of the softening law with the value of E_d , which is the result of the product between the compression softening parameter c_d and the concrete elastic modulus E_c (Figure 4.6).

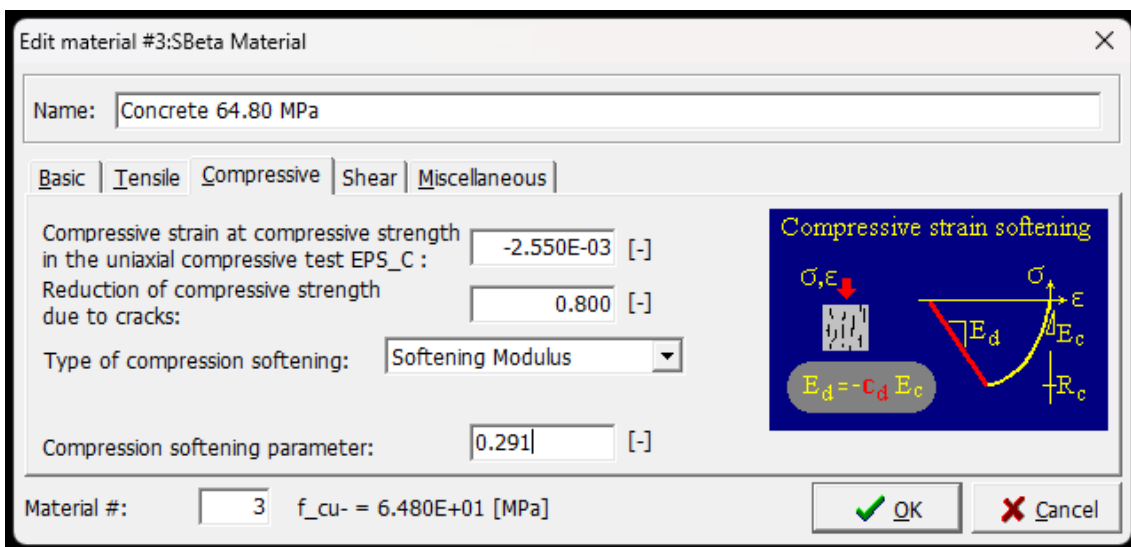


Figure 4.6: Compressive tab for SBeta Material

Shear

In this tab it has been necessary to define the *Shear retention factor* and the *Tension compression interaction*.

For the shear retention factor the choice is between *variable* or *fixed*. Selecting variable, it has been considered a reduction of the shear stiffness after cracking. As it can be show looking the figure below, it has been chosen the variable option (Figure 4.7).

Instead, for the tension compression interaction it is possible to choose among Linear, Hyperbola A and Hyperbola B. In this case it has been selected the linear option (Figure 4.8).

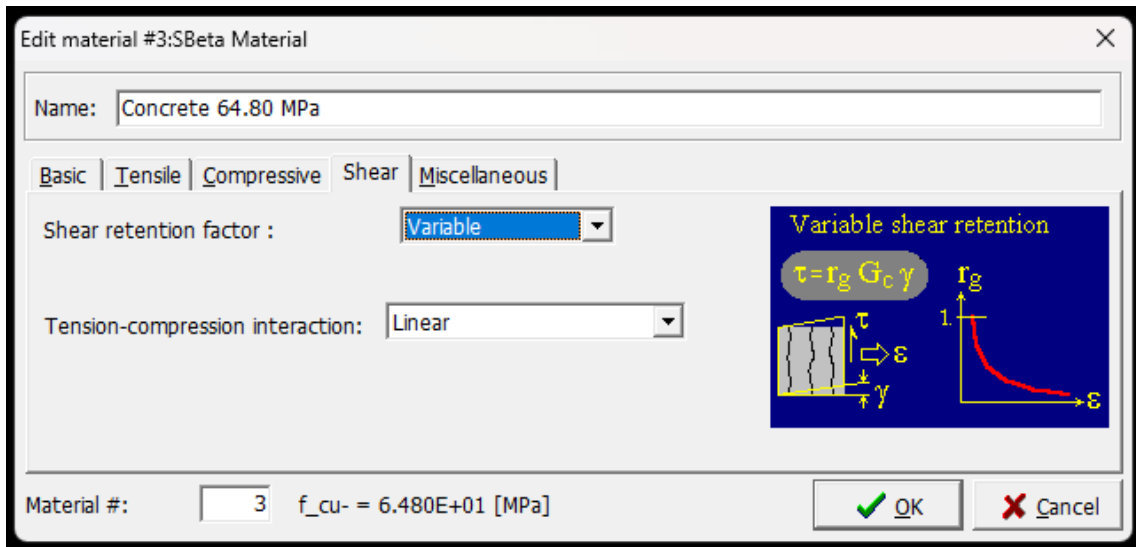


Figure 4.7: Shear tab - retention factor for SBeta Material

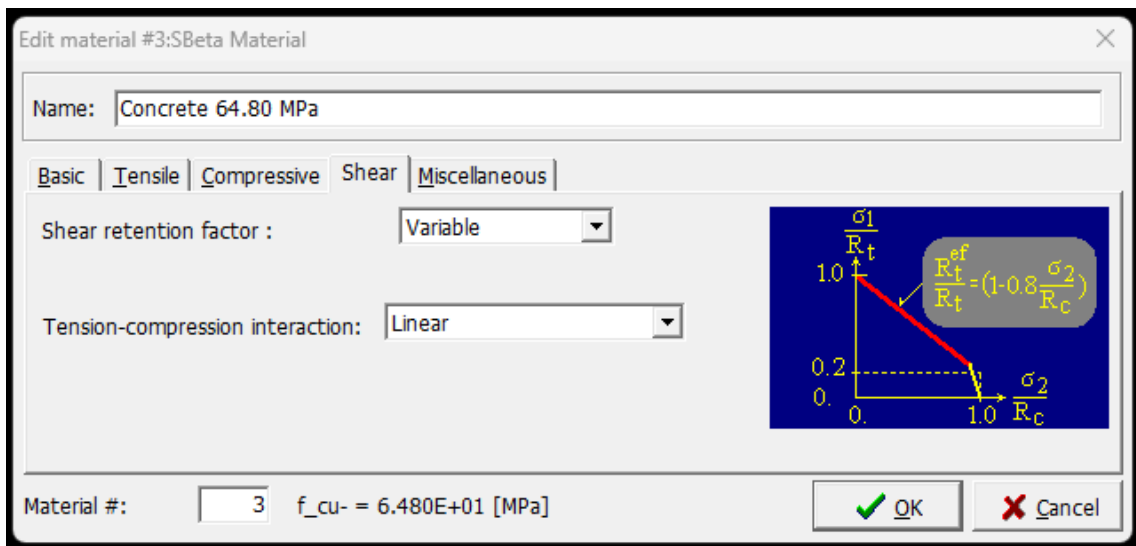


Figure 4.8: Shear tab: tension-compression interaction for SBeta Material

Miscellaneous

In the last tab, they have been defined the *Specific material weight* ρ in MN/m^3 and the *Coefficient of thermal expansion* α in $1/\text{k}$.

In order to take into account also the weight of the rebars embedded into the concrete matrix, it has been selected a specific material weight of $2.50\text{E-}02$ MN/m^3 , as it can be show in the figure below (Figure 4.9).

Regarding the coefficient of thermal expansion, it has been maintained the values proposed by the software.

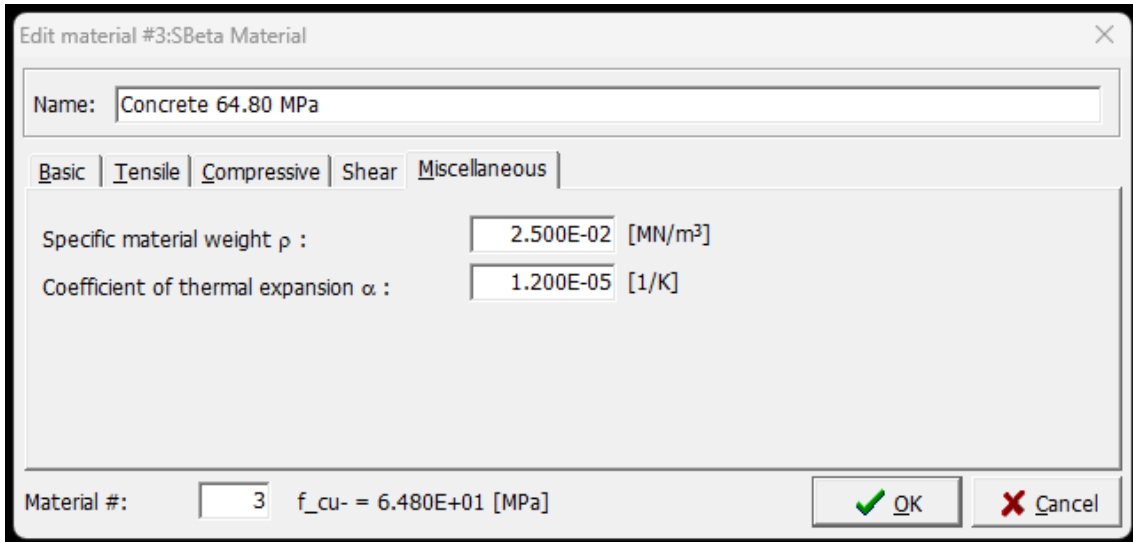


Figure 4.9: Miscellaneous tab for SBeta Material

4.1.1.2.2 Reinforcement

This type of material is assigned to the longitudinal and the transversal lines which simulate the presence of the reinforcement along the beam. In this case, two main tabs they have been compiled to define the material.

Basic

The reinforcement material models are characterized by the same behaviour in tension and in compression. In the basic tab it is necessary to indicate the type of stress-strain law. In the case steel reinforcement rebars it has been considered the Bilinear with Hardening model. In this type of model, also the limit stress and strength it has been considered (Figure 4.10).

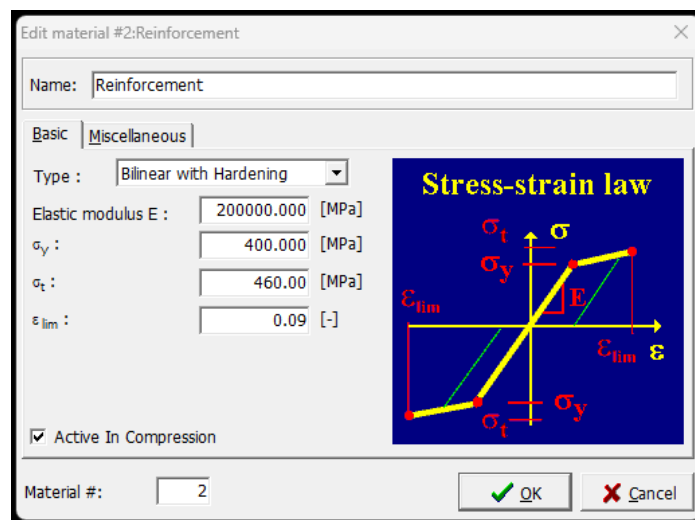


Figure 4.10: Basic tab for Reinforcement

Miscellaneous

In the second tab it has been set the specific weight of material to 0.00 MN/m³ because the rebars are already considered into the specific weight of concrete previously discussed. Regarding the coefficient of thermal expansion, it has not been changed (Figure 4.11).

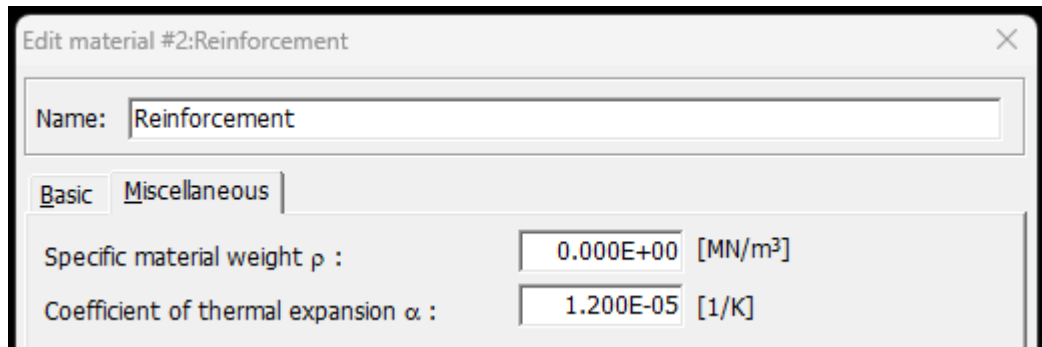


Figure 4.11: Miscellaneous tab for Reinforcement

4.1.1.2.3 Plane stress elastic isotropic

This type of material has been associated with the steel plates located on the face of the reinforced concrete beam where the load has been applied. The function of the steel plate is the redistribution of the load. They have been modelled a total of four steel plates: two plates situated on the top of the beam where the load is applied and other two plates situated on the bottom of the beam useful to apply the reaction of the supports.

Also in this case, it is necessary to compile two main tabs in order to define the material properties.

Basic and Miscellaneous

In this case the constitutive law is already fixed by the type of material model. It can be inserted only the value of the elastic modulus and the Poisson's ratio (Figure 4.12).

The second tab regarding the information of the specific weight, which is fixed at 0.00 MN/m³, and the coefficient of thermal expansion, which is not changed in terms of value from the proposed one (Figure 4.13).

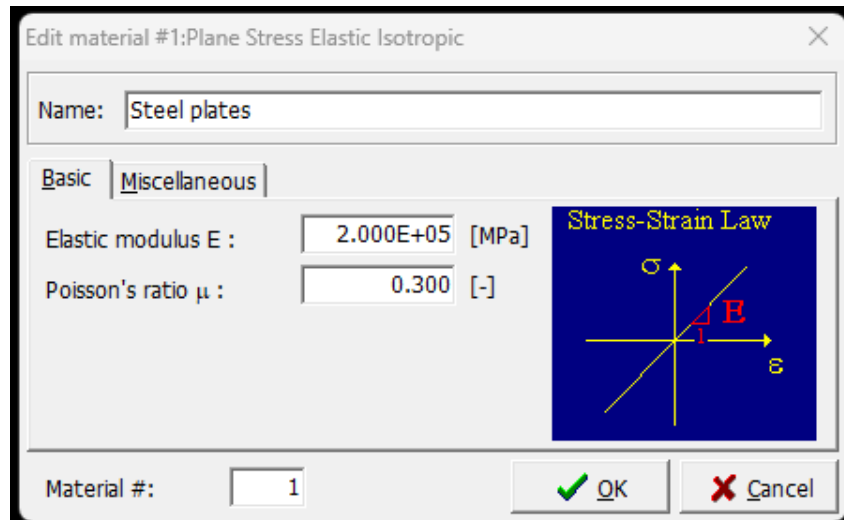


Figure 4.12: Basic tab for Plane Stress Elastic Isotropic

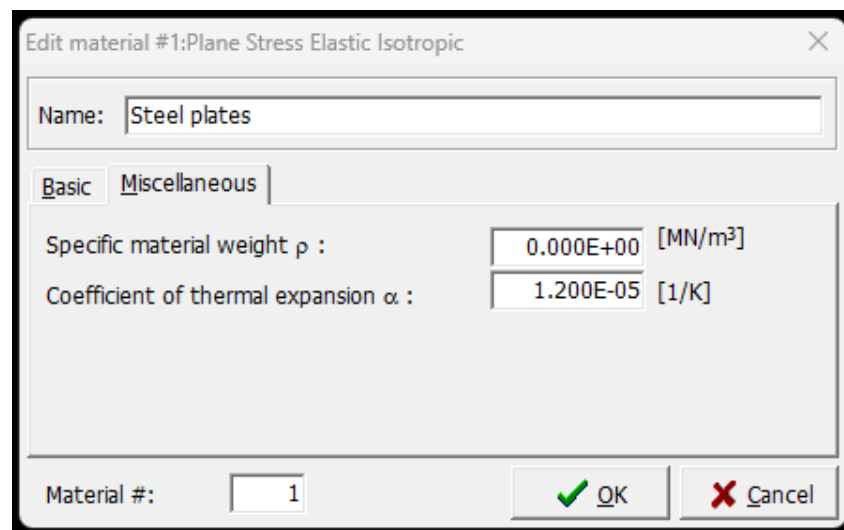


Figure 4.13: Miscellaneous tab for Plane Stress Elastic Isotropic

4.1.1.3 Topology

Defined the material properties, it is necessary to set the topology. Topology means the geometrical characteristics of the fem model. As it can be shown in the graphical interface (Figure 4.2), it is necessary to define *Joints*, *Line*, *Macro-elements*, *Opening*, *Bar Reinforcement* and *Contact Ambiguity*. Opening and Contact Ambiguity have not been considered in this work of thesis.

4.1.1.3.1 Joints

To create a new point, it is necessary to click on the tab and write the couple of coordinates in order to place it into the space (Figure 4.14). If it is required, it can be defined the refinement type.

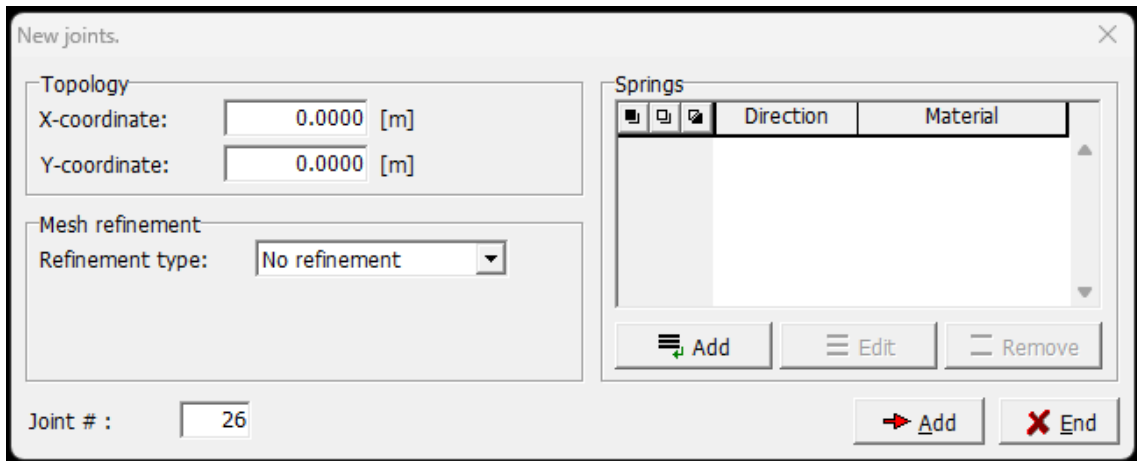


Figure 4.14: Joints tab - New joints

4.1.1.3.2 Line

Defined the joints it is necessary to collect them each other with the lines, which are the second topology element.

As it can be show in the figure below, using the Line tab it can be selected a different type of line: *Line*, *Arc* or *Circle*. For this work of thesis only the Line type is considered. To define a line, it is necessary to specify the origin and the end joint (Figure 4.15).

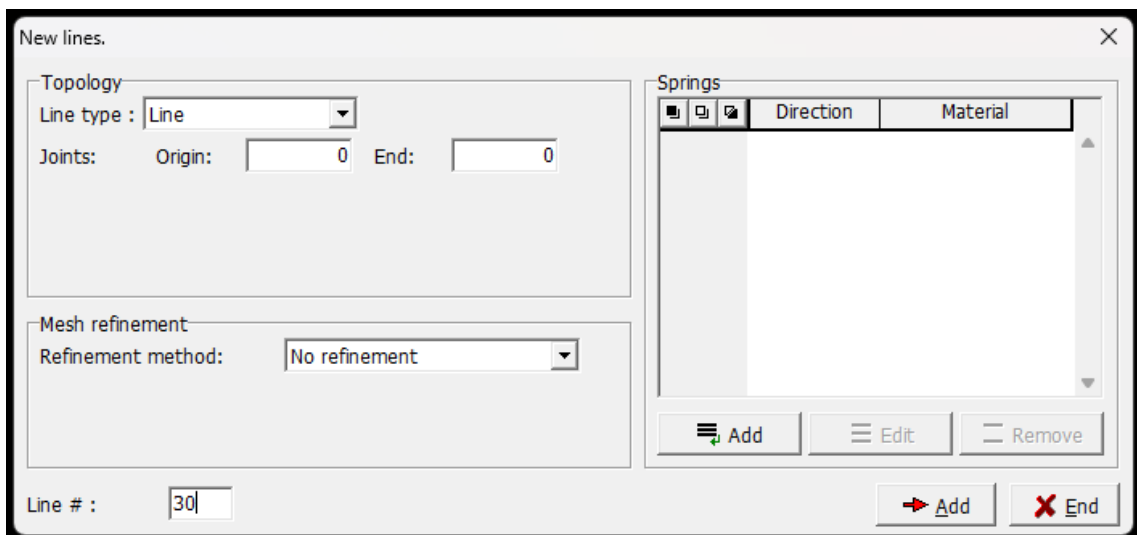


Figure 4.15: Line tab - New lines

4.1.1.3.3 Macro-elements

Macro-elements are identified by the lines which serve as perimeter surround them. In fact, to define a new macro-element it is necessary to define a *Boundary list*, which consists of a series of lines that include the macro-element

itself (Figure 4.16). The second characteristic is the *Mesh type*. It can be chosen between *Triangles*, *Quadrilaterals* and *Mixed*. After that, the *Element size* and the *Material* previously discussed have to be defined. Finally, *Thickness* has to be set, which consists of the base of the cross section of the beam and, last thing the *Quadrilateral elements* type has been chosen between *CCIsoQuad*, *CCQ10* and *CCQ10SBeta*.

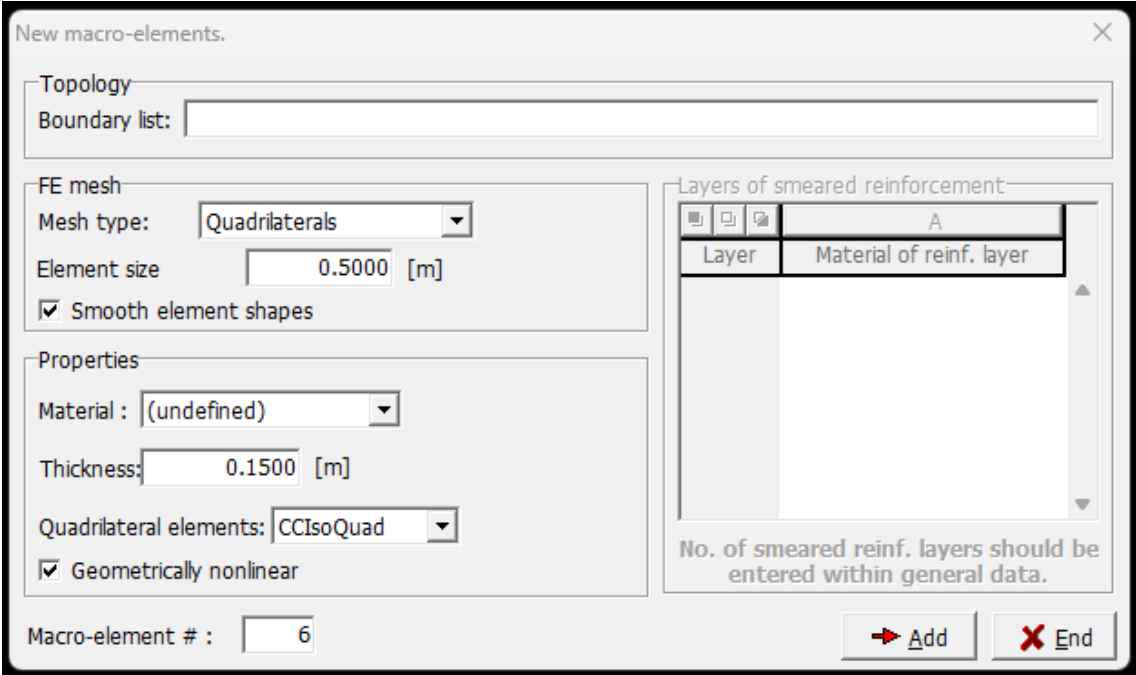


Figure 4.16: Macro-elements tab - New macro-elements

4.1.1.3.4 Bar reinforcement

To complete the topology treatment, it is necessary to compile the Bar Reinforcement tab. This tab is divided into two parts: *Topology* and *Properties*.

In the first part it can be chosen the *Segment type* between *Polyline of straight segment* and *Circle*. Defined the type, it can be create the segment inserting the coordinates (Figure 4.17).

In the second part it can be selected the material associated at the rebars and it is also possible to calculate the area of steel reinforcement setting the number of the bars and the diameter (Figure 4.18). It is also necessary to specify that a perfect bond between concrete and reinforcement steel is specified in this work of thesis.

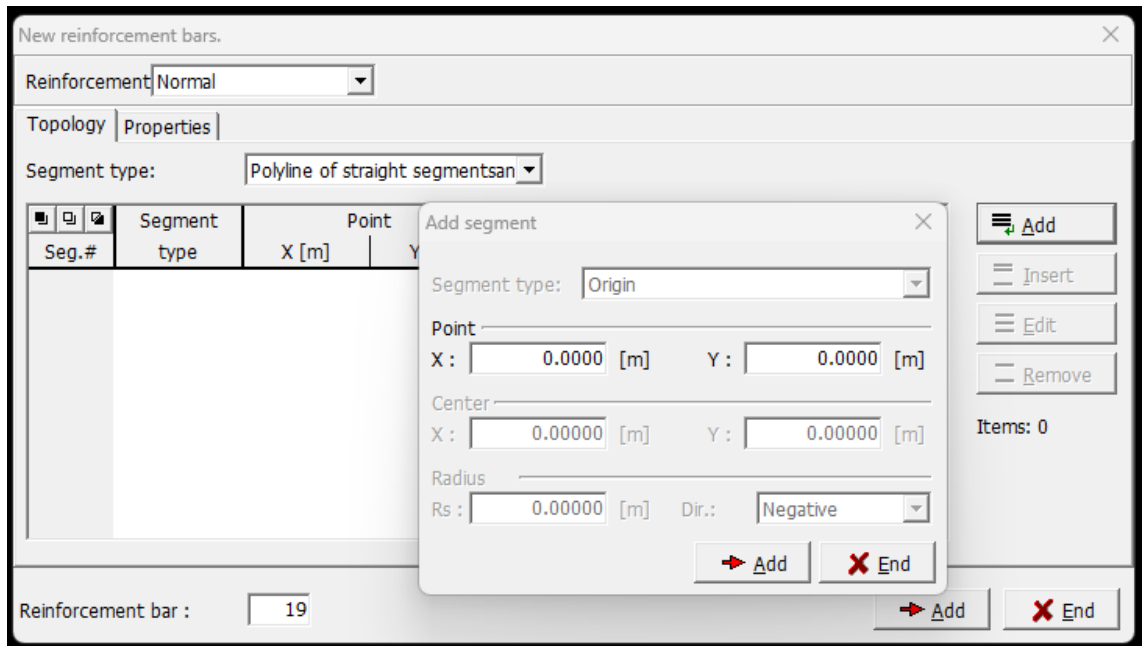


Figure 4.17: Bar Reinforcement tab – Topology

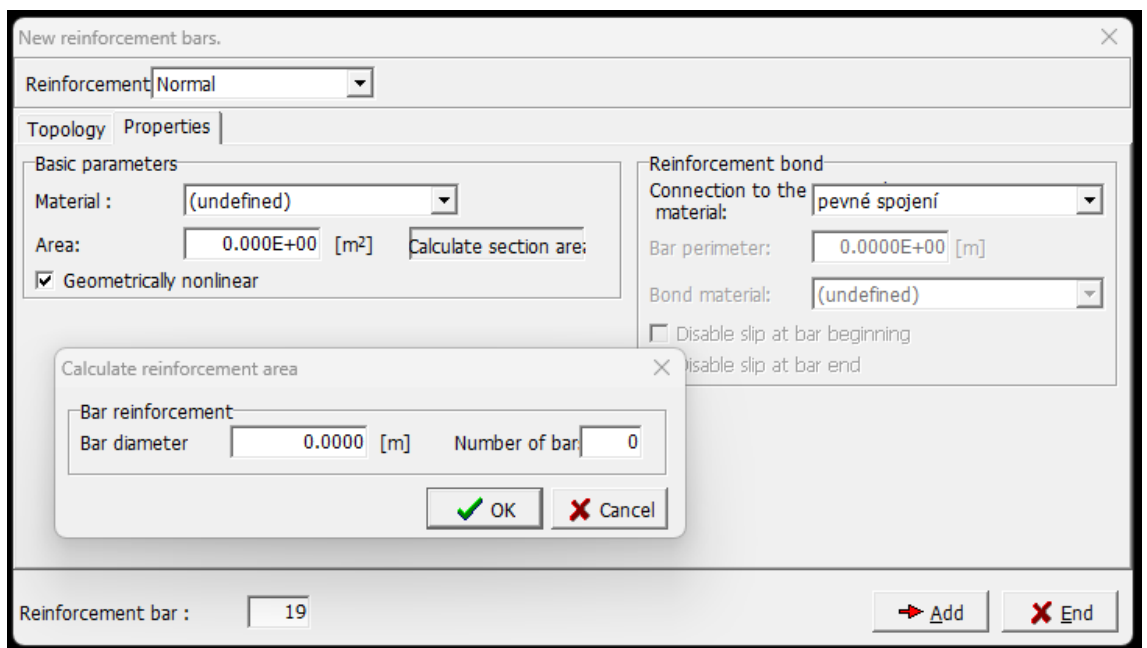


Figure 4.18: Bar Reinforcement tab – Properties

4.1.1.4 Load and supports

The next step of the pre-processing phase regarding the definition of the main load cases and the assignment of these load cases to all the topology elements, previously treated (joints, line, macro-elements and bar reinforcement).

The ATENA 2D software permits to define different types of load cases: body force, forces, supports, prescribed deformation, temperature, shrinkage and pre-

stressing. In this work of thesis, only the first three type are used and they are discussed in the following.

4.1.1.4.1 Supports load case

To consider the reinforced concrete beam simply supported in correspondence of the steel plates, it is necessary to define a load case. The information set are the LC name, the LC code and the direction of the dead load (Figure 4.19).

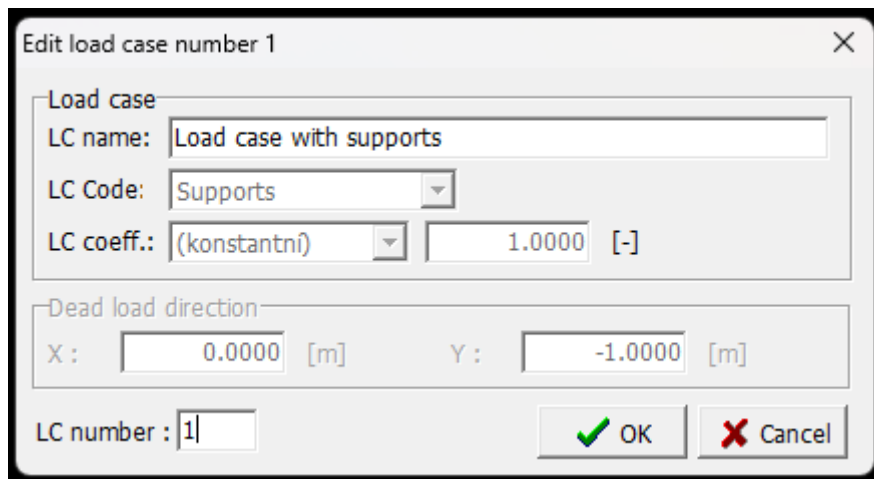


Figure 4.19: Definition of Supports load case

To assign this specific load case it is necessary to select the joints of the beam corresponding to the support, the joints where the support load case has to be applied. Selected these points and clicking on the button Replace, it is possible to specify the directions to be fixed (Figure 4.20).

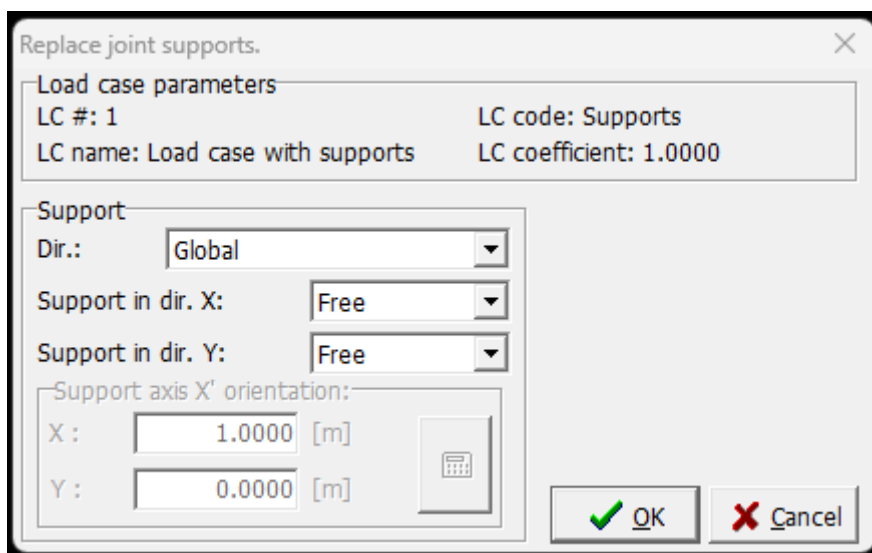


Figure 4.20: Support load case tab - Replace joint support

It is also proposed a graphical scheme with the supports load case applied on the joints in correspondence of the steel plates placed on the bottom face of the beam (Figure 4.21).

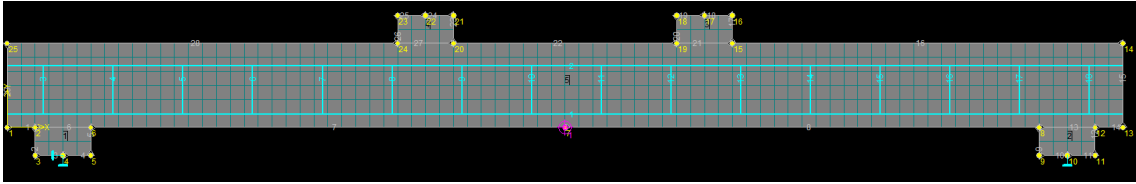


Figure 4.21: Graphical scheme of Supports load case

4.1.1.4.2 Body force load case

This second load case is useful to consider the self-weight of the structure. In the phase of creation, the main information are required again such as LC name, LC code and the direction of dead load (Figure 4.22). In this case it is not necessary to select the topology elements (i.e. joints, line and so on) to apply the load case.

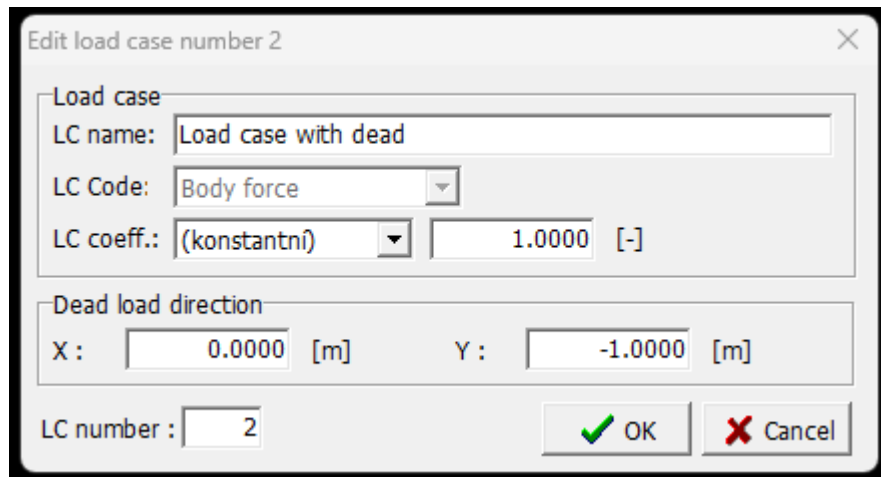


Figure 4.22: Definition of Body force load case

4.1.1.4.3 Forces load case

This third load case is used to define distributed load. The procedure to create the load case is the same to the ones described previously (Figure 4.23).

To assign the load case it is necessary to select the lines and click the button for adding a new load. In the window appeared it has been defined the type of forces (i.e. continuous full length, point load, partial and quadrilateral, quadrilateral), then the direction and the value of the load (Figure 4.24).

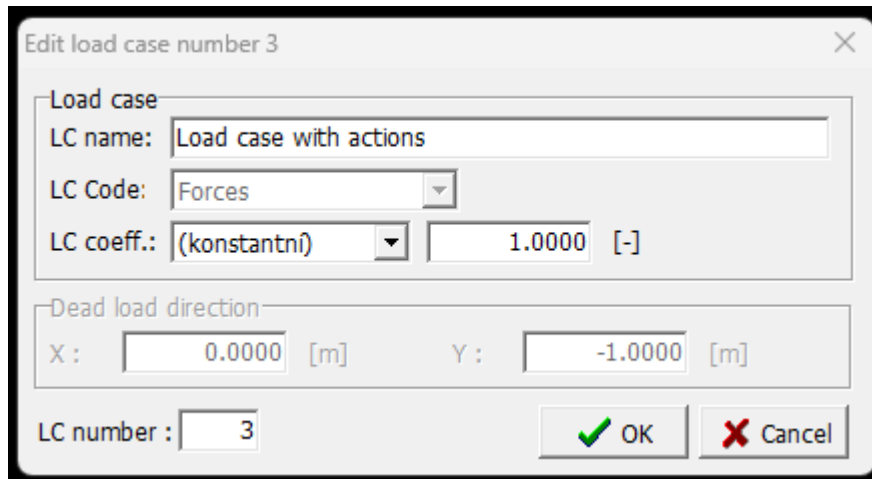


Figure 4.23: Definition of Forces load case

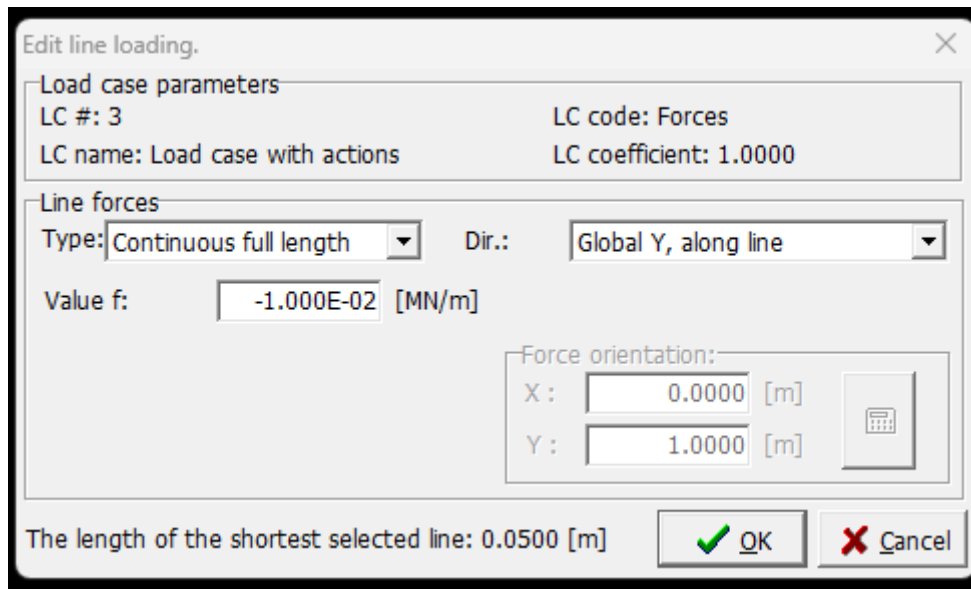


Figure 4.24: Forces load case tab - Line loading

In this case, the forces load case is applied on the steel plates placed on the top face of the beam. This load case simulates the incremental load for each step and the value is calculated take considering the length of the steel plate. Below is reported the beam with the forces load case applied (Figure 4.25).

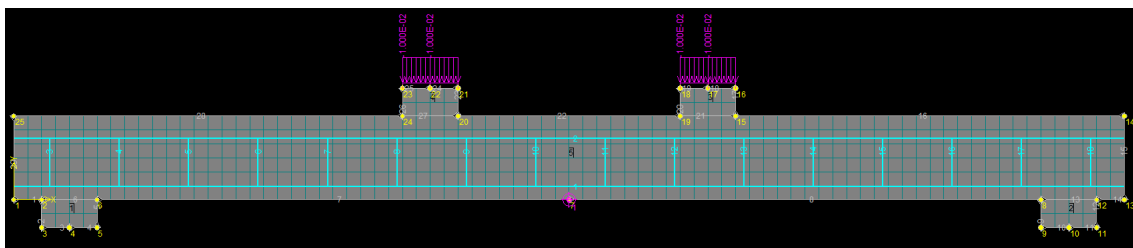


Figure 4.25: Graphical scheme of Forces load case

4.1.1.5 Run

In the *Run* section there are the final information regarding the input to be given to the software in the pre-processing phase. The main tabs are *Check data*, *Analysis steps*, *Monitoring points*, *Cuts*, *Moment lines* and *Solution parameters*.

In this work of thesis, *Cuts* and *Moment lines* are not considered. In the following a brief description for the other tabs.

4.1.1.5.1 Check data

This tab is a simple instrument which permit a rapid check of the model. The check data consists of an evaluation of the previous sections from materials to load and supports. If everything is correctly defined, in the check data window appear "Data O.K."

4.1.1.5.2 Analysis steps

This tab is very important for the analysis itself. In fact, it is defined the type of loading applied at each step, which is referred by the load case previously set (Figure 4.26).

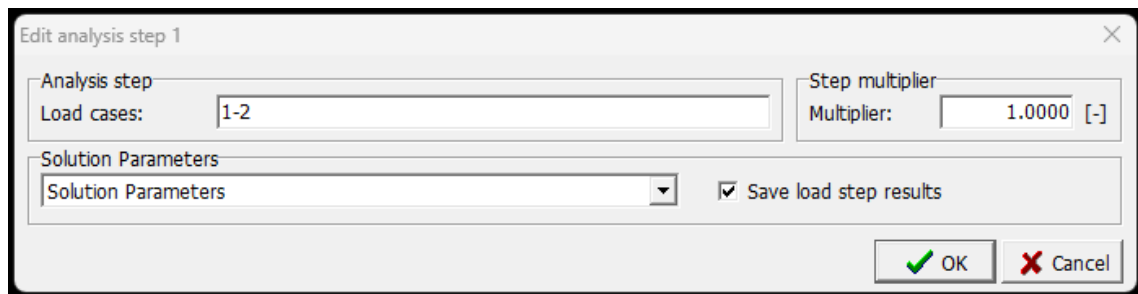


Figure 4.26: Definition of Analysis steps

In the section *Load cases*, they have been inserted the load cases presented in that step. For example, in the figure above in the first step of loading are applied together the LC1 (Load case with supports) and LC2 (load case with dead). The step multiplier is set at 1 the *Solution Parameters* section allow to define the way of solving the model.

4.1.1.5.3 Monitoring points

At the correspondence of the monitoring points of the model, for each step of the analysis some parameters can be saved, for example displacement or forces. Clicking the button *Add* into the *Monitoring Point* tab, it is possible to insert

a new monitoring point. In the window appeared (Figure 4.27), it is necessary to give a name to the monitoring point, define a Location through a couple of coordinates (X,Y) specifying the location (*Nodes* or *Integration points*). It is also required to establish the value to monitor (*Displacement*, *External_Forces* and *Reactions* if the location is nodes, as in our case). Finally, the item identifies the component of the value.

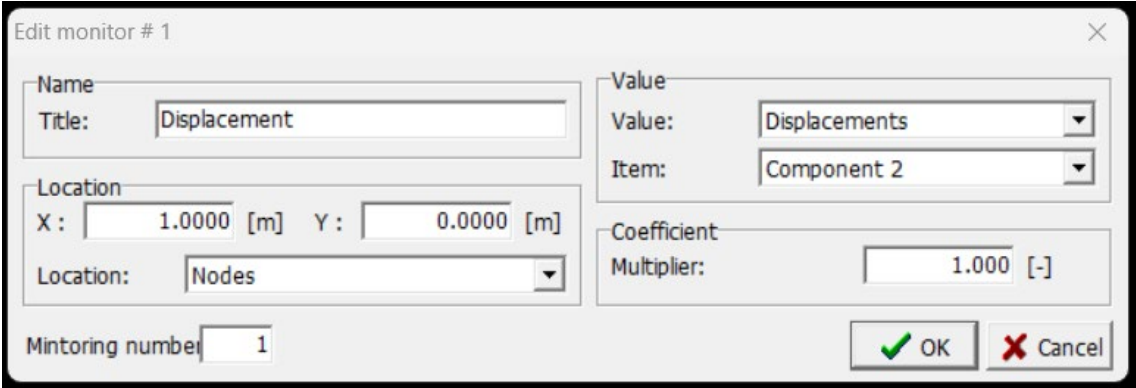


Figure 4.27: Monitoring points tab - Definition of monitoring points

4.1.1.5.4 Solution parameters

When adding a new solution parameter a window appears (Figure 4.28). In this case, apart from giving the title, it can be chosen one of the two basic solution methods: *Newton-Raphson* and *Arc Length*. Line search is useful to accelerate a convergence rate. Choosing Each iteration for Update Stiffness, meaning that the structural stiffness matrix is calculated and assembled each iteration and it is accomplished with the Stiffness Type Tangent.

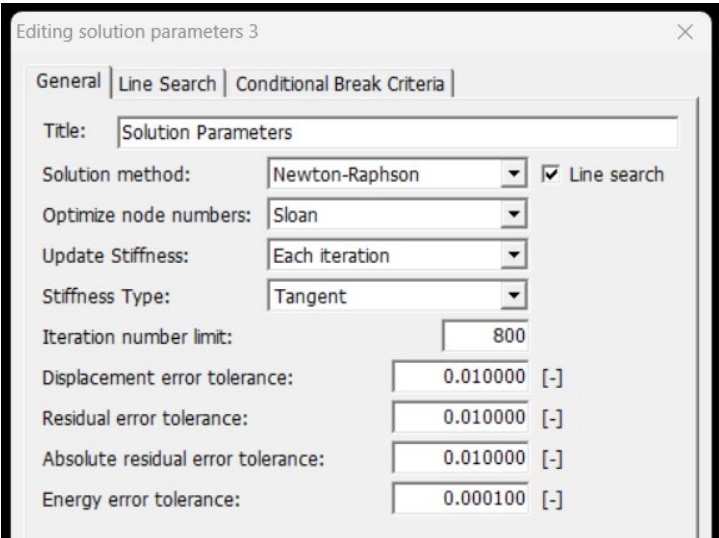


Figure 4.28: New solution parameters

Finally, the last four row represent the error tolerances. If the limits are respected the iteration stops and the calculation passes to the following step.

Regarding the Conditional Break Criteria, it can be set the methods to interrupt the computation if an error exceed the prescribed tolerance, as the product between the last four row of the previous figure and the prescribed factor in the figure below (Figure 4.29).

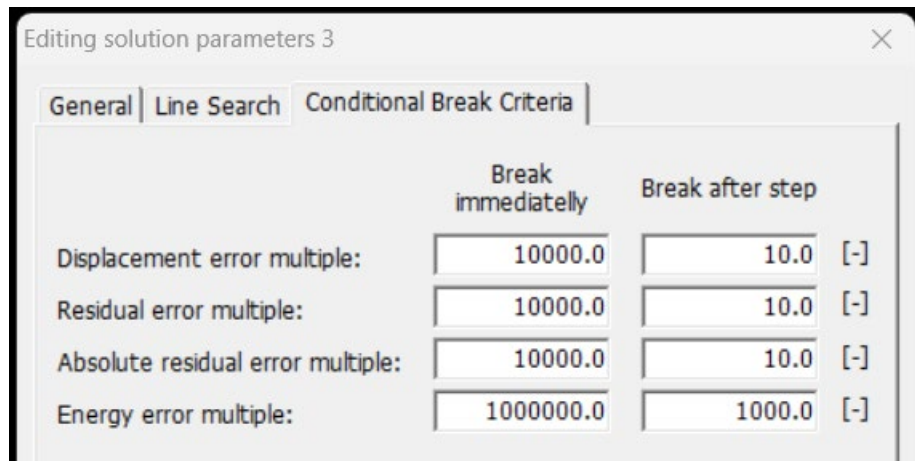


Figure 4.29: New solution parameters - Conditional Break Criteria section

4.1.2 Post processing

Concluded the pre processing phase, it is necessary to generate the mesh in order to perform the fem analysis. The graphical interface which appears at the end of the calculation is presented in the following figure (Figure 4.30).

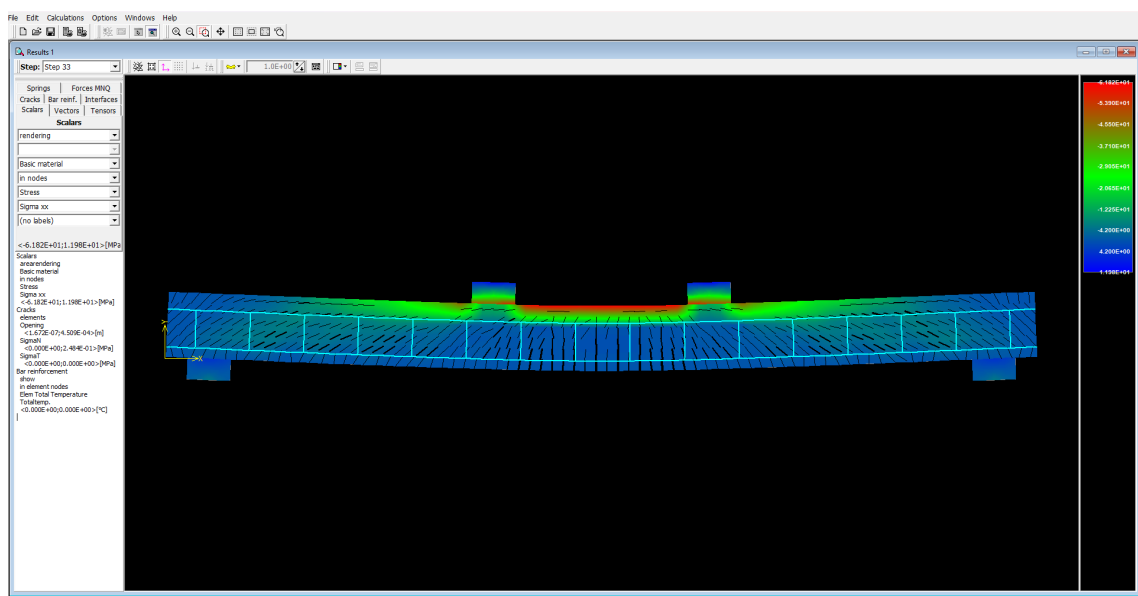


Figure 4.30: Post-processing graphical interface

This option is very useful because it is possible to study the results in a graphical view considering a legend organized with a colour scale. In particular, ATENA 2D permits to visualize the results also during the analysis, in this way it is guaranteed a continuous control from the user and not only at the end of the analysis.

Looking at the figure above, in the graphical interface of the post-processing phase it is possible to select a specific load step and visualize the results graphically. Focusing on the tabs placed below the load step, the results are presented in terms of *Springs*, *Forces MNQ*, *Cracks*, *Bar reinf.*, *Interfaces*, *Scalar*, *Vectors* and *Tensors*. In the following it will be explained the tabs which are used in this work of thesis, in particular *Cracks*, *Bar reinf.* and *Scalar*.

4.1.2.1 Cracks

Choosing the tab Cracks, cracks can be displayed. This option is used in this work of thesis in the figures presented in the following paragraph which treats the comparison between the experimental and numerical results. Using the pull-down menu it is possible to visualize specific results (Figure 4.31).

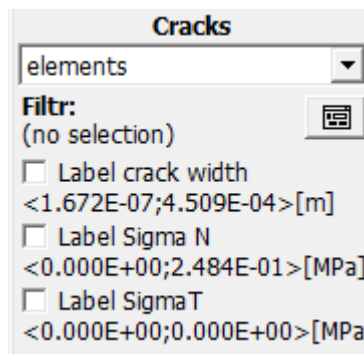


Figure 4.31: Example of cracks pull-down menu

The display type can be *no graphic* (cracks are not shown), *elements* (only one crack per element is shown) and *integration point* (one crack per integration point is shown).

4.1.2.2 Bar reinforcement

In the following it is presented the bar reinforcement tab (Figure 4.32). In this work of thesis, this tab is used to evaluate the values of the maximum strain associated with the failure step.

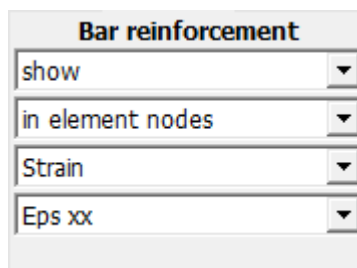


Figure 4.32: Example of bar reinforcement pull-down menu

The display type can be no graphic, show and show and labels. It can be chosen the nodes or in element nodes method. The latter is the most used. Then, it can be chosen the type of information searched between *Engineering Strain*, *Principal Engineering Strain*, *Stress*, *Principal Stress*, *Plastic Strain* and *Principal Plastic Strain*. As last thing, it is possible to choose the type of information (i.e. *Eps xx*, *Eps yy* or *Gamma xy*).

4.1.2.3 Scalars

Again, the display type can be chosen between no graphics, rendering, contour areas and contour lines (Figure 4.33). There are many possibilities of results visualization in terms of *Displacements*, *Elem Total Temperature*, *Strain*, *Principal Strain*, *Stress*, *Principal Stress*, *Von Mises Stress*, *Total Strain*, *Principal Total Strain*, *SBeta State Variables*, *Performance Index*, *Crack Width*.

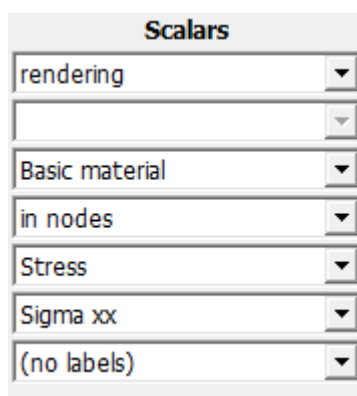


Figure 4.33: Example of Scalars pull-down menu

4.1.3 CCT and CCO files

As mentioned at the beginning of the main paragraph, ATENA 2D is able to read a CCT file format to insert into the program all the information regarding the pre processing phase (Figure 4.34).

FILETYPEATENA_TEXT	FILETYPEATENA_TEXT_1	FILETYPEATENA_TEXT_2
VERSION 2	VERSION 2	VERSION 2
BEG_HEADER	BEG_HEADER	BEG_HEADER
DESCRIPTION "RCB02_1"	DESCRIPTION "RCB02_2"	DESCRIPTION "RCB02_3"
COMMENT "CF"	COMMENT "CF"	COMMENT "CF"
NUMPLANES 0	NUMPLANES 0	NUMPLANES 0
STRUCTYPE "2D"	STRUCTYPE "2D"	STRUCTYPE "2D"
UNITSYSTEM "METRIC"	UNITSYSTEM "METRIC"	UNITSYSTEM "METRIC"
NUMDECIMAL 4	NUMDECIMAL 4	NUMDECIMAL 4
END_HEADER	END_HEADER	END_HEADER
BEG_MATERIALS	BEG_MATERIALS	BEG_MATERIALS
COUNT 3	COUNT 3	COUNT 3
BEG_MAT 1	BEG_MAT 1	BEG_MAT 1
VER_MAT 0	VER_MAT 0	VER_MAT 0
NAME "Steel plates"	NAME "Steel plates"	NAME "Steel plates"
TYPE	TYPE	TYPE
"CCPlaneStressElastIsotropic"	"CCPlaneStressElastIsotropic"	"CCPlaneStressElastIsotropic"
E 2.000E+05	E 2.000E+05	E 2.000E+05
Mu 0.300	Mu 0.300	Mu 0.300
Rho 0.000E+00	Rho 0.000E+00	Rho 0.000E+00
Alpha 1.200E-05	Alpha 1.200E-05	Alpha 1.200E-05
END_MAT 1	END_MAT 1	END_MAT 1
BEG_MAT 2	BEG_MAT 2	BEG_MAT 2
VER_MAT 0	VER_MAT 0	VER_MAT 0
Func_Type 4	Func_Type 4	Func_Type 4
....

Figure 4.34: CCT import file

This option is used in this work of thesis in order to create a huge number of fem models with the aim to perform the probabilistic analysis previously introduced and treated in the following chapter.

It is also possible to export the results of the analysis using the CCO file format. For a major comprehension, defined a monitoring point to save the values of the displacement for each load step, it is possible to export this information (Figure 4.35). This option has been used both for the probabilistic analysis previously discussed and for the primary calibration of the fem models in respect to the experimental values presented in the literature.

```

FILETYPE ATENA_MONITOR
VERSION 0
SPACE 2D

COUNT 1

MONITOR
id 1
name "Displacement"
coefficient 1.000
location_type 1
coordinates 1.0000 0.0000
identification 1
value
item
index 2
unit m
location 259 -1 -1
values
  1  2 -3.812E-05
  2  2 -1.739E-04
  3  2 -3.098E-04
  4  2 -4.461E-04
  5  2 -5.826E-04
  6  48 -1.057E-03
  7  70 -1.464E-03
  8  109 -1.925E-03
  9  800 -2.345E-03
 10  ....

```

Figure 4.35: CCO export file

4.2 Finite Elements Models: hypothesis and NLNAs results

This paragraph explains the numerical modelling assumptions essential to create the NLN models of the sixteen reinforced concrete beams previously treated in the experimental benchmark chapter. The FEM software “ATENA 2D” is used to generate these models. The domain of the reinforced concrete beams has been represented by quadrilateral plane stress finite elements, denoted as CCQ10SBeta.

The finite element mesh is a specific characteristic of each structural element, but it can vary between 2.5 cm and 5.5 cm. The values can change for

each structure because of the calibration process of the numerical model. The solution of the non-linear system is carried out using the standard Newton-Raphson iterative approach proposed by ATENA 2D. In general, a number of iterations is set in the ranging between 800 and 1500 and a convergence criteria based on forces and energy is considered. The specific tolerances are 1% and 0.01% respectively.

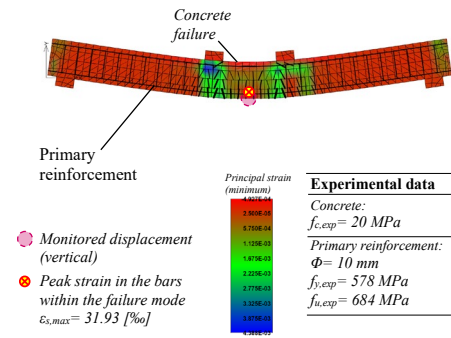
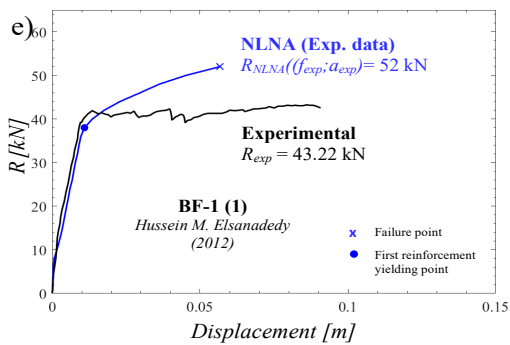
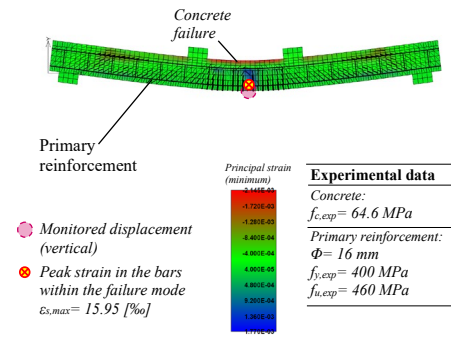
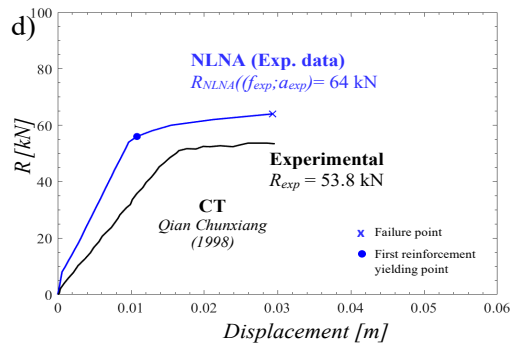
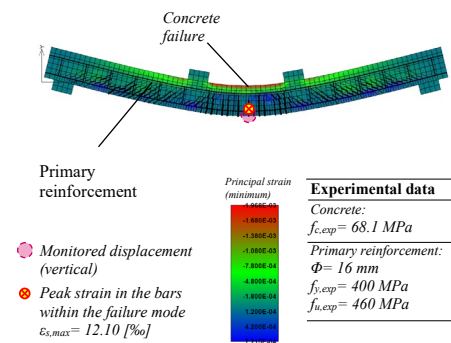
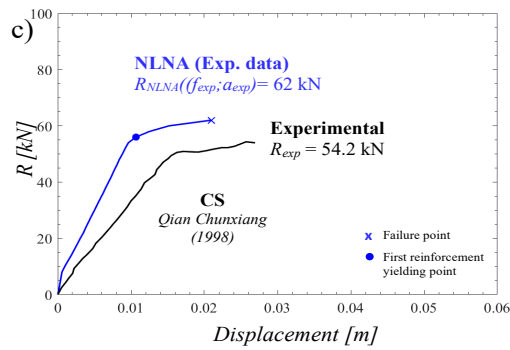
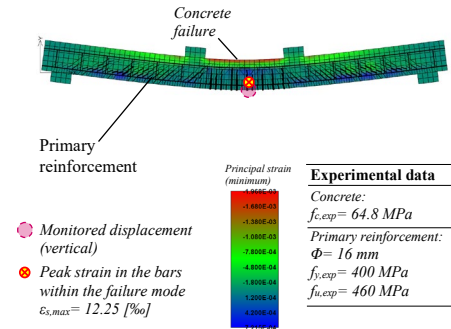
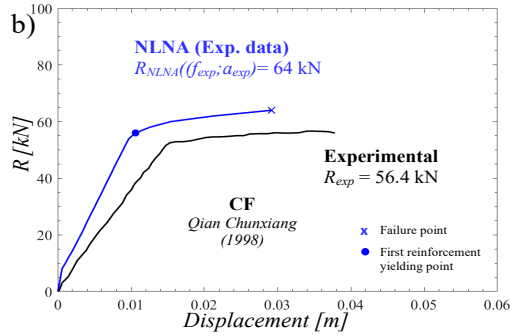
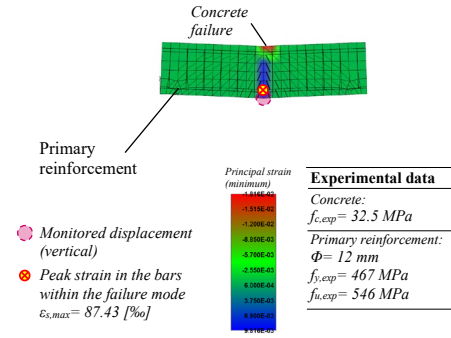
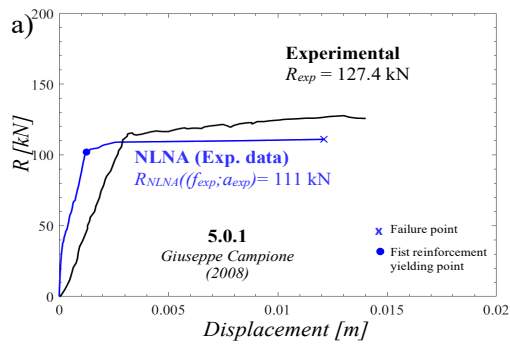
With respect to the constitutive models, ATENA 2D permits to consider the non-linear behaviour of the concrete under compression and tension using “*SBeta material mode*” into the software. This latter function can consider the mono-axial concrete behaviour as curvilinear response in compression with a post-peak linear compression softening (LCS). The LCS law is defined in a manner that after the achievement of peak load the resistance decrease of the 50% until the ultimate value of strain ϵ_u . Instead, the ultimate strain in the LTS law has been set between 2 and 15 times of the value of the strain corresponding of the concrete tensile resistance.

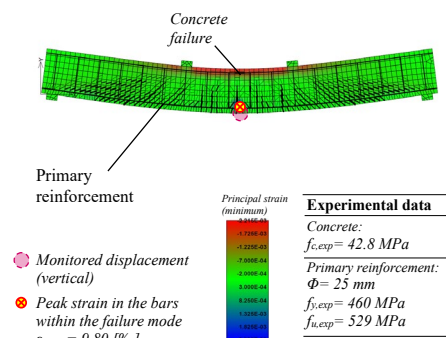
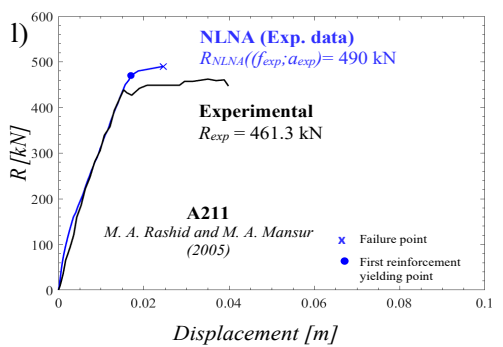
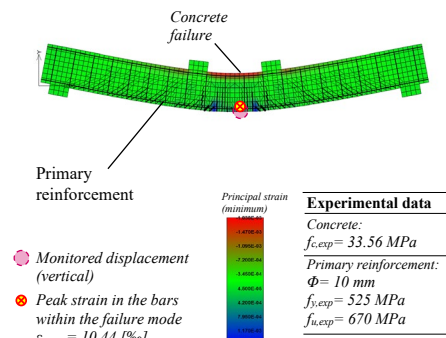
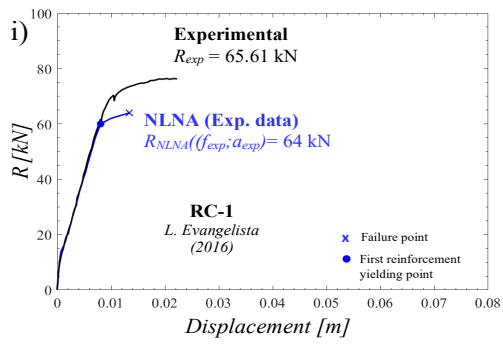
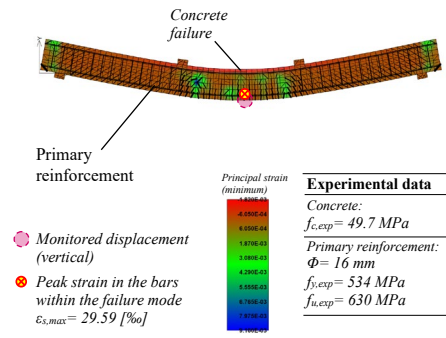
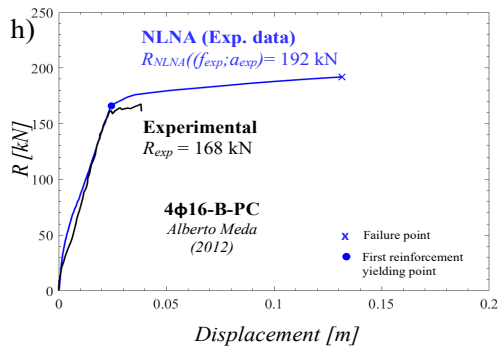
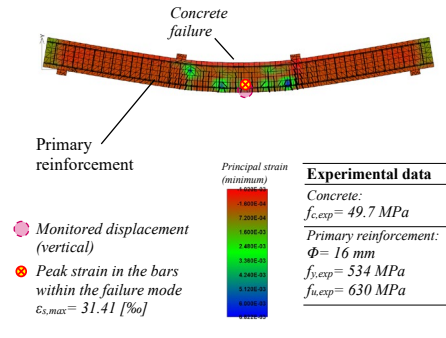
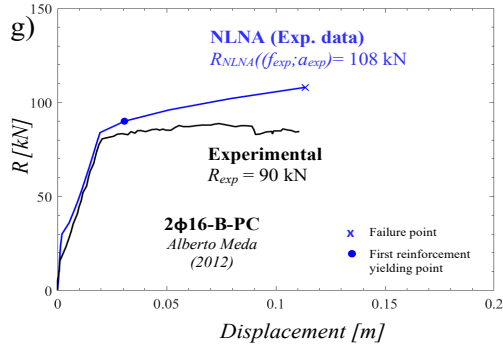
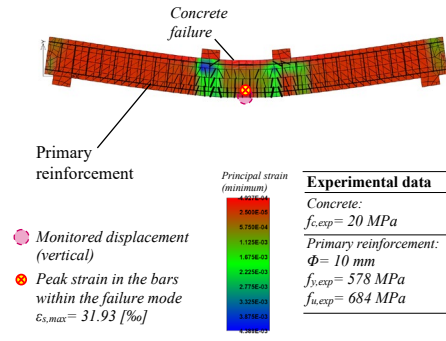
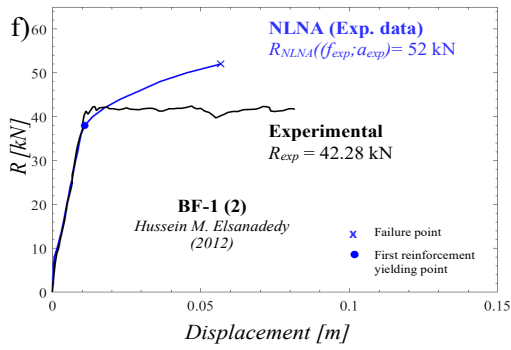
Regarding the cracking behaviour it has been considered the rotated crack model. Using this type of model, it is possible to take into account the progressive development and rotation of cracks within the concrete as load is applied, focusing on post-cracking behaviour.

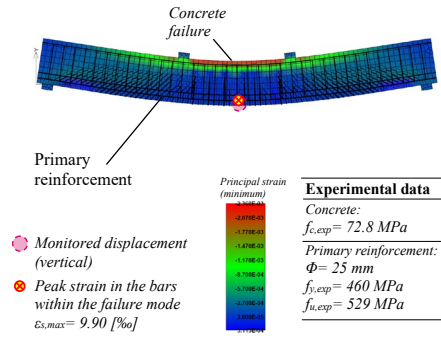
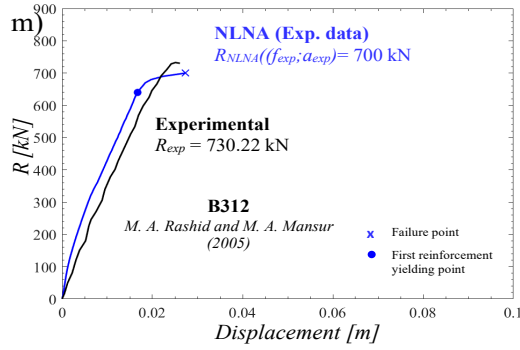
For the reinforcement it has been considered a bilinear constitutive law with hardening in both compression and tension. The Young’s modulus of the steel reinforcement is set for all the structures at 200000 MPa and an ultimate strain ϵ_u of 9%.

With these assumptions is possible to conduct the numerical simulation. In the first step has been applied the dead load, and then the increment load. The value of the load step is set according to a good level of accuracy and acceptable computational cost. In addition, the peak strain of the tensile reinforcement at the point of failure is recorded for each structure. In this work of thesis, they have been performed a total of $30 \cdot 16 = 480$ NLNAs.

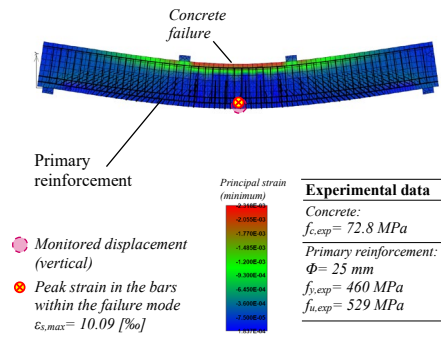
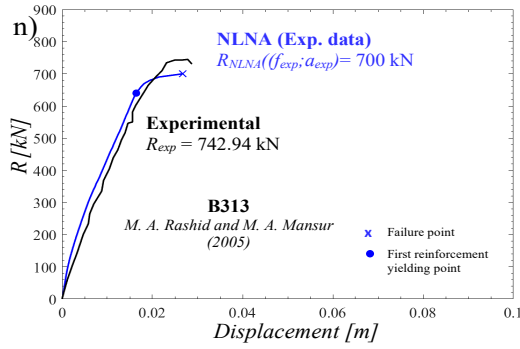
In the following it is presented the comparison between the experimental curve proposed in the literature and the curve obtained by NLNA considering the mean material properties (Figure 4.36).



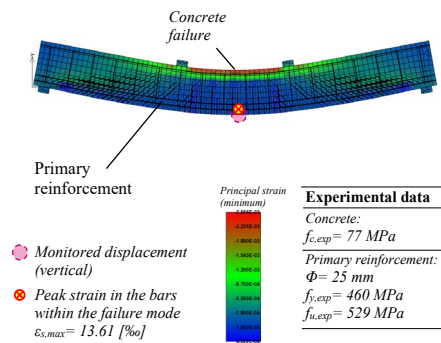
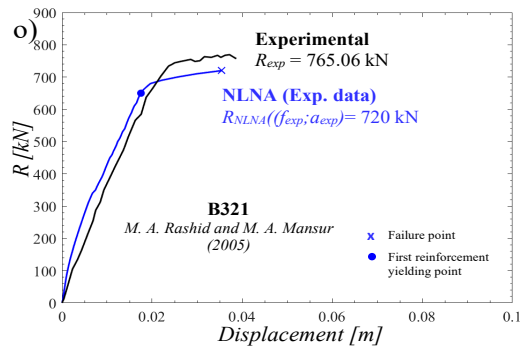




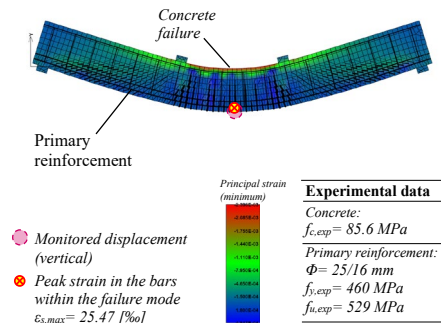
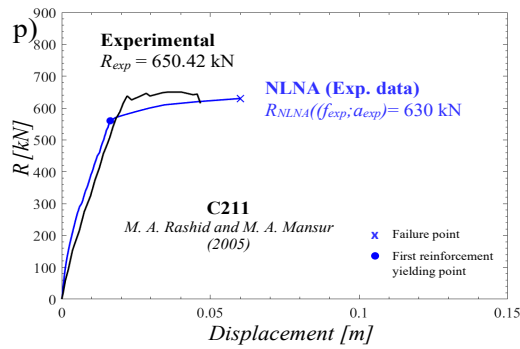
Experimental data	
Concrete:	$f_{c,exp} = 72.8 \text{ MPa}$
Primary reinforcement:	$\Phi = 25 \text{ mm}$ $f_{y,exp} = 460 \text{ MPa}$ $f_{u,exp} = 529 \text{ MPa}$



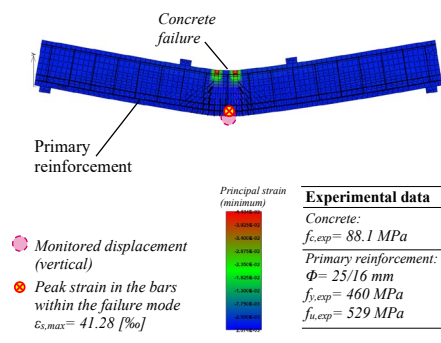
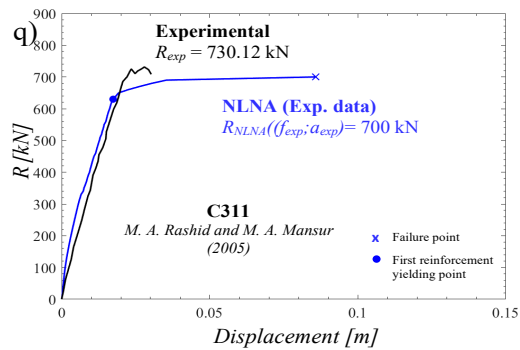
Experimental data	
Concrete:	$f_{c,exp} = 72.8 \text{ MPa}$
Primary reinforcement:	$\Phi = 25 \text{ mm}$ $f_{y,exp} = 460 \text{ MPa}$ $f_{u,exp} = 529 \text{ MPa}$



Experimental data	
Concrete:	$f_{c,exp} = 77 \text{ MPa}$
Primary reinforcement:	$\Phi = 25 \text{ mm}$ $f_{y,exp} = 460 \text{ MPa}$ $f_{u,exp} = 529 \text{ MPa}$



Experimental data	
Concrete:	$f_{c,exp} = 85.6 \text{ MPa}$
Primary reinforcement:	$\Phi = 25/16 \text{ mm}$ $f_{y,exp} = 460 \text{ MPa}$ $f_{u,exp} = 529 \text{ MPa}$



Experimental data	
Concrete:	$f_{c,exp} = 88.1 \text{ MPa}$
Primary reinforcement:	$\Phi = 25/16 \text{ mm}$ $f_{y,exp} = 460 \text{ MPa}$ $f_{u,exp} = 529 \text{ MPa}$

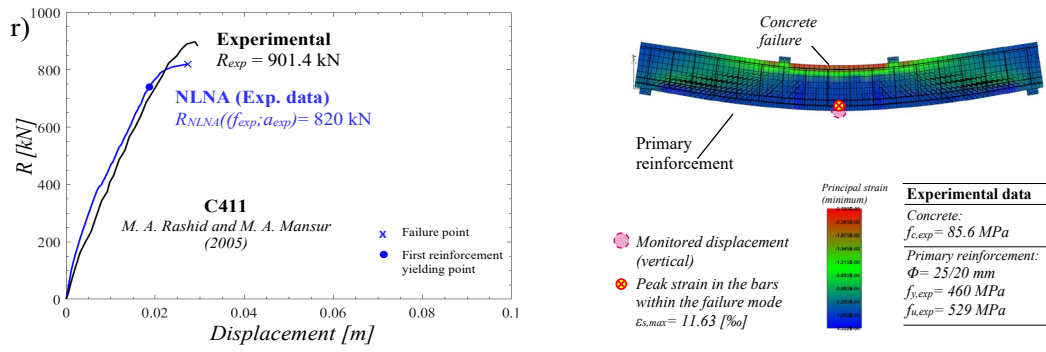


Figure 4.36: comparison between experimental results R_{exp} and NLNAs outcomes $R_{NLNA}(f_{exp}; a_{exp})$ and representation of the respective failure mechanism in concomitance of failure (a, b, c, d, e, f, g, h, l, l, m, n, o, p, q, r)

5 Probabilistic modelling

In this chapter they are explained the modelling assumptions utilized for the probabilistic analysis to evaluate the global structural response. This can be done adopting the LHS (Latin Hypercube Sampling) method.

5.1 Relevant random variables

Focusing on the LHS method, the sampling is carried out by means of 30 intervals with a sufficient size which permit to obtain an overall CoV for the involved variables and global response below 0.3.

According to the JCSS Probabilistic Model Code 2001 [11], they have been selected the relevant random variables listed into the table below. As it can be show, they has been assumed as mean value of the relevant random variables the experimental results reported into the selected scientific articles for all the 16 reinforced concrete beams.

Random variable	Probabilistic distribution	Mean value	CoV [-]	Statistical correlation
Concrete cylinder compressive strength f_c [MPa]	Lognormal	$f_{c,exp}$	0.15	-
Reinforcement tensile yielding f_y [MPa]	Lognormal	$f_{y,exp}$	0.05	f_u (0.75) ϵ_u (-0.45)
Reinforcement ultimate tensile strength f_u [MPa]	Lognormal	$f_{u,exp}$	0.05	f_y (0.75) ϵ_u (-0.60)
Reinforcement Young modulus E_s [MPa]	Lognormal	200000	0.03	-
Reinforcement ultimate strain ϵ_u [-]	Lognormal	0.09	0.09	f_y (-0.45) f_u (-0.60)

Table 5.1 - Characterization of the probabilistic models related to aleatory uncertainties associated to material properties

Evaluating the CoV $V_{R,m}$ it has been considered the aleatory uncertainties related to the materials properties at the global level. Regarding the geometrical properties, in this phase they are considered equivalent the experimental properties and the nominal ones. During the probabilistic analysis the random variables presented into the table above has been sampled using the LHS method previously mentioned and better presented in the following.

5.1.1 Latin Hypercube Sampling (LHS)

The *Latin Hypercube Sampling* (LHS) is a method used to reduce the computational effort of the Monte Carlo's simulation. The aim of this latter method is the definition of the probability of failure P_f and, consequently the Coefficient of Variation CoV of a generic aleatory variable (i.e. global structural resistance). The problem of the Monte Carlo's method regards the number of simulations. In fact, the number of the samples required for the simulations is proportional to the inverse of the target probability of failure (it means commonly $10^5 - 10^6$ simulations).

Using the LHS, the variables are sampled by their probabilistic distribution (in this case it has to be considered the probabilistic distribution of the random variables defined in the Table 5.1) and, successively, randomly combined each other. It is important to specify that the interval of probabilities (0,1) of the domain is uniformly sampled. In this way, the empirical CDF (obtained through LHS method) and the lognormal CDF can be plotted into the same graph (Figure 5.1).

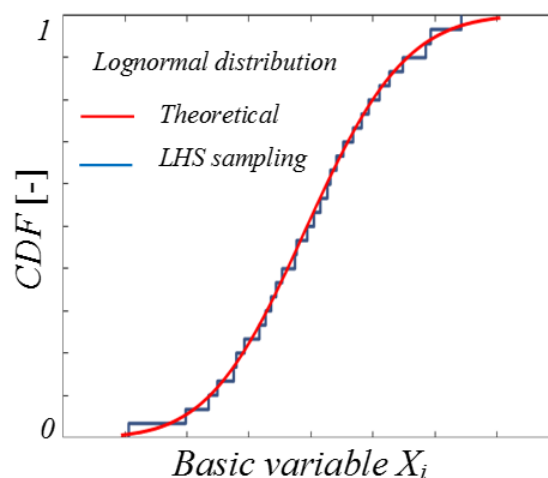


Figure 5.1: Comparison between the empirical CDF (LHS sampling in the figure) and the lognormal CDF (Theoretical in the figure) [9]

The LHS method is considered as an efficient procedure in this case where it is necessary to evaluate the CoV $V_{R,m}$ using NLNAs method. Using this type of sampling the number of numerical simulations required to define the probabilistic distribution of the global structural resistance are reduced. In fact, it has been demonstrated that 30-40 samples are sufficient to determine mean, variance and a proper probabilistic distribution of a variable if the value of the CoV is lower or equal to 0.2.

5.2 Probabilistic analysis of the global structural resistance

This paragraph groups the outcomes and the results of the probabilistic analysis. According to the LHS method, the random variables listed into the Table 5.1 are sampled and combined each other. They are used to determine a total of $30 \cdot 16 = 480$ NLNAs. As it can be shown in the following, the results of the NLNAs in terms of global structural resistance R have been used to define the “empirical” and the “best-fitted” Cumulative Density Function (CDF) for each reinforced concrete beam.

The “empirical” distribution represents the sampled values of the global structural resistance. Considering the 30 results of the simulations, the Anderson-Darling statistical test has been used to assess if the sampled values follow a lognormal distribution. The statistical test is passed if the value of “P-value” is higher than 0.05. Then, the statistical parameters $\mu_{R,m}$ and $V_{R,m}$ are estimated by means of the Maximum Likelihood (ML) method. It has been defined the so-called *mean-to-mean deviation* $\delta_{R,m}$, which represents the ratio between the mean value of the of the global resistance by the probabilistic analysis $\mu_{R,m}$ and the value of the global structural resistance evaluated using the experimental values of material and geometrical properties $R_{NLNA}(f_{exp}; a_{exp})$.

As the name suggests, the “best-fitted” distribution try to fit the sampled values of the “empirical” distribution by means of a lognormal distribution characterized by mean value $\mu_{R,m}$ and CoV $V_{R,m}$.

In the following the results of the probabilistic analyses for each reinforced concrete beam are presented (Figures 5.2 – 5.3).

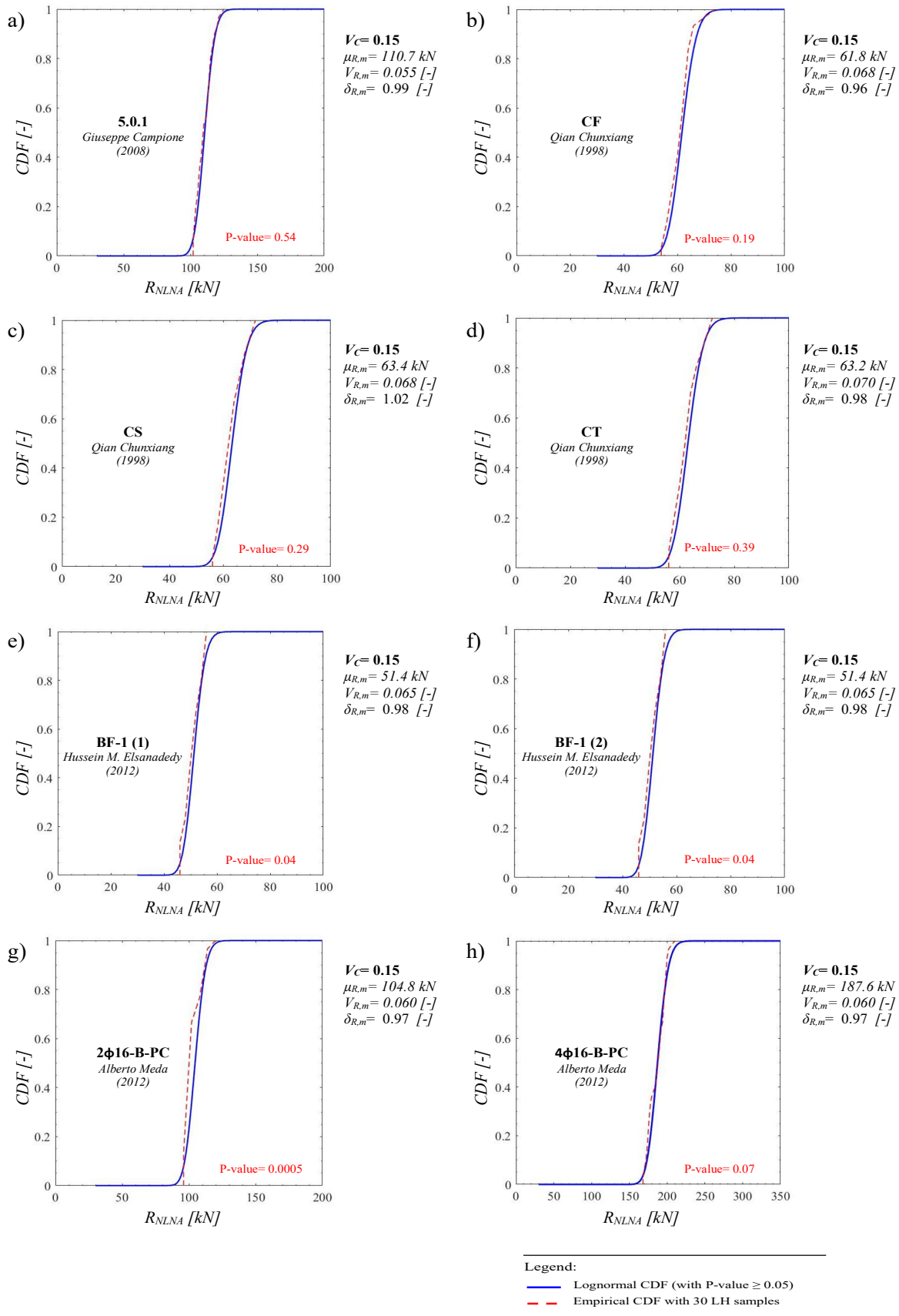


Figure 5.2: Empirical and lognormal CDFs (a, b, c, d, e, f, g, h)

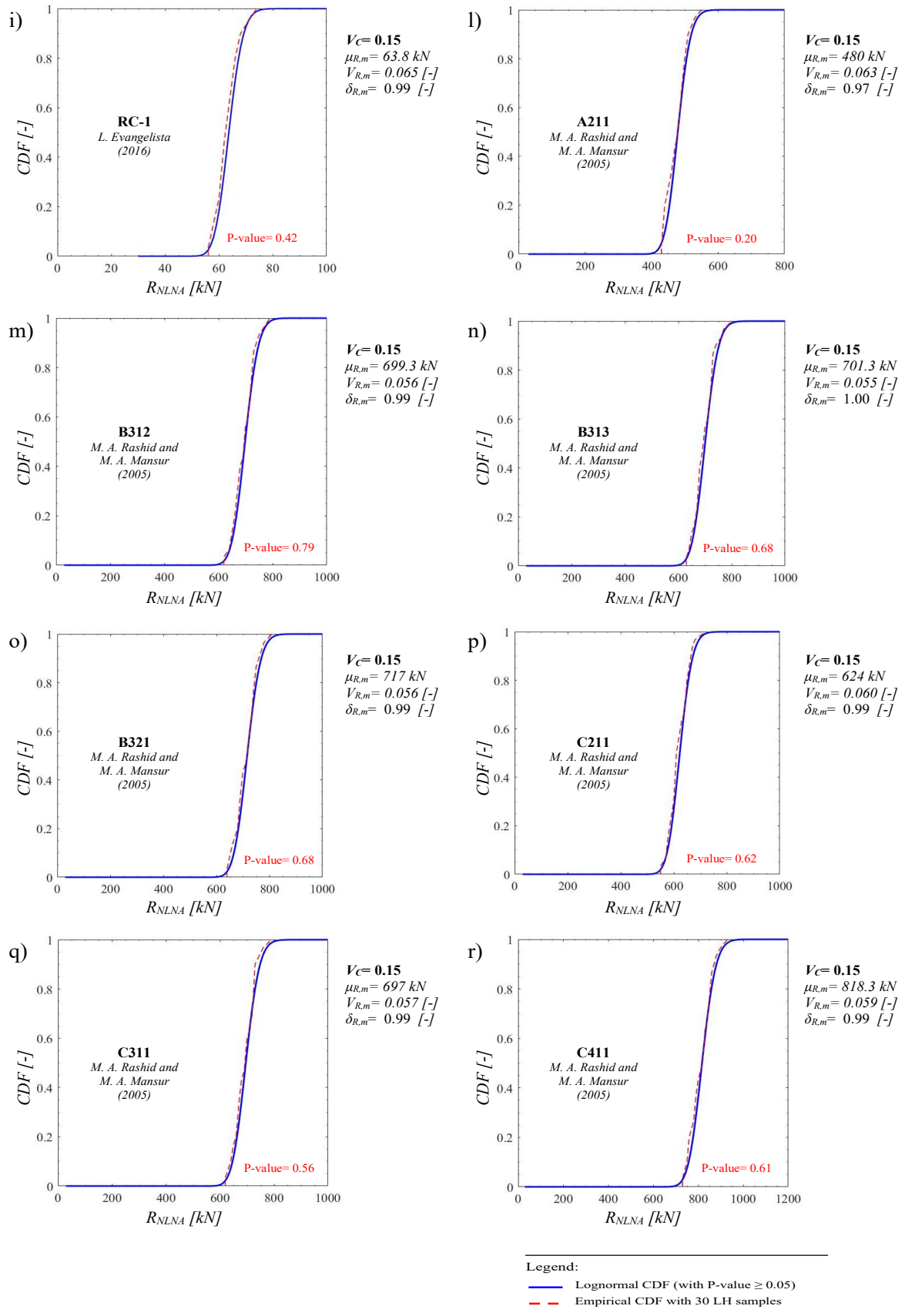


Figure 5.3: Empirical and lognormal CDFs (i, l, m, n, o, p, q, r)

In the following, the load-displacement curves of the probabilistic analysis are presented for each reinforced concrete beam. In a single graph they are grouped the 30 simulations performed for each structure (Figures 5.4 – 5.5).

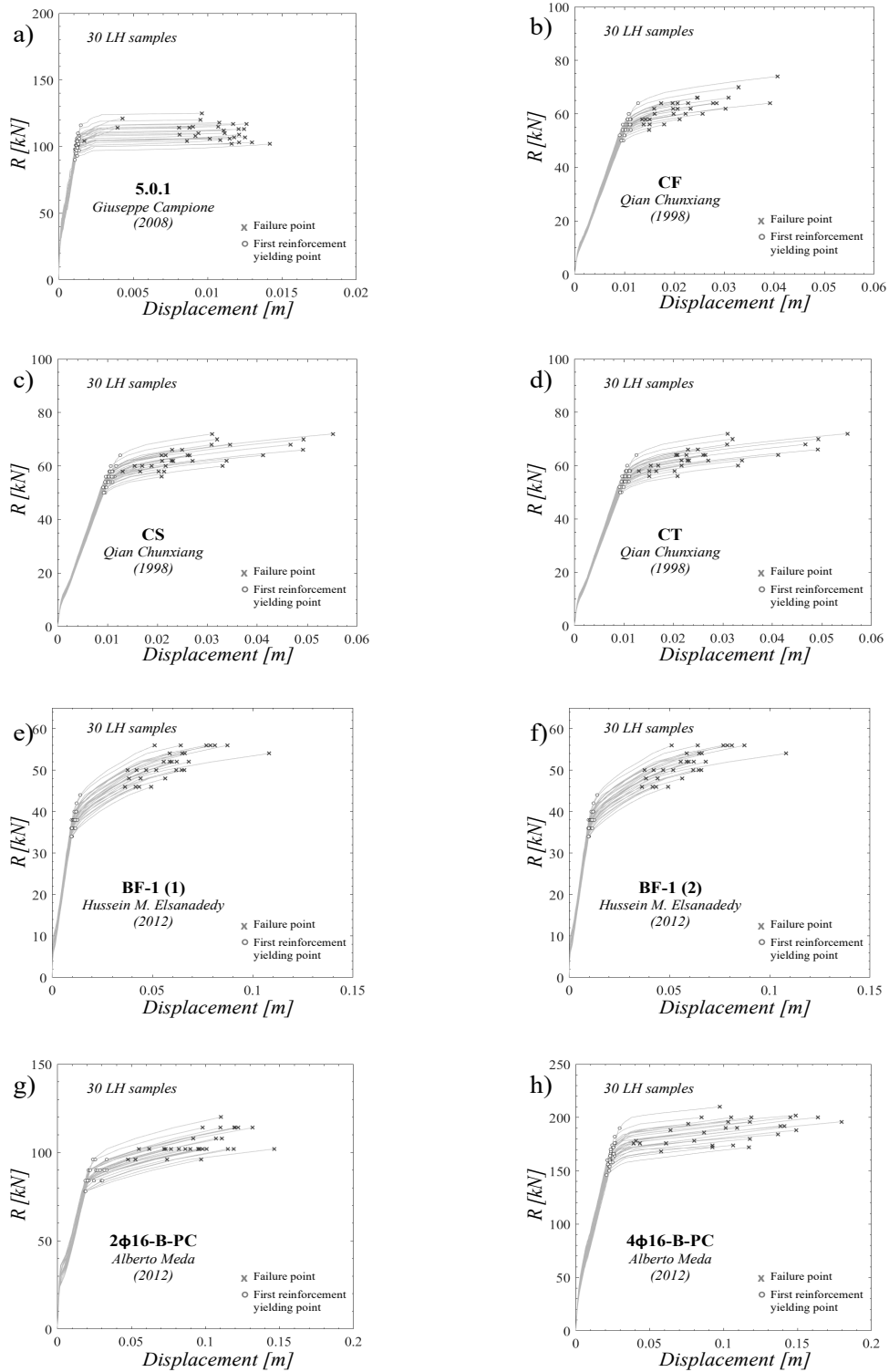


Figure 5.4: Load-Displacement curves of the 30 NLNAs (a, b, c, d, e, f, g, h)

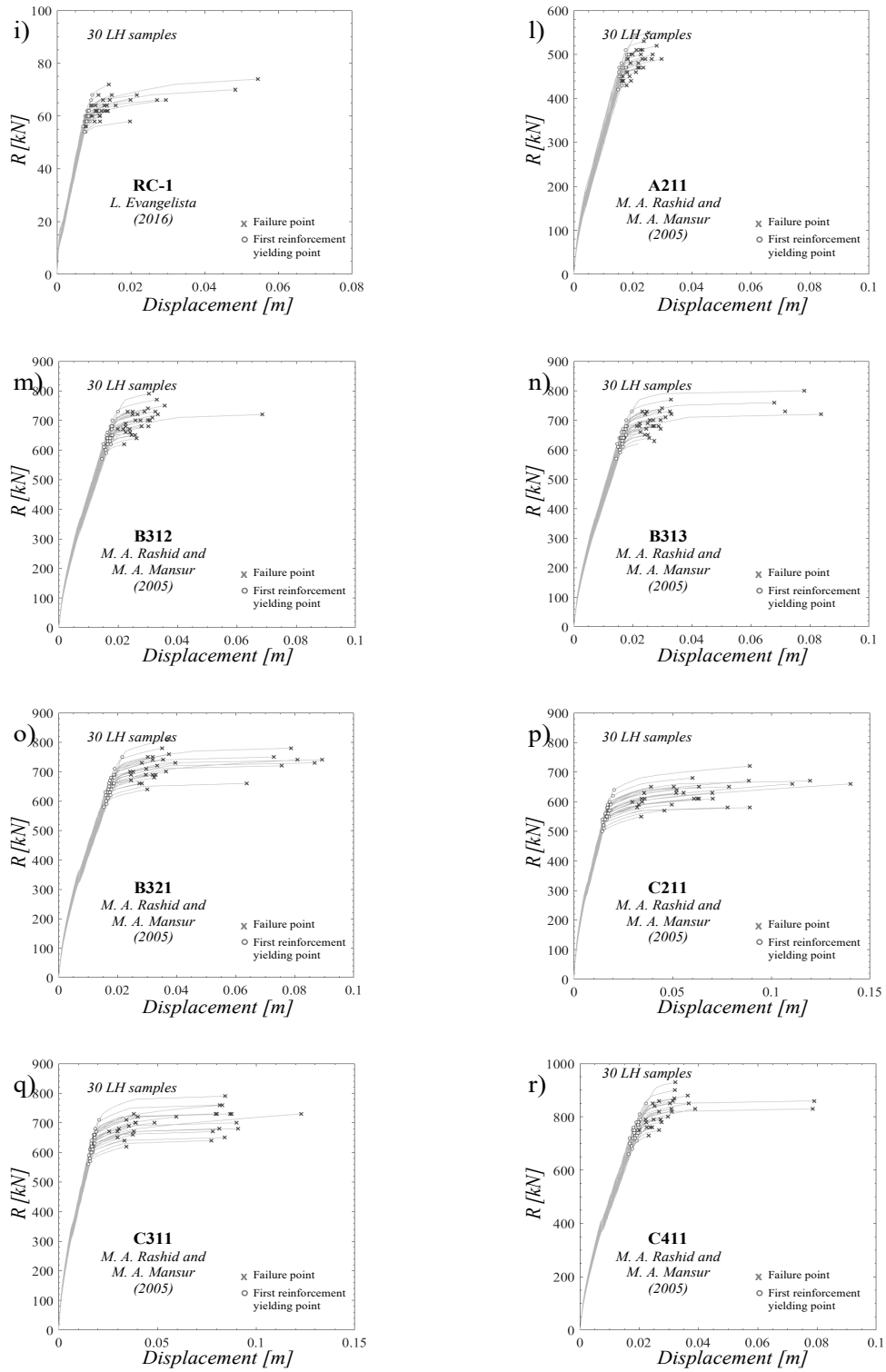


Figure 5.5: Load-Displacement curves of the 30 NLNAs (i, l, m, n, o, p, q, r)

6 Results and comments

Defined the values of the *mean-to-mean deviation* $\delta_{R,m}$ and the CoV of the global structural resistance $V_{R,m}$, it is possible to collate them to the geometrical response characteristics of the system, according to the aim of this work of thesis. These characteristics are the strain ratio $\varepsilon_{s,max}/\varepsilon_y$, the geometrical reinforcement ratio ρ and the mechanical reinforcement ratio ω .

Regarding the strain ratio, $\varepsilon_{s,max}$ is the maximum value of strain obtained performing the NLNA characterized by the experimental values of the materials and the nominal geometrical properties. The value of the yielding strain ε_y is evaluated according to the experimental material properties as an inherent characteristic of the steel reinforcement.

The second geometrical response characteristic of the system is the geometrical reinforcement ratio ρ defined using the Eq.(6):

$$\rho = \frac{A_s}{B \cdot d} \quad (6)$$

Where A_s represents the amount of steel reinforcement located in the tension zone, B is the thickness of the beam and the value d is the effective depth of the cross section.

The last characteristic is the mechanical reinforcement ratio ω , which considers also the resistance of the materials, as it can be shown from the Eq.(7) below:

$$\omega = \frac{A_s \cdot f_y}{B \cdot d \cdot f_c} \quad (7)$$

In the following, the statistical parameters $\delta_{R,m}$ and $V_{R,m}$ are correlated with the three geometrical response characteristics abovementioned and some comments are made to understand if there is a sort of tendency which links the obtained data (Figures 6.1 – 6.2).

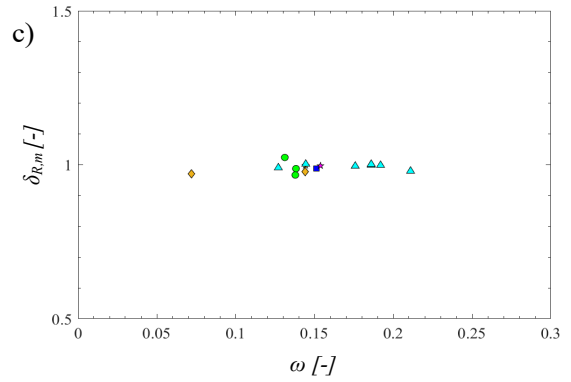
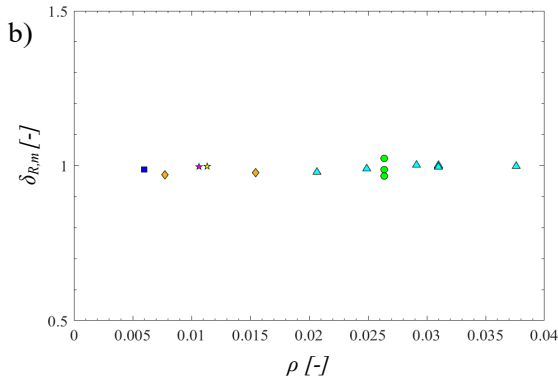
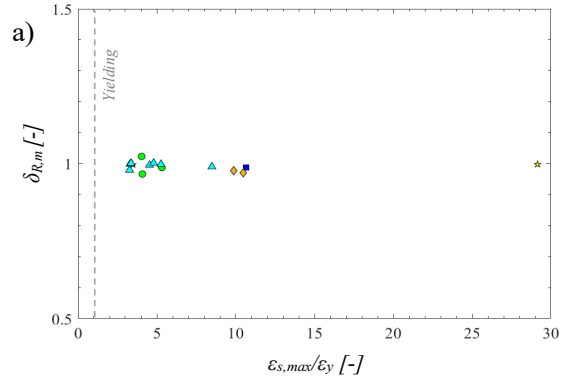
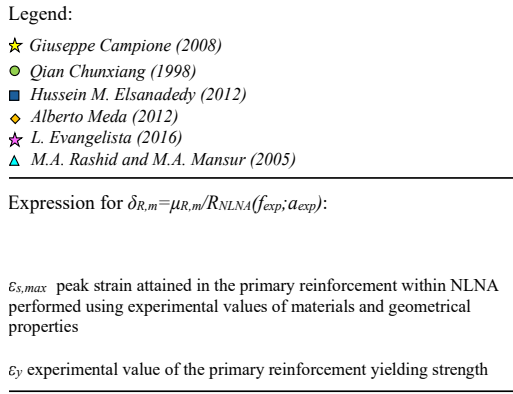


Figure 6.1: Variation trend of the *mean-to-mean deviation* $\delta_{R,m}$ with respect to a) the strain ratio $\epsilon_{s,max}/\epsilon_y$, b) the geometrical reinforcement ratio ρ , c) the mechanical reinforcement ratio ω

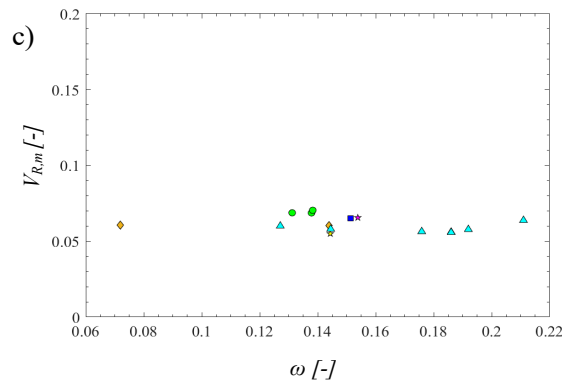
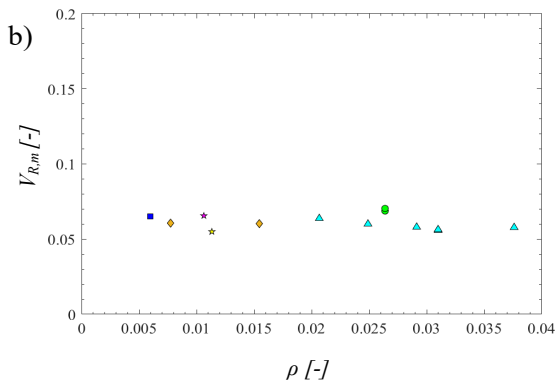
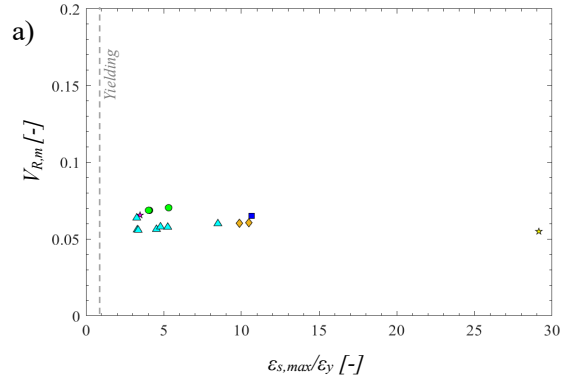
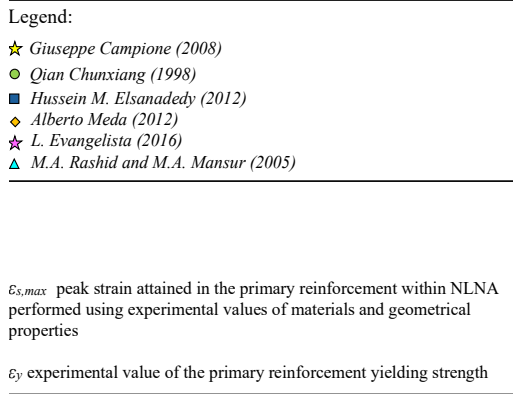


Figure 6.2: Variation trend of the *CoV of the global resistance* $V_{R,m}$ with respect to a) the strain ratio $\epsilon_{s,max}/\epsilon_y$, b) the geometrical reinforcement ratio ρ , c) the mechanical reinforcement ratio ω

Focusing of the results reported in the Figure above, the variation trend of the *mean-to-mean deviation* $\delta_{R,m}$ with respect to the strain ratio $\varepsilon_{s,max}/\varepsilon_y$ is comparable with the values obtained in the [7]. The same observation may be done regarding the variation trend of the CoV of the global resistance $V_{R,m}$ with respect to the same geometrical characteristic. For this reason, it is possible to expand the mentioned study [7] validating the strain-based method also for the design and the assessment of the structure characterized by a beam behaviour failing in bending. This is better discussed in the next paragraph.

Another relevant result which can be discussed is related to the variation trend of the strain ratio $\varepsilon_{s,max}/\varepsilon_y$ with respect to the geometrical reinforcement ratio ρ (Figure 6.3). It is possible to affirm that the greater is the geometrical reinforcement ratio ρ , the less is the value of the strain ratio $\varepsilon_{s,max}/\varepsilon_y$.

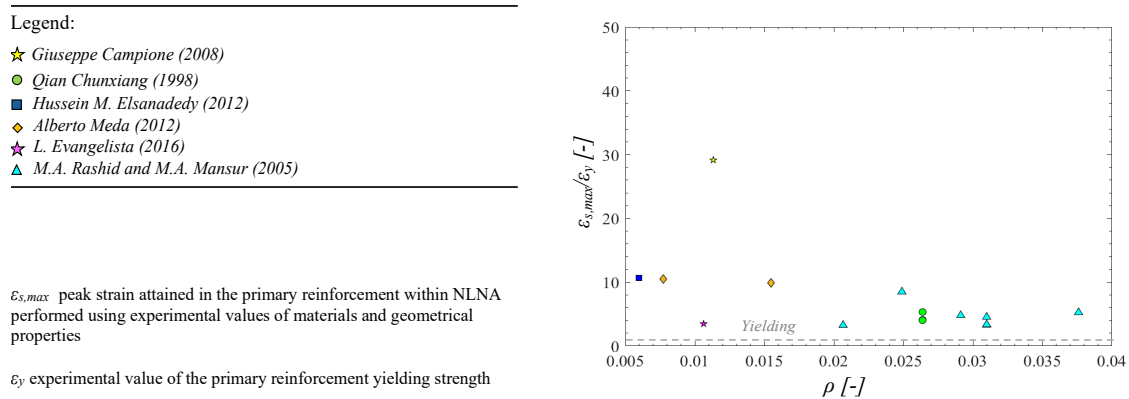


Figure 6.3: Variation trend of the strain ratio $\varepsilon_{s,max}/\varepsilon_y$ with respect to the geometrical reinforcement ratio ρ

6.1 Strain-based method for RC structures failing in bending

The aim of this paragraph is to expand the strain-based method for reinforced concrete structures subjected to flexural collapse, typically structural elements characterized by a beam behaviour. As it has been affirmed previously, the results regarding the variation trend of the statistical parameters $\delta_{R,m}$ and $V_{R,m}$ with respect to the strain ratio $\varepsilon_{s,max}/\varepsilon_y$ confirm the good outcomes of the study [7]. In fact, adding the results obtained in this work of thesis regarding the statistical parameters there is not a significant variation in terms of analytic law which correlates these statistical parameters ($\delta_{R,m}$ and $V_{R,m}$) with the geometrical response characteristic $\varepsilon_{s,max}/\varepsilon_y$, as better discussed in the following.

Thanks to this work of thesis, it has been expanded the strain-based method already presented in the [7] to the beam-behaviour structural elements which typically collapse according to a flexural failure. The experimental benchmark of the [7] is characterized by 10 deep beams (cases a) and b) of the Figure 6.4) and 6 reinforced concrete walls (cases c) and d) of the Figure 6.4). According to the scientific article [7], the structures have been selected in order to cover a various range in terms of material properties and considering the range of failure modes from brittle to ductile. However, these structures have been limited the application of the strain-based method to the non-slender structural elements.

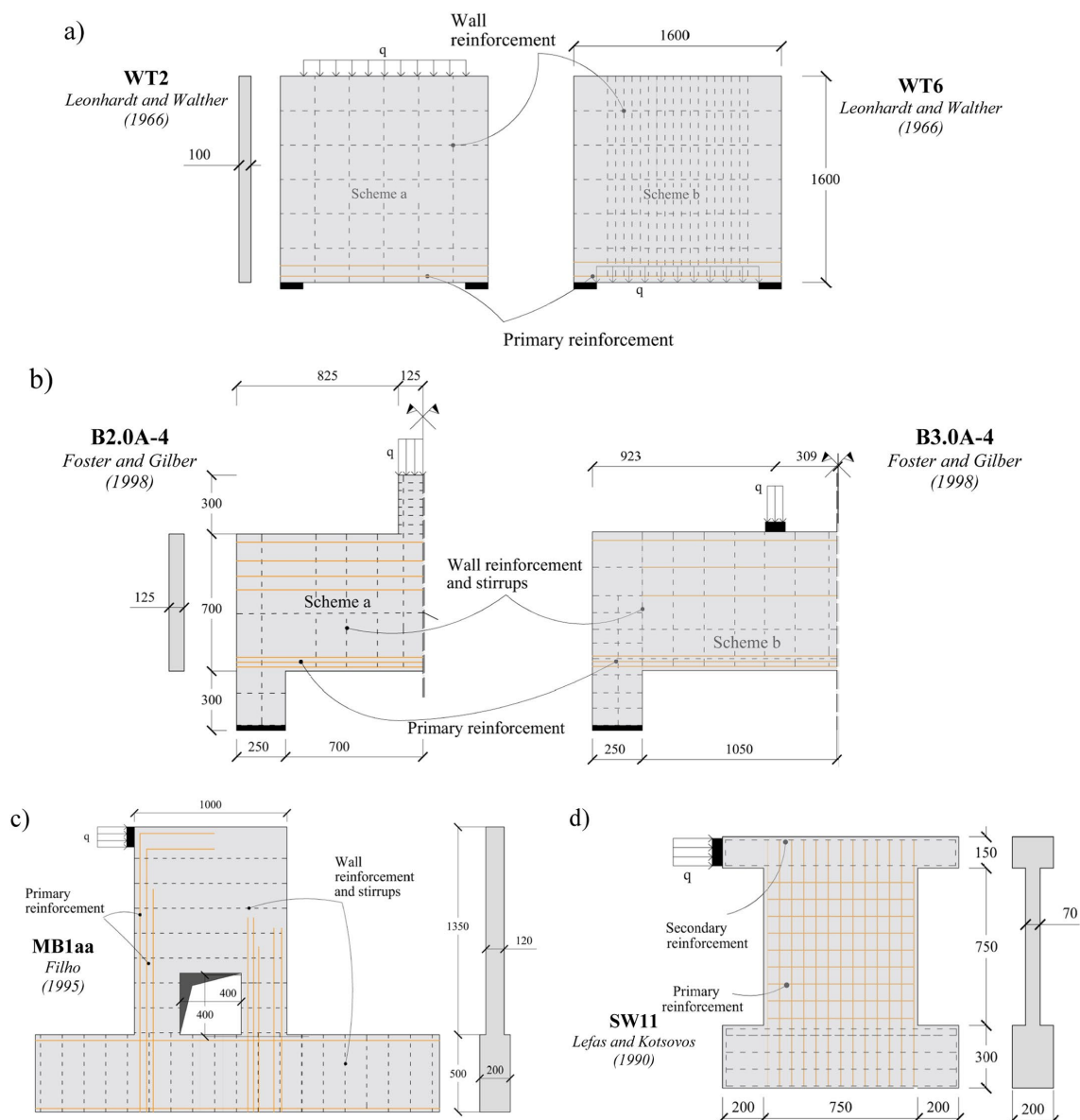


Figure 6.4: Experimental benchmark of the [...] consists of a) 5 deep beams, b) 5 deep beams, c) 5 reinforced concrete walls, d) one concrete wall

Considering the results obtained in the study [7] in terms of the variation trend of the statistical parameters $\delta_{R,m}$ and $V_{R,m}$, they are represented into the same graph with the outcomes of this work of thesis (Figures 6.5 – 6.6). In order to highlight the new results, all of the values of the [7] are represented with the colour grey.

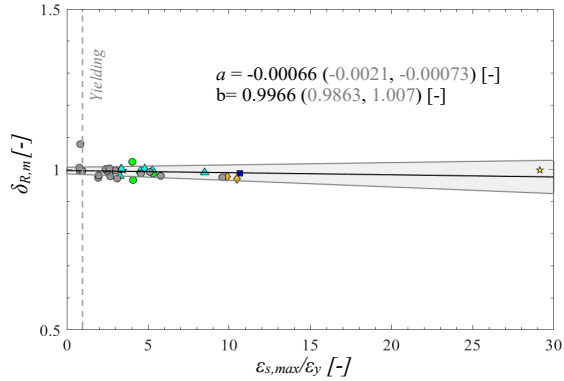
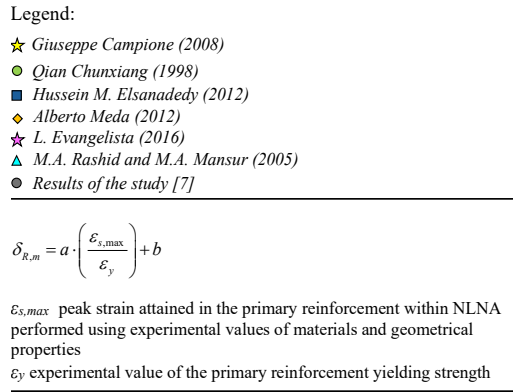


Figure 6.5: Trend of variation of the mean-to-mean deviation $\delta_{R,m}$ with respect to the strain ratio $\varepsilon_{s,max}/\varepsilon_y$ with the representation of the upper and lower bounds of the 95% confidence interval

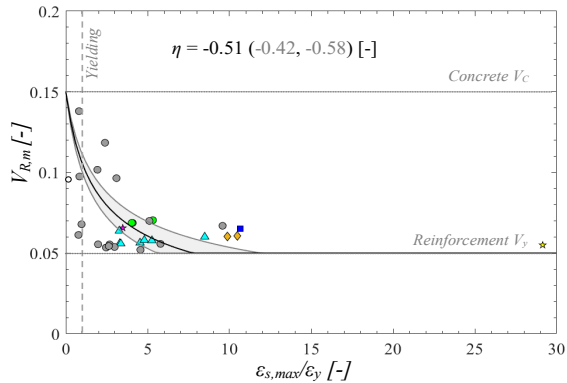
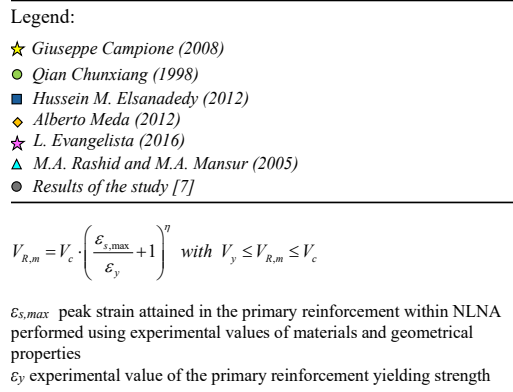


Figure 6.6: Trend of variation of the CoV $V_{R,m}$ with respect to the strain ratio $\varepsilon_{s,max}/\varepsilon_y$ with the representation of the upper and lower bounds of the 95% confidence interval

As reported into the legend of the Figures 6.5 – 6.6, considering the values of the statistical parameters of the 16 reinforced concrete beams they are been used the following expressions to consider the best-fitting of the results in terms of $\delta_{R,m}$ (Eq.(8)) and $V_{R,m}$ (Eq.(8)) as a function of the strain ratio $\varepsilon_{s,max}/\varepsilon_y$.

$$\delta_{R,m} = a \cdot \left(\frac{\varepsilon_{s,max}}{\varepsilon_y} \right) + b \quad (8)$$

$$V_{R,m} = V_c \cdot \left(\frac{\varepsilon_{s,max}}{\varepsilon_y} + 1 \right)^\eta \quad \text{with } V_y \leq V_{R,m} \leq V_c \quad \text{and} \quad V_c = 0.15 \quad (9)$$

In both the Eq.(8) and the Eq.(9), the coefficients a , b for the Eq.(8) and the exponent η for the Eq.(9) are estimated using the least square method in order to define the best-fitting law and the upper and lower bounds of the 95% confidence interval.

Focusing on the graphical representation of the $\delta_{R,m}$ with respect to the strain ratio $\varepsilon_{s,max}/\varepsilon_y$, it can be recognized a slightly linear decreasing as the values of the coefficients a and b suggest (Figure 6.5). Then, in the practical applications, the value of the mean-to-mean deviation $\delta_{R,m}$ can be reasonably assumed equal to 1.

Regarding the Coefficient of Variation $V_{R,m}$ of the global structural resistance with respect to the strain ratio $\varepsilon_{s,max}/\varepsilon_y$, two main comments can be made. Observing all the values reported into the graph, when the strain ratio $\varepsilon_{s,max}/\varepsilon_y$ is lower than 1, $V_{R,m}$ assumes the CoV of the cylinder compressive strength V_C . As second comment, when the strain ratio $\varepsilon_{s,max}/\varepsilon_y$ increases and achieves values in the range of 5-10, $V_{R,m}$ assumes the CoV of the main reinforcement yielding V_y .

6.1.1 Expressions for practical applications

It is now necessary to define the expressions for practical applications of the strain-based method useful to design or verify a reinforced concrete structure. As a reminder, the aim is the evaluation of the global resistance safety factor γ_R within the Global Resistance Method and according to the GRF. Knowing this value it is possible to calculate the global structural resistance R_d after the evaluation of the value of the global resistance obtained performing a NLN analysis considering the mean values of material properties and nominal values for geometric characteristics $R_{NLNA}(f_m; a_n)$. In the following the main steps are explained.

According to the Eq.(2), γ_R is calculated as a function of the CoV of the global structural resistance V_R , the related factor δ_R , the target value of the reliability index β_t and the FORM factor α_R .

Focusing on the Eq.(5), V_R is evaluated as a function of $V_{R,m}$ and $V_{R,g}$. Regarding the value of $V_{R,m}$, it is obtained using the Eq.(9) setting -0.4 as exponent η (Figure 6.7 (a)). This latter value is able to characterize a various range of V_C . For the value of $V_{R,g}$, it can consider reasonably 0.05.

As already discussed in the second chapter and according to the Eq.(3), the value of δ_R is equal to $\delta_{R,m}$. This latter value can be approximated to 1, according to the results obtained.

β_t and α_R are imposed values. Fixing the value of α_R equal to 0.8, it is possible to represent the value of the global resistance safety factor γ_R as a function of the strain ratio $\varepsilon_{s,max}/\varepsilon_y$ and the value of the target reliability index β_t (Figure 6.7 (b)).

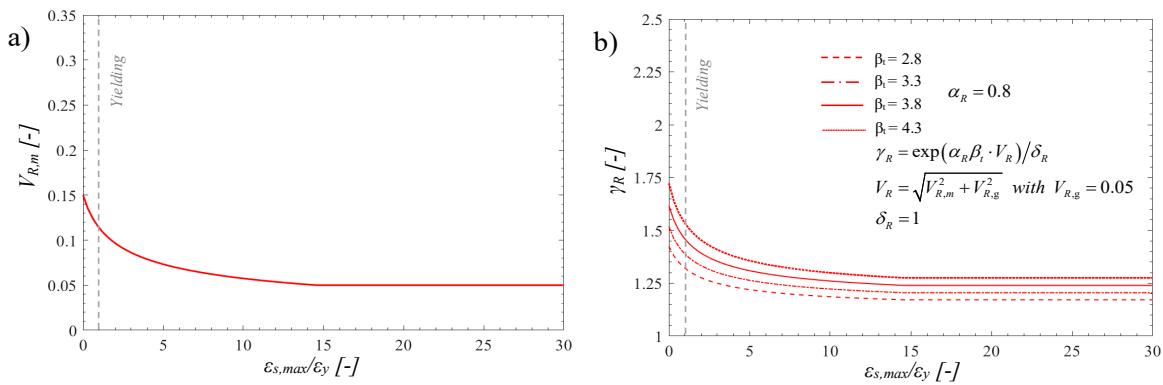


Figure 6.7: Representation of the Eq.(9) (a) assuming $\eta = -0.4$ and (b) as a function of β_t

It is important to remember that this proposed approach permits to evaluate the global resistance factor γ_R for both new and existing reinforced concrete structures.

In the practical application, a design who needs to design or verify a reinforced concrete structure has to perform only one NLNA considering the mean values for the material properties f_m and the nominal values for the geometrical ones a_n . In this way, the geometrical response of the system in terms of maximum strain at the failure step it is used to obtain the value of the global resistance factor γ_R . Knowing this latter value, it is possible to evaluate the global structural resistance R_d , according to the target reliability method.

6.2 Comparison with the other safety formats within the GRF

In this last paragraph, it has been carried out a comparison between the novel strain-based approach and the other safety formats used within the GRF. In this case it has been considered a target reliability index β_t equal to 3.8. In particular, two safety formats are compared with respect to the strain-based approach: the Estimation of Coefficient of Variation (ECoV method) and the Partial Factor Method (PFM). To comparison is carried out considering the design value of the global structural resistance defined for each safety format R_d and the design value of the of the global structural resistance resulting from the probabilistic analysis $R_{d,Prob}$ assumed lognormally distributed. All the types of uncertainties are considered as it has already been discussed in the previous chapters. As represented in the figure below (Figure 6.8), the comparative value is the ratio $R_d/R_{d,Prob}$. In general, the safety formats are considered in the safe side il the ratio $R_d/R_{d,Prob}$ is lower than 1. Looking at the graphs, it has been demonstrated the effectiveness of the strain-based approach.

Legend:

- ★ Giuseppe Campione (2008)
- Qian Chunxiang (1998)
- Hussein M. Elsanadedy (2012)
- ◆ Alberto Meda (2012)
- ☆ L. Evangelista (2016)
- ▲ M.A. Rashid and M.A. Mansur (2005)

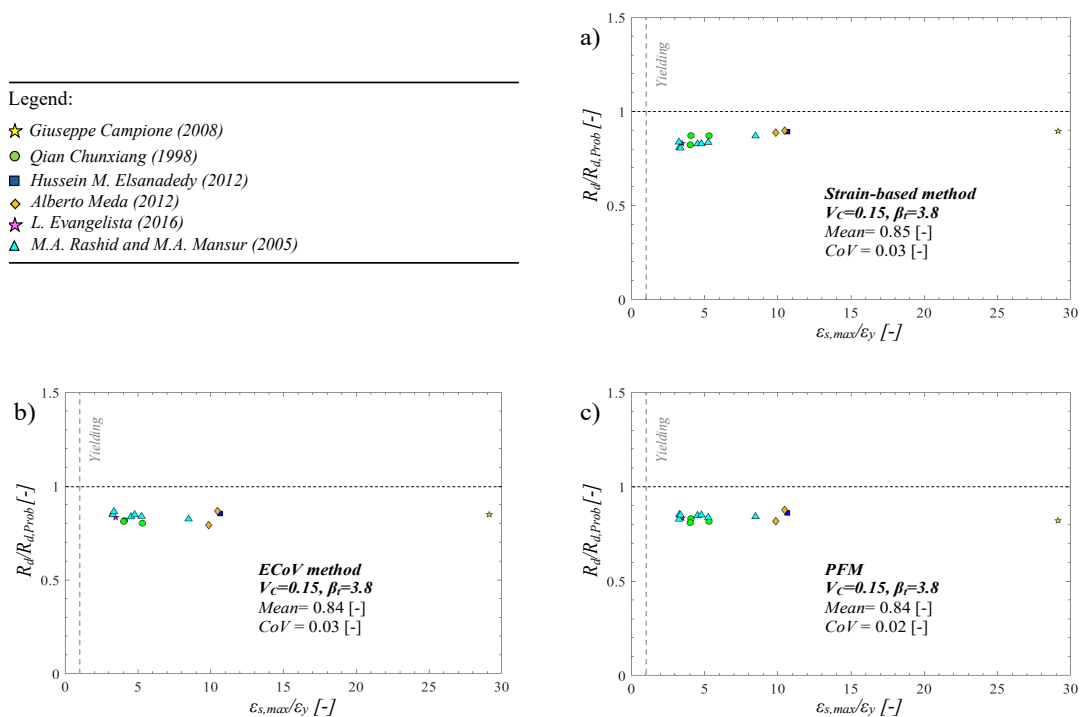


Figure 6.8: Comparison between the strain-based method, ECoV method and PFM, in terms of ratio between the estimated design value of the structural resistance R_d and the actual design global resistance from the probabilistic analysis $R_{d,Prob}$

7 Conclusions

This work of thesis has expanded the application of the novel strain-based method for estimating the design value of the global structural resistance R_d to beam-behaviour structural elements, subjected to flexural collapse. According to the Global Resistance Format (GFR), the global structural resistance is carried out by means of NLNAs. As first thing, an experimental benchmark consists of 16 reinforced concrete beams failing in bending have been considered. It has been developed a non-linear model for each beam and the related model uncertainties are considered by means of a proper factor. These non-linear models are used in the next phase to perform a probabilistic analysis of the global structural resistance taking into account the uncertainties related to the material properties. The aim of the probabilistic analysis is to characterize the mean value $\mu_{R,m}$ and the CoV $V_{R,m}$ of the global structural resistance for each beam.

The next phase regard the correlation between the $V_{R,m}$ and the geometrical response characteristics of the structural system (i.e. strain ratio $\varepsilon_{s,max}/\varepsilon_y$, the geometrical reinforcement ratio ρ and the mechanical reinforcement ratio ω). In this work of thesis, it has been only derived a correlation between the $V_{R,m}$ and the strain ratio $\varepsilon_{s,max}/\varepsilon_y$ useful to expand the strain-based approach already studied in mentioned articles to the beam-behaviour structural element. $\varepsilon_{s,max}$ represents the maximum strain of the primary reinforcement while ε_y is the yielding strain as an inherent property of the steel reinforcement. The terms of this ratio derive from the NLNA conducted considering the mean material properties and the nominal geometrical ones. However, the correlation between the $V_{R,m}$ and the strain ratio $\varepsilon_{s,max}/\varepsilon_y$ is carried out by means a best-fitting relationship estimated using the least square method considering the upper and lower bounds of the 95% confidence interval. After that, it is possible to define the global resistance safety factor γ_R according to the target reliability level.

Adopting this novel method, the computational effort for the designer and the potential errors are strongly reduced. In fact, it is necessary to perform only one analysis to evaluate the strain ratio which permits to evaluate the γ_R . It is

necessary to admit that this method investigated in this work of thesis is now validated for the flexural collapse. To validate this method also for the shear failure it is necessary another study.

Finally, a comparison between the strain-based method with respect to the other safety formats included in the GRF, such as ECoV method and the PFM, has been demonstrated the effectiveness of this novel strain-based method.

References

- [1] Giuseppe Campione, Maria Letizia Mangiavillano. Y. 2008. "Fibrous reinforced concrete beams in flexure: Experimental investigation, analytical modelling and design considerations". *Engineering Structures*, 2970-2980
- [2] Qian Chunxiang, Indubhushan Patnaikuni. Y. 1998. "Properties of high-strength steel fiber-reinforced concrete beams in bending". Elsevier, 71-73
- [3] Hussein M. Elsanadedy, Tarek H. Almusallam, Saleh H. Alsayed, Yousef A. Al-Salloum. Y. 2012. "Flexural strengthening of RC beams using textile reinforced mortar – Experimental and numerical study". *Compositive Structures*, 0263-8223
- [4] Alberto Meda, Fausto Minelli, Giovanni A. Plizzari. Y. 2012. "Flexural behaviour of RC beams in fibre reinforced concrete". *Composites: Part B*, 2930-2937
- [5] L. Evangelista, J. De Brito. Y. 2016. "Flexural Behaviour of Reinforced Concrete Beams Made with Fine Recycled Concrete Aggregates". *Journal of Civil Engineering*, 353-363
- [6] M. A. Rashid, M. A. Mansur. Y. 2005. "Reinforced High-Strength Concrete Beams in Flexure". *ACI Structural Journal*, 102-S47
- [7] Diego Gino, Elena Miceli, Paolo Castaldo, Antonino Recupero, Giuseppe Mancini. Y. 2024. "Strain-based method for assessment of global resistance safety factors for NLNAs of reinforced concrete structures". *Engineering Structures*, 304-117625
- [8] Paolo Castaldo, Diego Gino, Giuseppe Mancini. Y. 2019. "Safety formats for non-linear finite element analysis of reinforced concrete structures: discussion, comparison and proposals". *Engineering Structures*, 136-153

- [9] Diego Gino, Y. 2019. "Advances in reliability methods for reinforced concrete structures". Politecnico di Torino
- [10] Miceli Elena, Y. 2020. "Robustness assessment in reliability terms of reinforced concrete structures in seismic zone". Politecnico di Torino
- [11] JCSS, Y.2001. "JCSS Probabilistic Model Code"

List of figures

Figure 1.1: Comparison between local structural analysis and global structural analysis [8]..... 2

Figure 2.1: Strain-based methodology from the point of view of the analyst 8

Figure 2.2: Strain-based methodology from the point of view of the designer 9

Figure 3.1: Three-point bending test and four-point bending test 11

Figure 3.2: Geometry and steel arrangement of 5.0.1 13

Figure 3.3: Stress-strain curve of 5.0.1..... 14

Figure 3.4: Geometry and steel arrangement of CF, CS and CT 15

Figure 3.5: Stress-strain curve of CF 16

Figure 3.6: Stress-strain curve of CS..... 17

Figure 3.7: Stress-strain curve of CT 17

Figure 3.8: Geometry and steel arrangement of BF-1 (1) and BF-1 (2)..... 18

Figure 3.9: Stress-strain curve of BF-1 (1) and BF-1 (2) 19

Figure 3.10: Geometry and steel arrangement of 2φ16-B-PC and 4φ16-B-PC 20

Figure 3.11: Stress-strain curve of 2φ16-B-PC and 4φ16-B-PC 21

Figure 3.12: Geometry and reinforcement arrangement of RC-1 22

Figure 3.13: Stress-strain curve of RC-1 23

Figure 3.14: Geometry and reinforcement arrangement of A211, B312, B313, B321, C211, C311, C411 24

Figure 3.15: Stress-strain curve of A211,B312,B313, B321, C211, C311, C411 27

Figure 4.1: Key features of ATENA 2D (www.cervenka.cz)..... 28

Figure 4.2: Pre processing graphical interface 29

Figure 4.3: Basic tab for SBeta Material 30

 Figure 4.4: Tensile tab - Type of tension softening for SBeta Material..... 31

 Figure 4.5: Tensile tab - Crack model for SBeta Material 31

 Figure 4.6: Compressive tab for SBeta Material..... 32

 Figure 4.7: Shear tab - retention factor for SBeta Material 33

 Figure 4.8: Shear tab: tension-compression interaction for SBeta Material 33

 33

 Figure 4.9: Miscellaneous tab for SBeta Material 34

Figure 4.10: Basic tab for Reinforcement	34
Figure 4.11: Miscellaneous tab for Reinforcement.....	35
Figure 4.12: Basic tab for Plane Stress Elastic Isotropic	36
Figure 4.13: Miscellaneous tab for Plane Stress Elastic Isotropic.....	36
Figure 4.14: Joints tab - New joints.....	37
Figure 4.15: Line tab - New lines	37
Figure 4.16: Macro-elements tab - New macro-elements	38
Figure 4.17: Bar Reinforcement tab – Topology.....	39
Figure 4.18: Bar Reinforcement tab – Properties.....	39
Figure 4.19: Definition of Supports load case	40
Figure 4.20: Support load case tab - Replace joint support.....	40
Figure 4.21: Graphical scheme of Supports load case	41
Figure 4.22: Definition of Body force load case	41
Figure 4.23: Definition of Forces load case	42
Figure 4.24: Forces load case tab - Line loading	42
Figure 4.25: Graphical scheme of Forces load case.....	42
Figure 4.26: Definition of Analysis steps	43
Figure 4.27: Monitoring points tab - Definition of monitoring points	44
Figure 4.28: New solution parameters	44
Figure 4.29: New solution parameters - Conditional Break Criteria section	45
Figure 4.30: Post-processing graphical interface.....	45
Figure 4.31: Example of cracks pull-down menu	46
Figure 4.32: Example of bar reinforcement pull-down menu	47
Figure 4.33: Example of Scalars pull-down menu.....	47
Figure 4.34: CCT import file.....	48
Figure 4.35: CCO export file	49
Figure 4.36: comparison between experimental results R_{exp} and NLNAs outcomes $R_{NLNA}(f_{exp}; a_{exp})$ and representation of the respective failure mechanism in concomitance of failure (a, b, c, d, e, f, g, h, l, l, m,n,o,p,q,r).....	54
Figure 5.1: Comparison between the empirical CDF (LHS sampling in the figure) and the lognormal CDF (Theoretical in the figure) [9]	56
Figure 5.2: Empirical and lognormal CDFs (a, b, c, d, e, f, g, h).....	58
Figure 5.3: Empirical and lognormal CDFs (i, l, m, n, o, p, q, r).....	59

Figure 5.4: Load-Displacement curves of the 30 NLNAs (a, b, c, d, e, f, g, h).. 60

Figure 5.5: Load-Displacement curves of the 30 NLNAs (i, l, m, n, o, p, q, r)... 61

Figure 6.1: Variation trend of the mean-to-mean deviation $\delta R, m$ with respect to a) the strain ratio $\epsilon_{s, max}/\epsilon_y$, b) the geometrical reinforcement ratio ρ , c) the mechanical reinforcement ratio ω 63

Figure 6.2: Variation trend of the CoV of the global resistance $V_{R, m}$ with respect to a) the strain ratio $\epsilon_{s, max}/\epsilon_y$, b) the geometrical reinforcement ratio ρ , c) the mechanical reinforcement ratio ω 63

Figure 6.3: Variation trend of the strain ratio $\epsilon_{s, max}/\epsilon_y$ with respect..... 64

Figure 6.4: Experimental benchmark of the [...] consists of a) 5 deep beams, b) 5 deep beams, c) 5 reinforced concrete walls, d) one concrete wall 65

Figure 6.5: Trend of variation of the mean-to-mean deviation $\delta R, m$ with respect to the strain ratio $\epsilon_{s, max}/\epsilon_y$ with the representation of the upper and lower bounds of the 95% confidence interval..... 66

Figure 6.6: Trend of variation of the CoV $V_{R, m}$ with respect to the strain ratio $\epsilon_{s, max}/\epsilon_y$ with the representation of the upper and lower bounds of the 95% confidence interval..... 66

Figure 6.7: Representation of the Eq.(9) (a) assuming $\eta = -0.4$ and (b) as a function of βt 68

Figure 6.8: Comparison between the strain-based method, ECoV method and PFM, in terms of ratio between the estimated design value of the structural resistance R_d and the actual design global resistance from the probabilistic analysis $R_{d, Prob}$ 69

List of tables

Table 3.1: Experimental tests	12
Table 3.2: Material properties of 5.0.1	13
Table 3.3: Longitudinal steel reinforcement of 5.0.1	14
Table 3.4: Shear steel reinforcement.....	14
Table 3.5: Yielding and ultimate characteristics of 5.0.1	14
Table 3.6: Material properties of CF, CS and CT	15
Table 3.7: Longitudinal steel reinforcement of CF, CS and CT.....	16
Table 3.8: Shear steel reinforcement of CF, CS and CT.....	16
Table 3.9: Yielding and ultimate characteristics of CF, CS and CT.....	17
Table 3.10: Material properties of BF-1 (1) and BF-1 (2).....	18
Table 3.11: Longitudinal steel reinforcement of BF-1 (1) and BF-1 (2).....	19
Table 3.12: Shear steel reinforcement of BF-1 (1) and BF-1 (2).....	19
Table 3.13: Yielding and ultimate characteristics of BF-1 (1) and BF-1 (2).....	19
Table 3.14: Material properties of 2 ϕ 16-B-PC and 4 ϕ 16-B-PC	20
Table 3.15: Longitudinal steel reinforcement of 2 ϕ 16-B-PC and 4 ϕ 16-B-PC ...	21
Table 3.16: Shear steel reinforcement of 2 ϕ 16-B-PC and 4 ϕ 16-B-PC.....	21
Table 3.17: Yielding and ultimate characteristics of 2 ϕ 16-B-PC and 4 ϕ 16-B-PC	22
Table 3.18: Material properties of RC-1.....	22
Table 3.19: Longitudinal steel reinforcement of RC-1.....	23
Table 3.20: Shear reinforcement of RC-1	23
Table 3.21: Yielding and ultimate characteristics of RC-1	23
Table 3.22: Material properties of A211, B312, B313, B321, C211, C311, C411	25
Table 3.23: Longitudinal steel reinforcement of A211, B312, B313, B321, C211, C311, C411	25
Table 3.24: Shear steel reinforcement of A211, B312, B313, B321, C211, C311, C411.....	26
Table 3.25: Yielding and ultimate characteristics of A211, B312, B313, B321, C211, C311, C411	26

Table 5.1 - Characterization of the probabilistic models related to aleatory uncertainties associated to material properties..... 55